

The differential role of CR3 (CD11b/CD18) and CR4 (CD11c/CD18) complement receptors in human phagocytes

Ph.D. Thesis

Szilvia Zsófia Lukácsi

Supervisor:
Professor Zsuzsa Bajtay, D.Sc.

Doctoral School of Biology
Head: Professor Anna Erdei, D.Sc.

Immunology Ph.D. Program
Head: Professor Zsuzsa Bajtay, D.Sc.



Eötvös Loránd University, Institute of Biology
Department of Immunology

Budapest, 2019

Table of contents

List of abbreviations	5
1. Introduction	7
1.1. The expression and endosomal recycling of CR3 and CR4	7
1.2. The structural and signalling properties of CR3 and CR4.....	8
1.3. The diverse ligands bound by CR3 and CR4.....	11
1.4. The function of CR3 and CR4 in myeloid cells.....	14
1.4.1. The role of CR3 and CR4 in adherence and podosome formation	18
1.4.2. The role of CR3 and CR4 in phagocytosis	20
1.5. The pathological implications of CR3 and CR4.....	21
2. Aims	24
3. Materials and methods.....	25
3.1. Isolation of human monocytes and neutrophil granulocytes	25
3.2. Generation of monocyte-derived macrophages (MDMs) and monocyte-derived dendritic cells (MDDCs)	25
3.3. Blocking of CD11b/CD18 and CD11c/CD18 by antibodies	25
3.4. RNA silencing in macrophages	26
3.5. Induction of inflammatory condition using LPS treatment	26
3.6. Monitoring the expression of CD11b and CD11c during LPS induced activation	26
3.7. Analysis of β_2 -integrin conformational state	27
3.8. Analysis of adhesion by confocal microscopy	27
3.9. Analysis of adhesion with the computer-controlled micropipette	28
3.10. Analysis of adhesion by EPIC BT biosensor measurement	29
3.11. Analysis of the contact surface by confocal microscopy.....	29
3.11.1. Generation of the adhesive surface and adherent cell layer.....	29
3.11.2. Staining of the actin cytoskeleton and podosome counting.....	30
3.11.3. Staining of CD11b/CD11c on adherent cells.....	30
3.12. Phagocytosis of Staphylococcus aureus	30
3.13. Analysis of transmigration.....	31
3.14. Statistics	31
4. Results I. The function of CR3 and CR4 under physiological conditions. 32	
4.1. Adhesion to fibrinogen coated surfaces.....	32
4.1.1. The classical assay: CR4 dominates adhesion over CR3.....	32

4.1.2.	The computer controlled micropipette method: CR4 is important for a strong cell attachment	38
4.1.3.	Analysis of adhesion kinetics using the optical waveguide biosensor: CR4 dominates adhesion over CR3	40
4.2.	Migration	43
4.2.1.	Both CR3 and CR4 participate in the migration of MDMs and MDDCs	43
4.3.	Adhesive structures of human phagocytes – podosomes.....	44
4.3.1.	Podosome patterns	44
4.3.2.	Localization of CD11b and CD11c on the contact surface of adherent cells	44
4.4.	Phagocytosis of iC3b opsonized <i>Staphylococcus aureus</i>	47
4.4.1.	Comparing differently labelled <i>S. aureus</i> particles	47
4.4.2.	The role of CR3 and CR4 in the phagocytosis of iC3b opsonized <i>Staphylococcus aureus</i>	49
5.	Results II. The function of CR3 and CR4 under inflammatory conditions	52
5.1.	Receptor expression, activation status and recycling	53
5.1.1.	Under inflammatory conditions the expression of CR3 and CR4 is regulated differently on MDMs and MDDCs.....	53
5.1.2.	LPS treatment enhances β_2 -integrin cycling in both MDMs and MDDCs.....	54
5.2.	Adhesion to fibrinogen coated surfaces.....	57
5.2.1.	Under inflammatory conditions both CR3 and CR4 participate in the adhesion to fibrinogen	57
5.2.2.	LPS induced cell maturation decreases the force of adhesion significantly in MDDCs.....	58
5.2.3.	CR4 is prominently involved in the strong attachment of MDMs and MDDCs to fibrinogen	59
5.3.	Migration	60
5.3.1.	Under inflammatory conditions both CR3 and CR4 participate in the migration of MDMs and MDDCs	60
5.4.	Adhesive structures of human phagocytes – podosomes.....	61
5.4.1.	MDDCs lose their podosomes during LPS induced maturation	61
5.4.2.	Localization of CD11b and CD11c on the contact surface of adherent cells under inflammatory conditions	61
6.	Discussion.....	64

Summary	73
Összefoglalás.....	75
Acknowledgements.....	77
List of publications.....	78
Publications connected to the thesis.....	78
Other publications	78
References	80

List of abbreviations

ANA domain	ANaphylatoxin domain
APC	AlloPhycoCyanin
BMDCs	Bone Marrow derived Dendritic Cells
CCL19	Chemokine (C-C motif) Ligand 19
CCR7	C-C Chemokine Receptor type 7
cDC	Conventional or Classical Dendritic Cell
CDC42	Cell Division Control protein 42 homolog
CFTR	Cystic Fibrosis Transmembrane conductance Regulator
CLP	Common Lymphoid Progenitor,
CMP	Common Myeloid Progenitor
CR3	Complement Receptor type 3 (CD11b/CD18, $\alpha_M\beta_2$, Mac-1)
CR4	Complement Receptor type 4 (CD11c/CD18, $\alpha_x\beta_2$, p150,95)
CUB domain	Complement C1r/C1s, Uegf, Bmp1-fold containing domain
DCs	Dendritic Cells
ECM	ExtraCellular Matrix
EDTA	EthyleneDiamineTetraacetic Acid
FCS	Fetal Calf Serum
FHP	Filamentous Hemagglutinin Protein
FITC	Fluorescein IsoThioCyanate
fMLP	N-FormylMethionyl-Leucyl-Phenylalanine
FPR	Formyl Peptide Receptors
GM-CSF	Granulocyte-Macrophage Colony-Stimulating Factor
GTP/GDP	Guanosine TriPhosphate/ Guanosine DiPhosphate
HBSS	Hanks' Balanced Salt Solution
ICAM-1	Intercellular Adhesion Molecule 1
I-EGF domain	Integrin-Epidermal Growth Factor
IFN γ	InterFeroN γ
IL	InterLeukin
iNOS	inducible Nitric Oxide Synthase
JAM	Junctional Adhesion Molecule
KO	Knock Out
LAD	Leukocyte Adhesion Deficiency
LFA-1	Lymphocyte Function-associated Antigen 1 (CD11a/CD18, $\alpha_L\beta_2$)
LPS	LipoPolySaccharide
mAb	Monoclonal AntiBody

MDDC	Monocyte Derived Dendritic Cell
MDM	Monocyte Derived Macrophage
MFI	Mean Fluorescence Intensity
MG domain	MacroGlobulin domain
MIDAS	Metal-Ion-Dependent Adhesion Site
Mo	Monocyte
NET	Neutrophil Extracellular Trap
Neu	Neutrophil granulocyte
NIF	Neutrophil Inhibitory Factor
NK cell	Natural Killer cell
PBMC	Peripheral Blood Mononuclear Cells
PBS	Phosphate Buffered Saline solution
PDB	Protein Data Bank
pDC	Plasmacytoid Dendritic Cells
PLL-g-PEG	synthetic copolymer Poly(L-Lysine)-Graft-Poly(Ethylene Glycol)
PMN	PolyMorphoNuclear cell
PNRC	PeriNuclear Recycling Compartment
PSI domain	Plexin-Semaphorin-Integrin domain
Rap1	Ras-proximate-1
RGS14	Regulator of G-Protein Signalling-14
RhoA	Ras HOMolog gene family, member A
RIAM	Rap1-Interacting Adaptor Molecule
ROI	Region Of Interest
RT	Room Temperature
siRNA	Small Interfering RiboNucleic Acid
SLE	Systemic Lupus Erythematosus
SNP	Single Nucleotide Polymorphism
TED domain	ThioEster-containing Domain
TGF- β	Transforming Growth Factor β
TIP-DC	TNF- and iNOS-producing dendritic cells
TLR	Toll-Like Receptor
TNF- α	Tumour Necrosis Factor
uPAR	Urokinase Receptor
VCAM	Vascular Cell Adhesion Molecule
WASP	Wiskott–Aldrich Syndrome Protein

1. Introduction

The complement receptors CR3 (CD11b/CD18, also known as Mac-1; $\alpha_M\beta_2$) and CR4 (CD11c/CD18, also known as p150,95; $\alpha_X\beta_2$) belong to the family of β_2 -integrins and play an important role in phagocytosis, cellular adherence and migration. Their natural ligands include the iC3b complement component on opsonised targets, and fibrinogen or ICAM-1 as adhesion ligands¹⁻³. The ligand binding affinity of integrins is regulated by activation dependent conformational changes. Their extracellular domains undergo remarkable structural rearrangements to switch from a bent, inactive state into an extended, ligand-binding conformation.

A similar role is often assumed for CR3 and CR4 since they have an overlapping ligand binding specificity and high sequence homology (87%) in their extracellular domains⁴. However, their intracellular parts, important for signal transduction and connection with the cytoskeleton, differ in length and amino acid sequence displaying only a 56% similarity⁵. Our group set out to thoroughly investigate the individual role of CR3 and CR4, since studies published on these receptors reveal a pivotal role for them in leukocyte functions necessary for the resolution of infections⁶.

1.1. The expression and endosomal recycling of CR3 and CR4

The expression of CR3 and CR4 varies between cell types and species⁶. In humans both receptors can be found on myeloid cells, such as neutrophil granulocytes, monocytes, macrophages and dendritic cells⁷⁻⁹. In mouse CR4 has a high expression level only on dendritic cells and it additionally appears on certain subpopulations of monocytes, macrophages and neutrophils¹⁰⁻¹³. On lymphoid cells they are not expressed uniformly, only NK cells express CR3 constitutively^{14,15}. On T and B lymphocytes these receptors are usually present on subpopulations¹⁵, appear after activation^{16,17} or during pathological conditions^{18,19}.

Our group recently assessed the absolute number of cell surface CR3 and CR4 on human monocytes, neutrophils, monocyte-derived macrophages (MDM) and monocyte-derived dendritic cells (MDDC)^{6,8}. These data reveal that the expression level of the two receptors differs among these cell types. Comparing the number of CR3 and CR4 on the same cell type there is a strong shift in favour of CR3 in the case of monocytes and neutrophils, whereas on MDMs and MDDCs the CD11b:CD11c ratio is close to 1:1. The notable differences in receptor number probably contribute to the functional diversity

observed in the case of different immune cells. The ratio of these receptors in conjunction with ligand availability may influence the competition between these receptors, determining the outcome of the interactions.

The availability of integrins is regulated by continuous receptor trafficking. Instead of degradation, they are rapidly recycled between the cell membrane and endosomes²⁰. This mechanism extends the lifetime of integrins, for instance Lobert et al. showed a half-life of 12-24 hours for the $\alpha_5\beta_1$ -integrin²¹. Both clathrin-dependent and -independent ways were described for the endocytosis of integrins²², and the Rab family of small GTPases mediate the trafficking of membrane vesicles²³. For integrins, this rapid recycling can occur via distinct routes^{24,25}. The $\alpha_V\beta_3$ - and inactive β_1 -integrins were shown to cycle through a short, Rab4-dependent pathway, where these receptors are quickly returned to the plasma membrane from the early endosomes^{20,26}. In the Rab11-dependent long loop, first described for β_1 -integrins, receptors go through the perinuclear recycling compartment (PNRC) before returning to the cell surface^{26,27}. The fast recycling of integrins grants constantly new receptors for ECM engagement, providing environmental information and efficient migration.

There are few data available on the recycling route used by β_2 -integrins. In the cytoplasmic domain of the LFA-1 (CD11a/CD18, $\alpha_L\beta_2$) β chain Fabbri et al. found a membrane proximal sequence that is required for recycling²⁸, and later proved a clathrin-independent and Rab11 mediated route for this molecule²⁹. In an older publication by Bretscher, studying various cell lines, a high recycling rate was shown for CR3 in contrast to LFA-1, that has a very low, or no internalization²⁰. This difference suggests an α -chain based regulation, prompting the necessity for further research in this field.

1.2. The structural and signalling properties of CR3 and CR4

Integrins are transmembrane heterodimers, consisting of a non-covalently coupled α and β chain. They have a large extracellular region for ligand binding, a transmembrane domain and a short cytoplasmic tail, interacting with signalling molecules and the actin cytoskeleton^{30,31}. The α subunit head consists of a β -propeller and I-domain (Inserted) and it is connected to an elongated leg region, including three domains with a β -sheet structure, the thigh, calf-1 and calf-2³². The β subunit head is formed by an I-like domain and the leg includes a PSI (plexin-semaphorin-integrin) domain, a hybrid domain, four I-EGF (integrin-epidermal growth factor) domains and a β tail domain (TD)^{33,34}(Fig. 1).

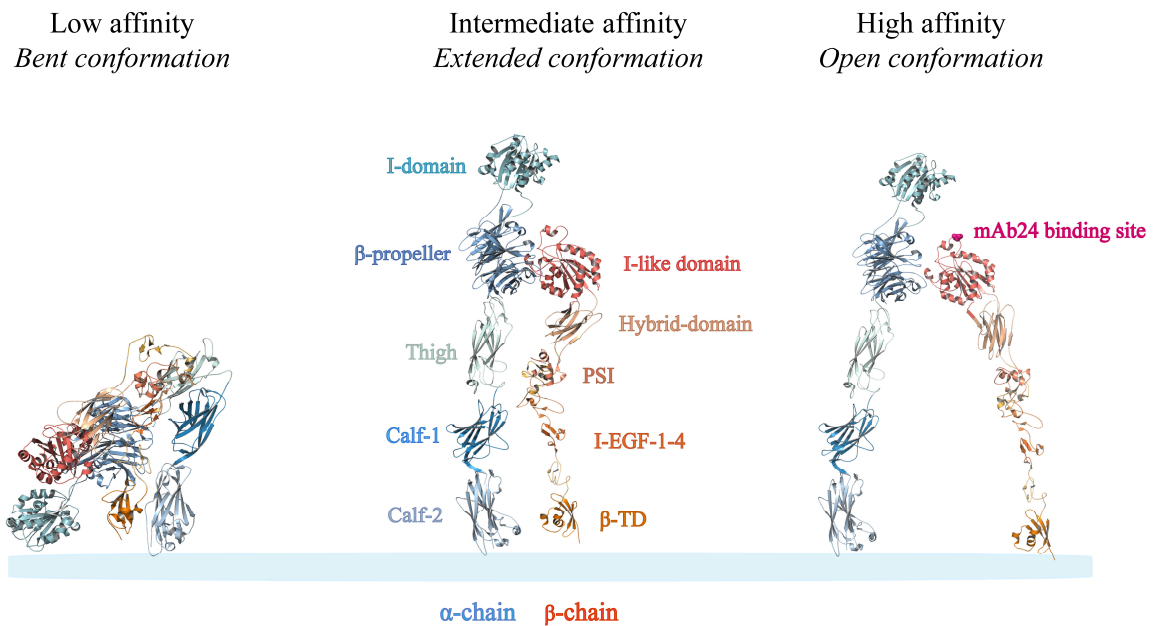


Figure 1. The affinity regulation of β_2 -integrins. The ligand binding affinity of integrins is regulated by activation dependent conformational changes. Integrins can convert between an inactive bent and an activated extended conformation. Both subunits are bent in the inactive form, positioning the head domains near the cell membrane. Inside-out signalling results in the extended conformation, orienting the I-domain away from the membrane. Ligand binding to the activated integrin triggers the outside-in signalling pathway, recruiting various cytosolic proteins. The combination of a lateral force exerted by the actin cytoskeleton and the resistance provided by the bound ligand stabilizes the high affinity, open state. The X-ray diffraction data of CR4 was used from PDB entry 5ES4³⁵ and the structure was visualized with PyMOL software. The transmembrane and cytoplasmic domains are not shown.

Integrins can be divided into two large groups by their head region composition, integrins which have the α I-domain and those that do not. Integrins lacking an α I-domain bind their ligands with the interaction of the β I-like domain and the β -propeller domain from the α subunit³⁶. Where it is present, the α I-domain is responsible for ligand recognition. The α chains coupled to the β_2 subunit have an I-domain, and it is indeed the recognition site for their most known ligands, like iC3b, fibrinogen and ICAM-1^{1,37,38}. The ligand binding occurs at the metal-ion-dependent adhesion site (MIDAS) and it is dependent on the presence of a bivalent cation³⁹. The MIDAS is formed by a conserved DxSxS motif and two non-contiguous amino acids in the α I-domain, and from the ligand, an acidic residue takes part

in the coordination of the metal ion^{31,40,41}.

The ligand binding affinity of integrins is regulated by activation dependent conformational changes. Integrins can transition between an inactive bent and an activated extended conformation⁴². Both subunits are bent in the inactive form, positioning the head domains near the cell membrane. The α subunit bends between the thigh and calf-1 domains, termed genu, and the β_2 subunit between the I-EGF1 and I-EGF2 domains^{43,44}. The close interactions of the α and β transmembrane and cytoplasmic domains keep integrins in the inactive state, to have an active conformation, these regions must be separated. This activation is achieved by molecules, most importantly talin, connecting integrins to the actin cytoskeleton. Talin interacts with the β tail in a membrane proximal region and at a conserved NPxY/F motif (NPLF in β_2) found in the mid section of the cytoplasmic region (between the 747th-755th residues)⁴⁵⁻⁴⁹. The binding of talin to the membrane proximal region disrupts the association of the α and β tails and initiates the separation of the transmembrane domains^{50,51}.

Within the headpiece, a low affinity closed, a high affinity open and an intermediate conformation in between can be distinguished⁵²⁻⁵⁴. The affinity regulation is in association with the conformation changes of loops containing the residues that coordinate ligand binding at the MIDAS region^{41,42,55}. The extension of the integrin legs enables a swing out movement for the PSI and hybrid domains, inducing the conformational changes in the I domain required for a high affinity, open state⁵⁶⁻⁵⁸. However, in an extended integrin both open and closed conformation was shown to exist, and ligand binding and tensile force play a crucial role in determining the headpiece position. The combination of a lateral force exerted by the actin cytoskeleton and the resistance provided by the bound ligand stabilizes the high affinity, open state^{59,60}. At the uropod, where actin depolymerisation takes place and the integrins are no longer attached to the cytoskeleton, the tensile force applied by the retracting membrane promotes detachment from the ligand by stabilizing the low affinity, closed conformation^{61,62}.

A small GTPase Rap1 (Ras-proximate-1) was shown to participate in the talin dependent inside-out activation of LFA-1⁶³ and CR3^{64,65}. RIAM (Rap1-interacting adaptor molecule) was proposed as a scaffold between Rap1 and talin, given its ability to bind both molecules^{66,67}. Macrophages and neutrophils from RIAM deficient mice show disrupted β_2 -integrin dependent adhesion and spreading⁶⁸. Using the human THP-1 monocytic cell line, Lim et al. found, that siRNA silencing of RIAM did not impair phagocytosis and spreading⁶⁵, instead later showed a role for the Regulator of G-Protein Signalling-14 (RGS14) in the

activation of CR3 during phagocytosis in the murine J774.A1 cell line⁶⁹. However Medraño-Fernández et al. proved later, that RIAM is important for complement mediated phagocytosis for HL-60 and THP-1 cell lines and human monocyte derived macrophages⁷⁰. Data obtained from the KO mice models suggest, that RIAM might be β_2 -integrin specific, as the function of platelet $\alpha_{IIb}\beta_3$ -integrin⁷¹ and β_1 -integrins on PMNs⁶⁸ is not disrupted in these mice. Additionally, talin deficient mice show a more severe phenotype compared to RIAM KO mice⁶⁸, underlining that the absence of talin effects the function of all integrins, but the absence of RIAM not.

1.3. The diverse ligands bound by CR3 and CR4

The many ligands described for CR3 and CR4 proved a promiscuous binding ability, with no apparent common motif in these molecules (Table 1.). Their ligands include complement proteins, ECM components and adhesion molecules, all recognised by the major ligand binding site in the α I-domain¹. The β -glucan components of fungal cells are recognized by a separate lectin site in CR3, located C-terminally from the I-domain⁷². An also I-domain independent binding site for bacterial lipopolysaccharides was shown as well in both CR3 and CR4^{73,74}.

	CR3	CR4
Complement proteins	iC3b ¹ , Factor H ⁷⁵	iC3b ⁷⁶ , Factor H ⁷⁷
Coagulation factors	fibrinogen ⁷⁸ , factor X ⁷⁹	fibrinogen ⁸⁰
ECM components	fibronectin ⁸¹ , laminin ⁸¹ , collagen ⁸² , vitronectin ⁸³	collagen ⁸⁴
Adhesion molecules	ICAM-1,2,4 ⁸⁵ , JAM-3 ⁸⁶	ICAM-1,2,4 ⁸⁷⁻⁸⁹ , VCAM-1 ⁸⁸
Pathogen derived molecules	β -glucan ⁹⁰ , LPS ⁷³ , Neutrophil inhibitor factor (NIF) ⁹¹ , FHP ⁹²	LPS ⁷⁴ , Rotavirus ⁹³

Table 1. The ligands of CR3 and CR4

The first identified, natural ligand for CR3 and CR4 was the iC3b complement component⁷⁶. This component is generated by the cleavage of surface bound C3b, deposited on complement activating surfaces. Although the iC3b molecule does not allow further complement activation, it serves as a potent opsonin recognized by complement receptors⁹⁴. Mapping the binding sites for CR3 and CR4 revealed that these receptors bind different residues in iC3b⁹⁵. The binding sites are illustrated on C3b on Figure 2., in the absence of a

resolved structure for iC3b. From the crystal structure of an C3d: α_M I-domain complex Bajic et al. described the amino acid residues in CR3 (Ser142, Ser144, Thr209) and the C3 TED domain (Lys1217, Asp1245, Asp1247, Arg1254) participating in the coordination of the bivalent cation³⁸. According to a study by Chen et al, CR4 can not bind to the TED domain of iC3b, but instead it recognises a sequence in the MG3-MG4 interface⁹⁶. Using electron microscopy, Xu et al. verified these results, and discovered an additional binding site for CR4 near the C345C domain⁹⁵. A different binding site for CR3 and CR4 could enhance the efficiency of phagocytosis by providing a more diverse pathogen recognition.

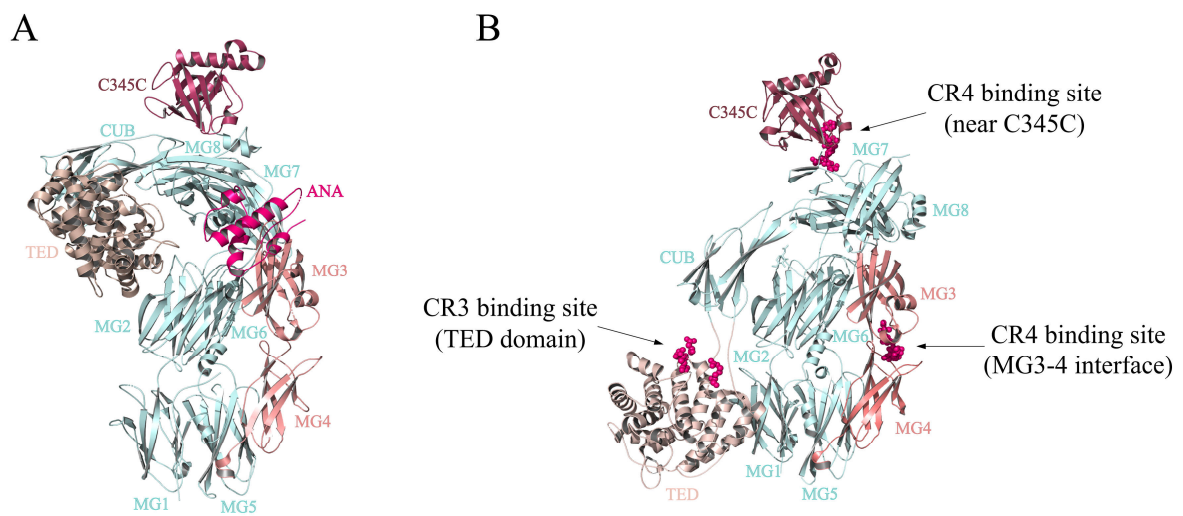


Figure 2. The crystal structure of C3 and C3b with the binding sites for CR3 and CR4

The C3 component (A) consists of two chains, α and β . The β chain contains the first five macroglobulin (MG1-5) domains and the MG6 domain is formed by the intertwined strands of both the α and β chain. The α chain starts with the anaphylatoxin (ANA) domain, that is cleaved during complement activation. It is followed by the MG7 and CUB domain. The C3b molecule (B) is covalently bound on the activating surface through the thioester-containing domain (TED), where the reactive moieties emerge only after the cleavage of C3a (ANA domain). The α chain ends with MG8 and the C345C domain⁹⁴. The X-ray diffraction data was used from PDB entry 5FO7⁹⁷ and 2A73⁹⁴, the structures were visualized with PyMOL software.

Another natural ligand of these receptors is fibrinogen, that is known as an indicator of tissue damage. The best known role of this molecule is maintaining hemostasis by the formation of fibrin clots at the site of vessel wall injuries. It is an acute phase protein, with an elevated hepatic and extrahepatic expression during inflammation, resulting in a higher circulating concentration in blood⁹⁸. During injury fibrinogen is deposited both intravascularly and into the extracellular matrix in the surrounding tissues⁹⁹. There is an increasing amount of evidence that this process also functions as an inflammatory stimulus for platelets and leukocytes^{100,101}.

Fibrinogen is an elongated hexamer, consisting of three pairs of peptide chains: 2 A α , 2 B β and 2 γ (Fig. 3). The outer D-domains are connected by coiled-coil segments to the central E-nodule, where the chains are linked by five disulphide bridges¹⁰². The first studies applying monoclonal antibodies specific for the CD11b I-domain identified CR3 on monocytes and neutrophils as a receptor for fibrinogen^{78,103}. Using synthetic peptides the binding site for CR3 was mapped to the C-terminal domain of the γ chain^{104,105}. From the two potential binding sequences γ 190-202 (P1) and γ 377-395 (P2), P2 was proved to contain the required recognition motif NRLTIG at γ 390-395^{106,107}. The binding of the P1 and P2 sequences were shown for CR4 as well¹⁰⁸, but several groups proved another binding site at the central E region of fibrinogen^{37,80,109}. Loike et al. proposed the N-terminal 17-19 amino acids of the A α chain for the binding site, as peptides containing this sequence inhibited the adhesion of neutrophils to the central nodule⁸⁰.

The binding sites in fibrinogen are cryptic in the native protein, and are only exposed upon proteolysis and immobilization¹¹⁰. Consequently, the soluble protein does not activate cells in the circulation, the proinflammatory effect is regulated by its deposition at the site of injury. Fibrinogen accumulates only in the inflamed tissues, marking it for the recruitment of leukocytes. The engagement of fibrinogen via CR3 and CR4 enhances antimicrobial functions such as cell adhesion, cytokine and chemokine production^{100,107}.

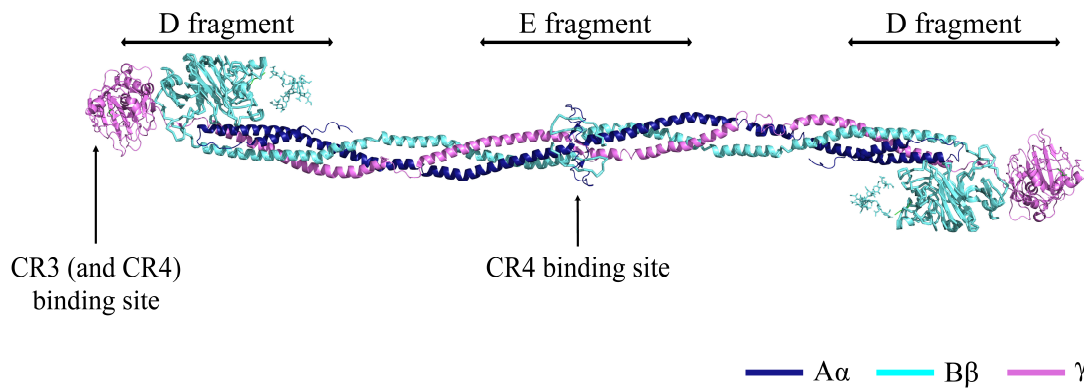


Figure 3. The structure of human fibrinogen. The elongated fibrinogen hexamer consists of three pairs of peptide chains 2A α , 2B β and 2 γ . CR3, and possibly CR4, recognise a *NRLTIG* motif in the γ chain, and there is an additional binding site for CR4 at the N-terminus of the A α chain. The outer globular parts are called D-domains, and the central nodule is termed E-domain. The X-ray diffraction data was used from PDB entry 3GHG¹¹¹ and the structure was visualized with PyMOL software.

1.4. The function of CR3 and CR4 in myeloid cells

CR3 and CR4 are known to play an essential role in cell motility and the elimination of pathogens via phagocytosis. Immune cells expressing these receptors will migrate through the endothelium and move in the direction of infection within the tissues. This is achieved with the help of podosomes, providing the surface for integrin-ligand connections. Innate immune cells will be the first to engage the invading pathogens, and to capture and internalize targets, these cells utilize a range of receptors. Pattern recognition receptors bind the pathogens directly, while complement or IgG opsonized targets become recognizable by complement- and Fc-receptors, significantly increasing the efficiency of phagocytosis^{112,113}. Additionally, these cells have receptors dedicated to sense the signs of danger, like bacterial products, the anaphylatoxic complement fragments C3a and C5a or chemokines produced by tissue resident cells^{114,115}. N-formylated oligopeptides originating from the invading bacteria or released by the mitochondria due to tissue damage are recognised by formyl peptide receptors (FPRs)¹¹⁶. These receptors are expressed on neutrophils, monocytes, macrophages and immature dendritic cells¹¹⁷⁻¹¹⁹, and have an important role in initiating the immune response by promoting leukocyte recruitment, enhanced phagocytosis and the release of reactive oxygen species¹²⁰.

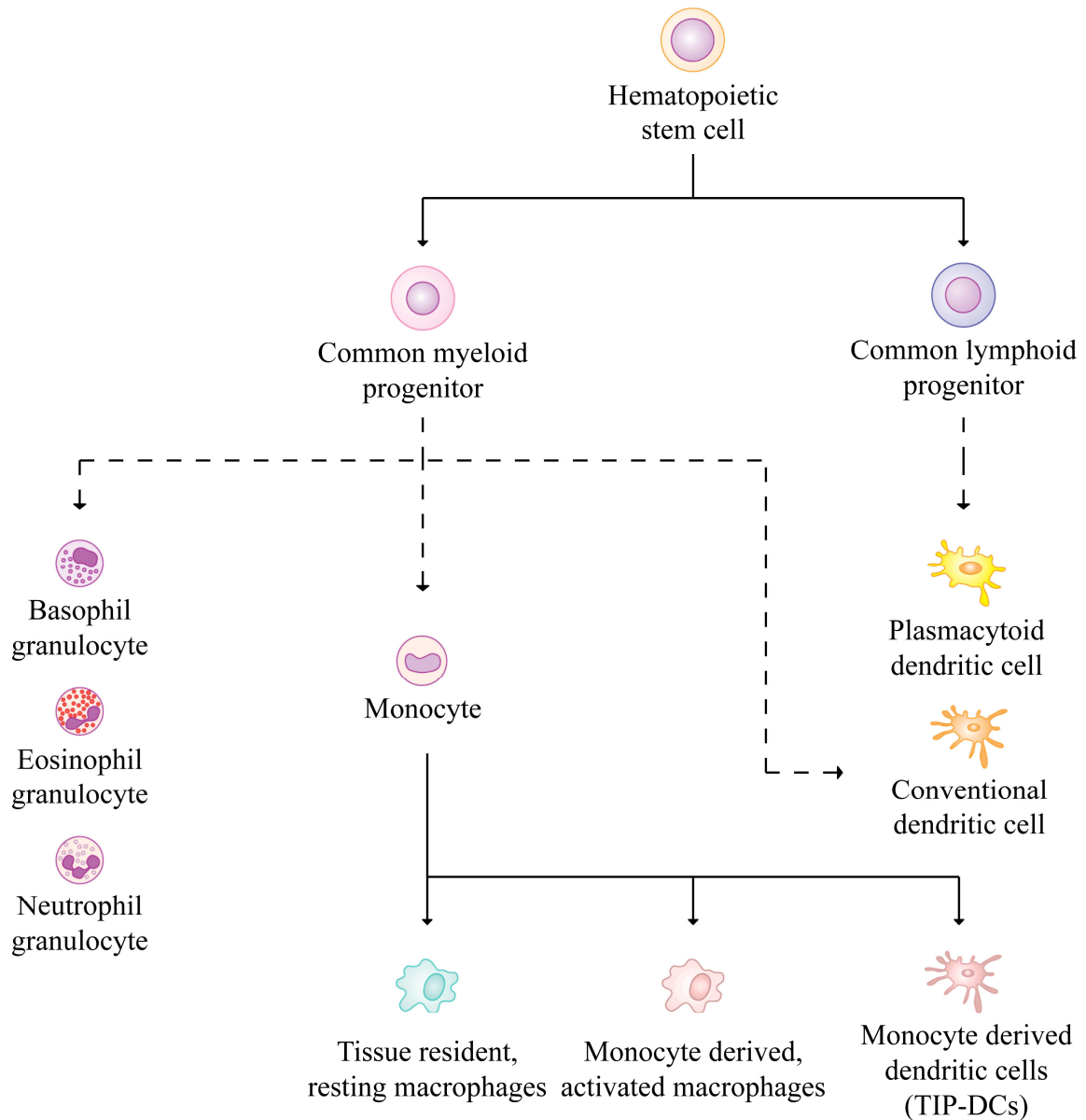


Figure 4. The ontogenesis of granulocytes, monocytes, macrophages and dendritic cells. Granulocytes, monocytes and conventional dendritic cells develop from the common myeloid progenitor cell through lineage committed precursors (not shown in this figure), and plasmacytoid dendritic cells differentiate from the common lymphoid progenitor. Monocytes migrate into the tissues, where they repopulate the pool of resident macrophages. When monocytes are recruited to sites of inflammation, they differentiate into monocyte derived cells with an activated phenotype. The figure was based on the handbook: Anna Erdei, *Immunológia (Medicina, 2012)*¹²¹.

Myeloid cells originate from the common myeloid progenitor (CMP) lineage of the hematopoietic stem cells in the bone marrow (Fig. 4). Granulocytes have three major populations that were first distinguished based on their histological staining: neutrophils, basophils and eosinophils. Basophil and eosinophil granulocytes comprise only a small percent of leukocytes in the blood and their best known functions are mediating allergic reactions and defence against parasites, respectively^{122,123}. Neutrophil granulocytes give 50-70% of circulating leukocytes and these cells are the first to migrate to the site of injury in large numbers. They bear numerous pattern recognition and phagocytic receptors, as well as granules containing proteases and anti-microbial peptides¹²⁴. Additionally, upon activation neutrophils can release a mixture of nuclear DNA and enzymes, called the neutrophil extracellular trap (NET)¹²⁵. Thus neutrophils quickly and effectively eliminate pathogens through phagocytosis and NET release.

In humans, monocytes are divided into 3 groups based on the expression of CD14 and CD16: classical (CD14⁺ CD16⁻), intermediate (CD14⁺ CD16⁺) and non-classical (CD14^{low} CD16⁺)¹²⁶. Classical monocytes stay in the circulation for one day after exiting the bone marrow, then migrate into tissues to repopulate the pool of resident macrophages¹²⁷. Recent fate mapping studies in mice revealed that only a small population of tissue resident macrophages differentiates from monocytes, but instead most subsets are embryonic in origin with the capacity for self-renewal¹²⁸. During inflammation, classical monocytes are quickly recruited to the site of injury, where they directly exert proinflammatory functions as “inflammatory monocytes” or differentiate into monocyte derived cells^{129,130}. These monocytes show great plasticity during maturation, the phenotype of monocyte derived macrophages and dendritic cells (or TIP-DCs) strongly depends on the tissue microenvironment^{131,132}. Non-classical monocytes comprise 10% of blood monocytes, and can also differentiate from classical monocytes, through the intermediate phenotype¹³³. These monocytes have a longer circulating time of approximately 7 days, during which they monitor the integrity of blood vessels via an LFA-1 mediated crawling on the endothelium^{134,135}. Non-classical monocytes were also associated with a proinflammatory phenotype, that could contribute to disease progression^{136,137}.

Specialized populations of resident macrophages can be found in most tissues over the body: alveolar macrophages in the lungs, microglia in the brain, osteoclasts in the bone, Kupffer cells in the liver, marginal zone and sinus macrophages in the lymphoid organs¹³⁸. Their characteristic gene expression profile and function is defined by the local microenvironment, which contributes to specific tissue homeostasis^{139,140}. The common

features of all macrophage subpopulation are the recognition and elimination of pathogens, the advancement of the immune response through cytokine secretion and antigen presentation and lastly, the promotion of tissue repair and regeneration. During immune surveillance, macrophages sense the possible danger signals in the environment, which induces their activation. The traditional classification of activated macrophages includes the classically activated M1 and the alternatively activated M2 macrophages. The M1 polarization is induced by IFN- γ , TNF- α or bacterial products, like lipopolysaccharide (LPS), resulting in a proinflammatory phenotype¹⁴¹. These macrophages secrete high levels of proinflammatory cytokines, reactive oxygen species, contributing to an effective pathogen elimination and consequent tissue damage¹⁴². The presence of IL-4, IL-13 or IL-10 cytokines supports the development of M2 macrophages, that is characterized by its anti-inflammatory properties. They produce IL-10 and TGF- β , phagocytose debris and apoptotic cells and help tissue regeneration^{143,144}. It is important to mention, that this strict dichotomy is the simplification of macrophage activation, that can vary on a wide spectrum depending on the activating stimulus and the microenvironment¹⁴⁵. Instead of using the terms M1 and M2 macrophages, researchers studying macrophage activation should always state the activating conditions in their experiments¹⁴⁶.

Dendritic cells are known for their importance as antigen presenting cells and in the initiation of adaptive immune responses. They can differentiate from both the common lymphoid (CLP) and myeloid (CMP) progenitor, giving rise to plasmacytoid (pDC) and conventional (cDC) dendritic cells, respectively. pDCs have a lower expression of costimulatory and MHCII molecules than cDCs and a limited potential to prime naïve T-cells^{147,148}. They secrete high amounts of type I interferons upon TLR7 and TLR9 ligation with nucleic acids, providing an effective immune defence against viral infections¹⁴⁹. Conventional dendritic cells reside in both lymphoid and non-lymphoid tissues in an immature state, where they continuously monitor their environment. They maintain tolerance by presenting self-antigens and initiate an immune response upon encountering foreign ones¹². Immature dendritic cells have a high phagocytic capacity to internalize pathogens, but the proteolytic degradation of antigens is more restricted than in macrophages. The lower concentration of lysosomal enzymes and a higher pH in the endosomes could contribute to the preservation of antigens for presentation¹⁵⁰. Dendritic cells migrate to the lymph nodes after antigen uptake, and during this journey they go through a maturation process¹⁵¹. Maturation induces functional changes including chemokine receptor and costimulatory molecule expression and the rearrangement of the

actin cytoskeleton. The chemokine receptor CCR7 is upregulated during maturation and migration to the T-cell area is directed by the stromal cell produced CCL19 and CCL21. Concomitantly, dendritic cells lose their capacity for phagocytosis and become potent activators of naïve T-cells.

Myeloid cells populate the possible entry points in the tissues and provide the first line of defence against invading pathogens. They are involved in the quick elimination of microbes and in the initiation and regulation of adaptive immune responses. Human myeloid cells express CR3 and CR4 in high numbers, which receptors are essential in these processes. Studying the role of these receptors could take us closer to understand these basic immune cell functions.

1.4.1. The role of CR3 and CR4 in adherence and podosome formation

CR3 and CR4 are known to mediate cell adhesion, spreading and migration through the establishment of cell-cell and cell-extracellular matrix connections³⁰. Most publications only discuss in detail the functions of LFA-1 and CR3, and the commonly used mouse models are either CD11b- or CD18-deficient^{152,153}. However, studies on human granulocytes and monocytes showed that LFA-1, CR3 and CR4 all contribute differently to endothelial adhesion^{154,155}. These studies also demonstrate that the cell type and the stimuli used can influence the participation of these receptors. Thacker and Retzinger showed, that human monocyte derived dendritic cells bind to fibrinogen, that stimulates the secretion of cytokines in a CD18-dependent manner, however they could not discriminate between the specific receptors¹⁵⁶. Georgakopoulos et al showed, that CR3 and CR4 contribute differently to adhesion on fibrinogen and their participation is dependent on the experimental conditions, namely the type of stimuli and culture conditions of human blood monocytes¹⁵⁷.

Immune cells of the monocytic lineage use specific adhesive structures for cell adhesion and migration, called podosomes. Podosomes are known to mediate short-lived adhesion spots that are formed and quickly remodelled during migration. Cell movement can be achieved with podosome disassembly at the uropod and formation at the leading edge¹⁵⁸. The first studies describing these structures showed an F-actin core and an adhesion ring surrounding it on the contact surface of adherent cells (Fig. 5)¹⁵⁹⁻¹⁶¹. High-resolution microscopy helped to understand the ultrastructure of podosomes, revealing that instead of a continuous ring, integrins are positioned in small islets around the core¹⁶². The core is built up from branched actin fibers, surrounded by unbranched antiparallel contractile filaments reaching the site of adhesion¹⁶³. This contractility contributes to the mechanosensory

function of podosomes in the detection of matrix rigidity¹⁶⁴. Additionally, individual podosomes are connected with each other through actomyosin filaments, regulating their distribution and synchronized function¹⁶⁵. These data suggest a complex network of adhesive structures that is achieved with the cooperation of individual podosomes and local actin polymerization.

The importance of β_2 -integrins in podosome formation and podosome mediated adhesion has been proven, but the individual role of these receptors had not been studied so far. Burns et al. found, that β_2 -integrins are specifically recruited to podosomes in human MDCCs on a fibronectin surface (a ligand for both β_1 - and β_2 -integrins), whereas β_1 -integrins show a disperse distribution¹⁶⁶. In a β_2 -integrin-null mouse model, Gawden-Bone et al. showed that in the absence of β_2 -integrins podosome assembly is disrupted¹⁶⁷. With the development of super-resolution techniques more and more podosome associated molecules are described. Studying the individual role of these proteins in detail, such as integrins, is indispensable for the understanding of podosome function.

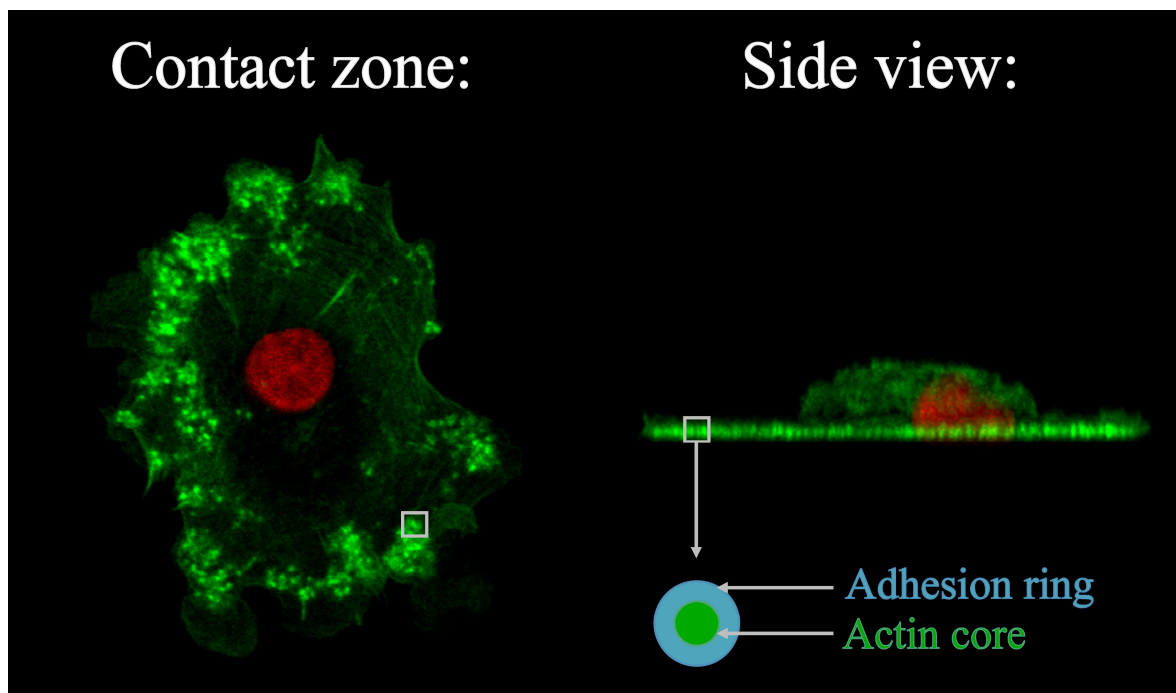


Figure 5. The structure of podosomes. Podosomes are found in the contact surface of adherent cells. These structures have an F-actin core surrounded by an adhesion ring, and can be visualized by staining the actin cytoskeleton with a fluorophore conjugated phalloidin probe (shown in green). Cell nuclei were stained with Draq5 DNA dye (in red).

1.4.2. *The role of CR3 and CR4 in phagocytosis*

Well accepted role of CR3 and CR4 are the phagocytosis of opsonized pathogens, tumour- and apoptotic cells. In the literature however, the participation of these receptors is not consistent. It seems to depend on the cell types and the experimental conditions applied in these experiments. The outcome is also affected by the microbe used to study phagocytosis, since some pathogens are able to utilize complement receptors for the infection of host cells^{168,169}, and CR3 and CR4 was shown to directly bind bacterial or viral components as well^{92,93}.

Experiments employing human monocytes proved a more prominent role for CR3 in the phagocytosis of opsonized *Mycobacterium leprae*¹⁷⁰, *Borrelia burgdorferi*¹⁷¹ and *Plasmodium falciparum* infected erythrocytes¹⁷², and no significant contribution of CR4 to the CR3 mediated uptake of *Mycobacterium tuberculosis*¹⁷³ and *Staphylococcus aureus*¹⁷⁴ was found.

Neutrophils also preferentially use CR3 over CR4 for serum-mediated phagocytosis of *Francisella tularensis*¹⁷⁵ and this receptor is also involved in the nonopsonic phagocytosis of *Salmonella enterica*¹⁷⁶ or *Mycobacterium kansasii*¹⁷⁷.

In the case of human macrophages, the role of CR3 and CR4 in phagocytosis could be influenced by the subset of these cell types and the invading pathogen they encounter. Both CR3 and CR4 were shown to be involved in the binding and/or phagocytosis of opsonised *Cryptococcus neoformans*¹⁷⁸, *Mycobacterium leprae*¹⁷⁹ and *Francisella tularensis*¹⁷⁵ by MDMs. However, in alveolar macrophages CR4 was shown to be the major receptor in the uptake of *Mycobacterium tuberculosis*¹⁷³.

1.5. The pathological implications of CR3 and CR4

Ailments caused by the deficiency of β_2 -integrins shed light on their importance in the resolution of infections. The absence or malfunction of these receptors have functional consequences, affecting both innate and adaptive immunity.

Leukocyte adhesion deficiency (LAD) is a rare autosomal recessive disorder first described almost 40 years ago. The symptoms for these patients are recurrent bacterial and fungal infections and impaired wound healing, as a consequence of reduced leukocyte adherence and recruitment¹⁸⁰. This deficiency has several types, with all forms of mutations affecting a step in the cell adhesion cascade¹⁸¹. LAD-I is caused by a variety of mutations in the ITGB2 gene, coding the β_2 -integrin subunit¹⁸². Patients having the mutated gene show reduced expression of all β_2 -integrins, including LFA-1, CR3 and CR4¹⁸⁰. The position of the mutation influences the severity of the disease, with moderately deficient cases expressing 5-10% of normal β_2 -integrin levels, and the more severe cases expressing less than 1%^{183,184}. Neutrophils and mononuclear cells from LAD-I patients fail to adhere and to migrate to the site of inflammation, and show defects in the phagocytosis of complement opsonized particles¹⁸⁴⁻¹⁸⁷. LAD-II is linked to the mutation of the Golgi-localised GDP-fucose transporter, important for the posttranslational fucosylation of selectin ligands¹⁸⁸. In the absence of functional selectin ligands, leukocytes fail to stick and roll on the blood vessels, a motion that initiates adhesion¹⁸⁵. LAD-III is caused by a mutation in the Kindlin-3 gene, which is crucial for the activation of β_1 -, β_2 - and β_3 -integrins. These receptors are expressed in normal levels on leukocytes and platelets of LAD-III patients, but they stay in an inactive state¹⁸⁹. Besides the symptoms caused by deficient adherence described in LAD-I, patients with LAD-III also show severe bleeding tendencies, as the aggregation of platelets is impaired without functional β_3 -integrins¹⁹⁰. A fourth type of adhesion deficiency (LAD-IV) was recently described in cystic fibrosis patients, affecting the chemotaxis and adhesion of monocytes, but not disrupting neutrophil functions. Mutations of the cystic fibrosis transmembrane conductance regulator (CFTR) gene seem to influence the RhoA and CDC42 dependent activation of β_1 -, β_2 -integrins in a monocyte specific manner, contributing to the pathogenesis of cystic fibrosis^{191,192}.

When talking about impaired immune cell motility and functions, the Wiskott–Aldrich Syndrome (WAS) should also be mentioned, that is an X-linked complex disorder caused by the lack of Wiskott–Aldrich Syndrome protein (WASP) expression. WASP is a regulator of actin polymerisation and its expression is restricted to the hematopoietic lineage¹⁹³. This disease is strongly linked to the defects of cytoskeletal reorganisation essential for immune

functions such as migration, antigen uptake and immunological synapse formation, thus effecting both innate and adaptive immunity¹⁹⁴. The lack of cell polarization and impaired chemotaxis was observed in human monocytes¹⁹⁵, PMNs¹⁹⁶, macrophages¹⁹⁷ and dendritic cells¹⁹⁸ of WAS patients. As the assembly and disassembly of podosomes is a dynamic process mediated by fast actin reorganisation, it is not surprising, that WASP is required for their formation in myeloid cells^{199,200}, and the integrins forming their adhesion rings also require a cytoskeletal connection²⁰¹. Podosome assembly^{199,200,202} and the clustering of β_2 -integrins^{166,196} are disrupted in PMNs, macrophages and dendritic cells of WAS patients and WASP-deficient mice²⁰².

CR3 was also shown to have a role in the pathogenesis of systemic lupus erythematosus (SLE). A single nucleotide polymorphism in the CD11b chain (rs1143679) is identified as a risk factor in SLE²⁰³. The rs1143679 SNP means an arginine to histidine change (R77H) in the CD11b molecule that was shown to cause functional changes. The expression of cell surface CD11b is not altered, and the receptor can undergo activation induced conformational changes^{204,205}. MacPherson et al. showed reduced iC3b mediated phagocytosis and severely compromised adhesion to ICAM-1, ICAM-2 and iC3b in cell lines transfected with the mutant genes²⁰⁴. Rhodes et al. observed reduced iC3b mediated phagocytosis and adhesion in monocytes and monocyte-derived macrophages of donors homozygous for this mutation, moreover the TLR inhibitory function of CR3 engagement also seemed to be compromised²⁰⁵. The impairment of iC3b mediated phagocytosis was also confirmed by Fossati-Jimack et al. on monocytes, macrophages and neutrophils, however they found no alterations in neutrophil adhesion and TLR mediated cytokine release by monocytes and dendritic cells²⁰⁶. Though these results might be controversial, it is evident, that this mutation effects CR3 mediated functions, which can be a result of the altered regulation of ligand binding under shear forces for the mutant receptor²⁰⁷.

These severe deficiencies are rare and hard to study, but underline the essential role of these adhesion related molecules. There are knock-out mice modelling these human syndromes, but the manifestations of these mutations are not always consistent with those observed in humans. Table 2. shows the main features of these deficiencies in humans, the comparison of human LAD cases and mouse models was reviewed in detail by Etzioni et al²⁰⁸.

	Mutation and phenotype	Defects in human blood cells
Leukocyte Adhesion Deficiency	recurrent infections, impaired wound healing without pus formation	
	LAD-I <i>β₂-integrin subunit (ITGB2 gene)</i>	impaired adhesion, leukocyte recruitment and phagocytosis ^{184–187}
	LAD-II <i>GDP-fucose transporter (SLC35C1)</i>	impaired leukocyte rolling on blood vessels ¹⁸⁵
	LAD-III <i>Kindlin-3</i> developmental defects severe bleeding	impaired adhesion and platelet aggregation ¹⁹⁰
	LAD-IV <i>CFTR</i> persistent lung inflammation	impaired adhesion and chemotaxis of monocytes, but not of PMNs ¹⁹¹
Wiskott-Aldrich Syndrome	<i>WASP</i> thrombocytopenia, eczema, immunodeficiency, autoimmunity and tumours	impaired cell polarization and chemotaxis ^{195–198} , disrupted podosome assembly ^{199,200,202}
SLE association	<i>CR3 (rs1143679)</i> autoimmunity	compromised adhesion and phagocytosis ^{204–206}

Table 2. The pathological conditions associated with CR3 and CR4

2. Aims

CR3 and CR4 are cell surface receptors involved in cell adherence, migration and phagocytosis, some of the most important functions of myeloid cells. The individual function of these receptors has not been studied in depth before partly due to technical difficulties.

Our aims were:

1. To differentiate the participation of CR3 and CR4 in:
 - a) cell adherence to a fibrinogen coated surface
 - b) podosome formation
 - c) migration
 - d) phagocytosis of iC3b opsonized *Staphylococcus aureus*
2. To compare these functions on human neutrophil granulocytes and monocytes isolated from the blood of healthy donors, and in vitro differentiated monocyte derived macrophages and dendritic cells.
3. To study these processes under both physiological and inflammatory conditions induced by bacterial lipopolysaccharide.

3. Materials and methods

3.1. Isolation of human monocytes and neutrophil granulocytes

Monocytes were isolated from buffy coat obtained from healthy donors and provided by the Hungarian National Blood Transfusion Service. Informed consent was provided for the use of blood samples according to the Helsinki Declaration. Peripheral blood mononuclear cells (PBMC) were separated by Ficoll-Paque PLUS (GE Healthcare Bio-Science, Uppsala, Sweden) density gradient centrifugation and monocytes were isolated negatively by using the Miltenyi Monocyte IsolationKit II (Miltenyi Biotech, Bergisch Gladbach, Germany). Purity of isolated monocytes was analysed by flow cytometry using anti-CD14 antibody (ImmunoTools GmbH, Friesoythe, Germany).

For the isolation of neutrophil granulocytes PBMC were removed by Ficoll-Paque PLUS density gradient centrifugation, then dextran sedimentation was performed using Dextran T-500 (Pharmacia Fine Chemicals, Uppsala, Sweden). Red blood cells were lysed in hypotonic buffer. Purity of isolated neutrophils was analysed by flow cytometry using anti-CD16 and anti-CD14 antibodies (ImmunoTools GmbH).

3.2. Generation of monocyte-derived macrophages (MDMs) and monocyte-derived dendritic cells (MDDCs)

To generate MDDCs and MDMs, monocytes were isolated with Miltenyi CD14 MicroBeads from PBMC. Cells were cultivated in RPMI-1640 Medium (Sigma-Aldrich Inc., St Louis, MO) supplemented with gentamicin (Sigma-Aldrich) and 10% FCS (Sigma-Aldrich). To generate MDMs 40 ng/ml rHu GM-CSF (R&D systems, Minneapolis, USA) was added to the isolated monocytes. To generate MDDCs 40 ng/ml rHu GM-CSF (R&D systems) and 15 ng/ml rHu IL-4 (R&D systems) were added to the monocytes. Cytokines were resupplied on day 3 of differentiation. Studies were carried out on day 5.

3.3. Blocking of CD11b/CD18 and CD11c/CD18 by antibodies

In blocking experiments the anti-CD11b (monoclonal mouse IgG1 clone TMG6-5, provided by István Andó at BRC Szeged, Hungary or monoclonal mIgG1 clone ICRF44, Biolegend, San Diego, CA, USA) or anti-CD11c antibody (monoclonal mouse IgG1 clone 3.9, Biolegend,) was used. These antibodies are specific for the ligand binding domain of the corresponding integrin and were used in sterile, azide-free form at saturating concentration previously titrated by flow cytometry. The effect of receptor specific

antibodies was compared to samples incubated with an isotype matched control antibody (mouse IgG1 clone MOPC-21, Biolegend). To exclude Fc-receptor mediated phagocytosis and the binding of the blocking monoclonal antibodies we used an Fc-receptor blocking reagent (Miltenyi Biotech) prior to the antibody treatment. Cells were incubated with the receptor-specific antibodies for 30min at 4°C then used in the functional studies without washing, since unblocked integrins are known to recycle to the cell surface from an intracellular pool²⁰, that would decrease the efficiency of receptor blocking.

3.4. RNA silencing in macrophages

RNA silencing was performed according to the method of Prechtel²⁰⁹. We used commercially available predesigned Qiagen (Germany) AllStar Negative control siRNA and Qiagen Genome Wide predesigned siRNA for CD11c (Hs_ITGAX_6) and CD11b (Hs_ITGAM_5). Cells were transfected on day 3 and day 5 of differentiation with 20µg siRNA to generate CD11b silenced, CD11c silenced or negative control silenced MDMs at day 6. The expression of CD11b and CD11c was analysed on day 6 by flow cytometry with anti-CD11b-FITC and anti-CD11c-APC (ImmunoTools GmbH). Subsequent experiments were carried out on the same day.

3.5. Induction of inflammatory condition using LPS treatment

MDMs and MDDCs were treated with 100 ng/ml bacterial lipopolysaccharide (LPS, Sigma-Aldrich) on the 5th day of differentiation to induce cell activation. Cells were cultured in 12-well cell culture plates at 10⁶ cells/ml with LPS or without LPS (untreated control) for different time periods.

3.6. Monitoring the expression of CD11b and CD11c during LPS induced activation

The expression of CD11b and CD11c was measured by flow cytometry at different time points during the LPS induced cell activation. LPS treated and untreated control cells were harvested after 30 minutes, 24 hours or 48 hours, and washed with ice cold PBS (phosphate buffered saline solution) supplemented with 0,4% sodium azide and 1% FCS. Cells were labelled with anti-CD11b-FITC and anti-CD11c-APC (ImmunoTools GmbH) for 20 minutes on ice. The expression of the receptors was compared to the appropriate untreated control sample at each time point. Samples were analysed on Cytoflex flow cytometer

(Beckman Coulter) using CytExpert software for data acquisition and Kaluza Analysis software for data analysis.

3.7. Analysis of β_2 -integrin conformational state

The conformation state of β_2 -integrins was determined using the activation epitope specific mouse monoclonal mAb24 antibody labelled with Alexa488 (BioLegend). 5×10^5 cells were resuspended in 400 μ l of RPMI-1640 medium and labelled with mAb24-Alexa488 antibody for 20 minutes on ice under sterile conditions. Without washing, the tubes were moved to a 37°C CO₂ incubator or left on ice (0-minute controls). To induce activation, 100 ng/ml LPS was added to the cells at the beginning of the 37°C incubation. After the incubation time cells were washed with ice cold PBS supplemented with 0,4% sodium azide and 1% FCS and put on ice immediately, to stop the receptor internalization. Samples were analysed on Cytoflex flow cytometer at 0 minutes and 30 minutes. Confocal microscopy images were prepared at 0, 5 and 30 minutes by Olympus IX81 confocal microscope (60x objective) and FluoView500 software.

3.8. Analysis of adhesion by confocal microscopy

The wells of a CELLview cell culture dish with glass bottom (Greiner Bio-One, Kremsmünster, Austria) were coated with 10 μ g/ml fibrinogen (Merck, Darmstadt, Germany) in PBS for 1 hour at 37°C. After that wells were washed 2 times with PBS and free surfaces were blocked with synthetic copolymer poly(L-lysine)-graft-poly(ethylene glycol) (PLL-g-PEG, SuSoS AG, Dübendorf, Switzerland) for 30min at RT. After washing the wells 2 times with PBS, 5×10^4 cells in RPMI1640-10% FCS were immediately transferred to the wells and let to adhere for 30min at 37°C in a CO₂ incubator. After the incubation samples were fixed with 2% paraformaldehyde (Sigma-Aldrich) for 10min and unbound cells were removed by washing 2 times with PBS. The number of adhered cells was determined by staining the nuclei with Draq5 (BioLegend) diluted 1:1000 (5 μ M) in PBS and incubated for 15min at RT. Samples were analysed by Olympus IX81 confocal microscope (10x objective) and FluoView500 software. 10 representative fields were scanned in each well, the number of adhered cells was determined by ImageJ software. To analyse the contact zone of the cells the actin cytoskeleton was stained with phalloidin-Alexa488 (Molecular Probes, Invitrogen, Eugene, Oregon, USA). The probe was 80x diluted in PBS-0,1% Triton-X (Sigma-Aldrich) and cells were stained for 15min at 37°C and after that washed 2 times with PBS. Samples were analysed by Olympus IX81 confocal

microscope (60x objective) and FluoView500 software. Pictures were further analysed by ImageJ software.

3.9. Analysis of adhesion with the computer-controlled micropipette

Single cell adhesion force was analysed with an imaging-based automated micropipette (Cell-Sorter) with the collaboration of Rita Ungai-Salánki, Barbara Francz, Tamás Gerecsei and Bálint Szabó in the Department of Biological Physics, Eötvös Loránd University as described previously^{210,211}. Briefly, Petri dishes were coated by 10µg/ml fibrinogen (Merck) in phosphate buffered saline solution (PBS) for 1 hour at 37°C. Dishes were washed 2 times with PBS and the surface was blocked with the synthetic copolymer poly(L-lysine)-graft-poly (ethylene glycol) (PLL-g-PEG, SuSoS AG) in order to inhibit non-specific cell adhesion for 30 min at RT. After washing the Petri dish again with PBS, $7,5 \times 10^4$ cells in RMPI-10% FCS were placed onto the coated surface. Cells were incubated for 30 minutes at 37°C in 5% CO₂ atmosphere. Cultures were washed 3–4 times with Hanks' Balanced Salt solution with sodium bicarbonate without phenol red buffer (HBSS, Sigma-Aldrich) to remove floating cells. Region of interest (ROI) of the Petri dish was scanned by a motorized microscope (Zeiss Axio Observer A1) equipped with a digital camera (Qimaging Retiga 1300 cooled CCD). Cells were automatically recognized by the CellSorter software. To minimize the duration of the measurement, the shortest path of the micropipette was calculated by software²¹². Individual cells were visited and probed by the glass micropipette. The micropipette with an aperture of 70µm approached the surface to a distance of 10µm. Vacuum was generated in a standard syringe connected to the micropipette via a high speed normally closed fluid valve. To probe cell adhesion the valve was opened for 20ms generating a precisely controlled fluid flow and corresponding hydrodynamic lifting force acting only on the targeted cell. The hydrodynamic lifting force was calculated by running computer simulation solving the Navier-Stokes equation in a geometry corresponding to the experimental setup²¹¹. After each cycle of the adhesion force measurement the ROI of the Petri dish was scanned again, and the vacuum was increased to the next level. The micropipette visited again each location determined after the initial scan. Suction force was increased as long as most of the cells were removed. We counted the number of cells in the images before and after each cycle of the adhesion force measurement and calculated the ratio of still adhering cells of the population placed onto the surface at the beginning of the experiment.

3.10. Analysis of adhesion by EPIC BT biosensor measurement

Adhesion kinetics were measured on the Corning EPIC biosensor in collaboration with Norbert Orgován and Róbert Horváth in the Institute of Technical Physics and Material Sciences (Nanobiosensorics “Lendület” Group) as described previously in details²¹³. Briefly, each well of a standard microtiter plate contains an optical grating at its bottom which permits the illuminating light to be incoupled in the waveguide. Light beams in the waveguide interfere with each other; destructive interference precludes wave guiding, while constructive interference leads to resonance and to the excitation of a guided light mode. The latter can be achieved only at a discrete illuminating wavelength, called resonant wavelength (λ). The guided light mode generates an exponentially decaying evanescent field in a 100–200nm thick layer over the sensor, which probes the local refractive index (RI) at this interface. Any process accompanied by RI-variations in this layer (bulk RI change, molecular adsorption, cell spreading, or dynamic redistribution in the cells) untunes the resonance by altering the phase-shift of the propagating light when it is reflected from the interface (leading to destructive interference at the original resonance wavelength). The primary output of the EPIC sensor is then the shift of the resonant wavelength, $\Delta\lambda$.

Wells were coated by 10 μ g/ml fibrinogen (Merck) in phosphate buffered saline for 1 hour at 37°C. After that wells were washed 3 times with PBS and free surfaces were blocked with synthetic copolymer poly(L-lysine)-graft-poly(ethylene glycol) (PLL-g-PEG, SuSoS AG) for 30min at RT. After washing 3 times with PBS, 2x10⁴ cells in RPMI-10% FCS were immediately transferred to the wells and the registration of the $\Delta\lambda$ was continuously monitored throughout the experiment (120 min).

3.11. Analysis of the contact surface by confocal microscopy

3.11.1. Generation of the adhesive surface and adherent cell layer

The wells of a CELLview cell culture dish with glass bottom (Greiner Bio-One) were coated with 10 μ g/ml fibrinogen (Merck) in phosphate buffered saline (PBS) solution for 1 h at 37 °C, free surfaces were blocked with synthetic copolymer poly(L-lysine)-graft-poly(ethylene glycol) (PLL-g-PEG, SuSoS AG) for 30 min at 37 °C. After washing, 10⁴ cells in RPMI1640 supplemented with 10% FCS were plated onto the adhesive surface. Cells were let to adhere for 60 min at 37 °C in a CO₂ incubator, then fixed with 2% paraformaldehyde for 10 min at 37 °C. Unbound cells were removed by washing two times with PBS.

3.11.2. Staining of the actin cytoskeleton and podosome counting.

To analyse the podosome formation on the contact zone the actin cytoskeleton of adhered cells was stained with phalloidin-Alexa488 (Molecular Probes) diluted 1:100 in PBS-0,1% Triton X-100 (Reanal, Budapest, Hungary) for 15 min, then washed 2 times with PBS. Nuclei were stained with Draq5 (BioLegend) diluted 1:1000 (5 μ M) in PBS for 15 min. Samples were analysed by an Olympus IX81 confocal microscope (60x objective) applying Fluowiev500 confocal workstation.

The number of podosomes was counted using the method described by Cervero et al.²¹⁴. Briefly, the podosome number and contact zone area of the cells was determined using ImageJ software. Podosome density was calculated as the number of podosomes per 100 μ m² cell covered area. Cells were analysed on 5 representative microscopy fields per sample.

3.11.3. Staining of CD11b/CD11c on adherent cells

Fixed samples were permeabilized with 0.1% Tween-20 (Reanal) in PBS for 20 min at 37 °C. The permeabilizing solution was replaced with a blocking solution: 0.2% gelatine (Merck) in 0.1% Tween-20 in PBS and incubated for 1 h at 37 °C. The antibodies were diluted in the blocking solution; primary antibodies were incubated overnight at 37 °C, then secondary antibodies for 2 h at 37 °C. Cells were washed with 0.1% Tween-20 in PBS 3 times for 5 min each before adding the secondary antibody. Antibodies used for staining: anti-CD11b (EP1345Y, Abcam, Cambridge, UK), anti-CD11c (EP1347Y, Abcam), goat anti-rabbit IgG-A647 (Molecular Probes). After the secondary antibody staining cells were washed 3 times for 5 min each with 0.1% Tween-20 in PBS. The actin cytoskeleton was stained with phalloidin-Alexa488 (Molecular Probes) 1:80 diluted in 0.1% Tween-20 PBS for 45 min at 37 °C. Samples were analysed by an Olympus IX81 confocal microscope (60x objective) applying Fluowiev500 confocal workstation.

3.12. Phagocytosis of *Staphylococcus aureus*

To test the phagocytic capacity of immune cells *Staphylococcus aureus* (Wood strain without protein A) BioParticles (Molecular Probes) conjugated with Alexa488 or pHrodo Green was used. *S. aureus* was opsonized with normal human serum for 1 h at 37 °C, then washed extensively and offered to the cells under different conditions. During opsonization, *S. aureus* activates the alternative pathway of the complement system, and iC3b, the main ligand of CR3 and CR4, is deposited on its surface^{215,216}. All reagents were diluted in Hank's Balanced Salt Solution (HBSS) buffer supplemented with 5% FCS and 5mM glutamine, pH

7.4. The cells were incubated with the blocking antibodies for 30 min on ice before the phagocytosis. Without a washing step *S.aureus* was offered to them at 200 µg/ml concentration for 90 min at 37 °C in a CO₂ incubator or on ice. 100 µl of bacteria suspension diluted to 400 µg/ml (containing 1.2×10⁷ *S. aureus* particles) were added to 100 µl volume of cell suspension (5×10⁵ cells), resulting in a 200 µg/ml final concentration. The ratio of cells to bacteria was 1:24. After 90 min, phagocytosis was stopped by washing the samples with ice cold PBS and placing the cells on ice. Samples were analysed immediately by flow cytometry using BD FACS Calibur flow cytometer and CellQuest software for data acquisition and FCS Express 3.0 software for data analysis.

3.13. Analysis of transmigration

Cell migration was analysed using 24 well Transwell plates (polycarbonate membrane with 5 µm pore, Corning, Corning, NY, USA). 10⁵ cells in 100 µl RPMI-1640 medium was plated in the upper chamber, and the lower chamber was filled with 600 µl of chemoattractant or medium (negative control). For the untreated cells 62.5 nM N-Formylmethionine-leucyl-phenylalanine (fMLP, Sigma-Aldrich) was used as a chemoattractant and the migration was stopped after 1 hour. For the LPS treated cells we used 200 ng/ml CCL19 (BioLegend), and the migration was stopped after 2 hours for MDDCs and 4 hours for MDMs. At the end of the incubation time, EDTA was pipetted to the lower chamber without removing the membrane at a final concentration of 12.5 mM. After 5 minutes at 37°C cells were resuspended from the lower chamber and the bottom of the membrane, placed on ice and measured immediately. The number of transmigrated cells was measured in a volume of 250 µl/sample by flow cytometry (Cytoflex, BC).

3.14. Statistics

Statistical tests were performed with GraphPad Prism 5 software, p<0,05 was considered significant.

4. Results I. The function of CR3 and CR4 under physiological conditions

A similar role is often assumed for CR3 and CR4, since they have an overlapping ligand binding specificity and high sequence homology in their extracellular domains⁴. In humans they are simultaneously expressed in all myeloid cells, whereas in mice CR4 is expressed constitutively only on DCs. The different expression pattern in mouse and human cells suggests a separation of functions. Their importance in host defence is underlined by pathological conditions affecting the function of these receptors, like leukocyte adhesion deficiency, that is characterized by serious and recurrent infections.

Our group set out to thoroughly investigate the individual role of CR3 and CR4 in human myeloid cells. The most studied functions of these receptors are cell adhesion, migration and phagocytosis. First, we studied their participation in these processes during physiological conditions, with myeloid cells isolated from the blood of healthy donors.

4.1. Adhesion to fibrinogen coated surfaces

We set out to study the participation of CR3 and CR4 in the adhesion of human monocytes, monocyte derived macrophages (MDMs) and dendritic cells (MDDCs). We used fibrinogen coating for the adhesion assay, because it is a specific ligand for CR3 and CR4 on these cells. The adhesive capacity of cells was assessed by fundamentally different approaches: a widely used classical adhesion assay and two state-of-the-art biophysical methods. The classical method consists of counting the number of cells attached to the fibrinogen coated surface, whereas with the biophysical methods we gain information about the quality of adherence. The computer controlled micropipette is capable of measuring the strength of adhesion and the optical waveguide biosensor records adhesion kinetics. The biophysical measurements were carried out with the help of our collaboration partners at the Institute of Technical Physics and Material Sciences (Róbert Horváth, Nanobiosensorics “Lendület” Group) and at the Department of Biological Physics, Eötvös Loránd University (Bálint Szabó).

4.1.1. The classical assay: CR4 dominates adhesion over CR3

To study the individual role of CR3 and CR4 we used ligand binding site specific monoclonal antibodies prior to the cell attachment. To exclude the Fc-receptor mediated binding of antibodies an Fc-receptor blocking reagent was used, and the effect of receptor specific antibodies was compared to samples incubated with an isotype matched control

antibody. In the classical adhesion assay the effect of receptor specific treatment was quantified as the number of adherent cells on the fibrinogen coated surface, data are shown as the percent of adherent cells compared to the isotype treated control. As shown in Figure 6. the blocking of CD11c significantly decreased the number of adherent cells in the case of monocytes and MDDCs, and slightly, but not significantly blocked the adherence of MDMs too. Blocking CD11b had no effect on the number of adhered cells in the case of MDMs and MDDCs, but it was slightly reduced for monocytes.

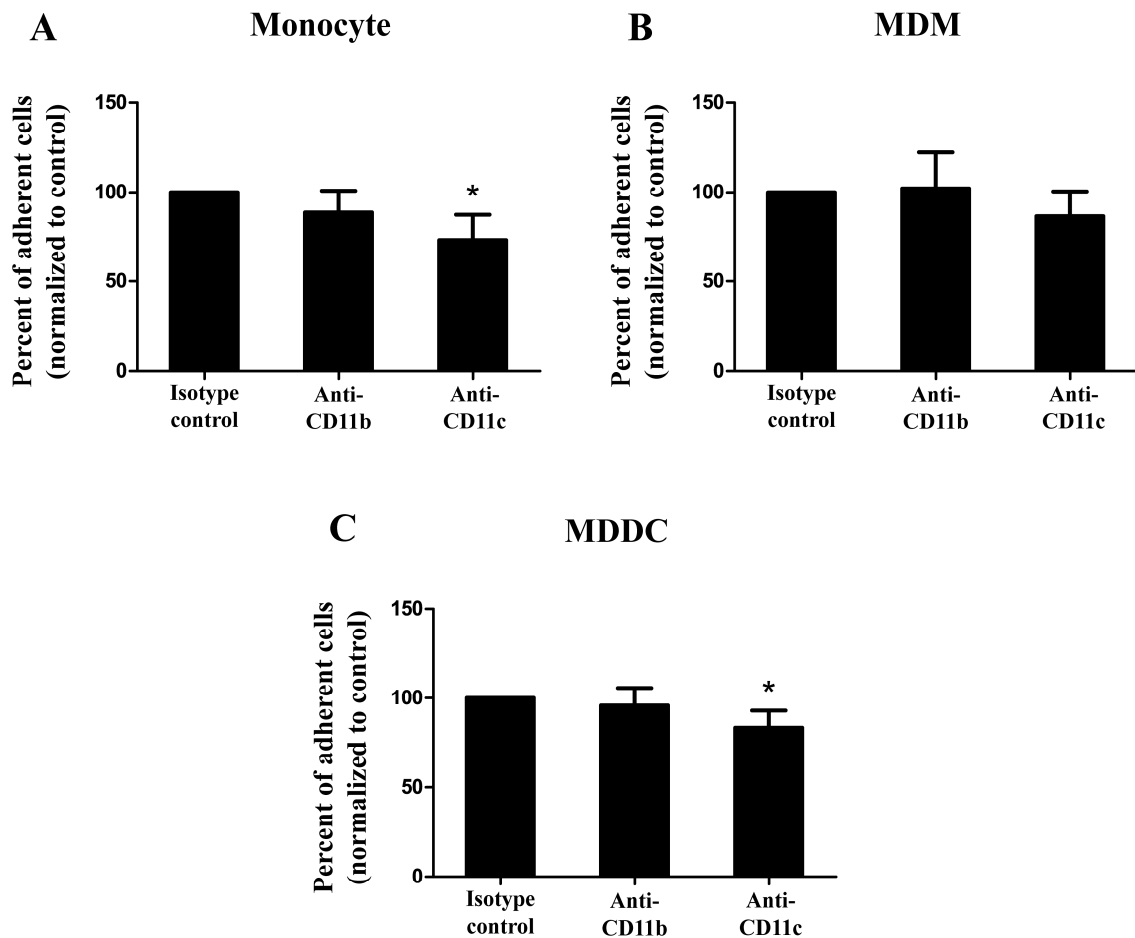


Figure 6. Number of adherent cells after blocking CD11b or CD11c with antibodies. Monocytes (A), MDMs (B) and MDDCs (C) were treated with ligand binding site specific monoclonal anti-CD11b or anti-CD11c or isotype control antibodies prior to the adhesion assay. Cells were let to adhere on a fibrinogen coated surface and unbound cells were washed away. Nuclei were stained with Draq5 DNA dye and counted with ImageJ software. The number of adhered cells was normalized to the isotype control antibody treated samples, shown as 100%. Results of 3 donors are shown as mean \pm SD. One-way ANOVA with Tukey's post-test was used to determine significant differences compared to control, $*=p < 0.05$.

Myeloid cells are known to spread on two-dimensional surfaces, creating a large contact area with the substrate. Since this process is regulated by integrin-ligand interactions and actin polymerization, we assessed the quality of adhesion by measuring the area of this contact surface. The actin filaments were stained with a phalloidin-Alexa488 probe and 420 nm optical sections of the contact zone were analysed by confocal microscopy. The blocking of CD11b resulted in a bigger contact area for MDMs (Fig. 7E) and a more polarized and slightly larger surface for MDDCs (Fig. 7H) and monocytes (Fig. 7B). In contrast, the blocking of CD11c decreased the size of the contact area for MDMs (Fig. 7F) drastically, but it did not affect the size of MDDCs (Fig. 7I) and monocytes (Fig. 7C).

To quantify these changes we measured the area of the contact zone based on the actin staining using ImageJ software. As shown in Figure 8 we established 3 size categories for the larger MDMs (Fig. 8A) and MDDCs (Fig. 8B) and 2 for the smaller monocytes (Fig. 8C) and determined their proportion in the population of adherent cells (Fig. 9). The calculated area data was consistent with the changes observed on the confocal microscopy pictures. Blocking CD11b with antibodies shifted the population towards cells with a large contact area on all three cell types and minimised the number of smaller area cells, showing that CD11b acts against spreading (Fig. 9). The blocking of CD11c decreased the spreading area of MDMs (Fig. 9B), resulting in the majority of small area cells, but it did not affect the area of monocytes (Fig. 9A) and MDDCs (Fig. 9C).

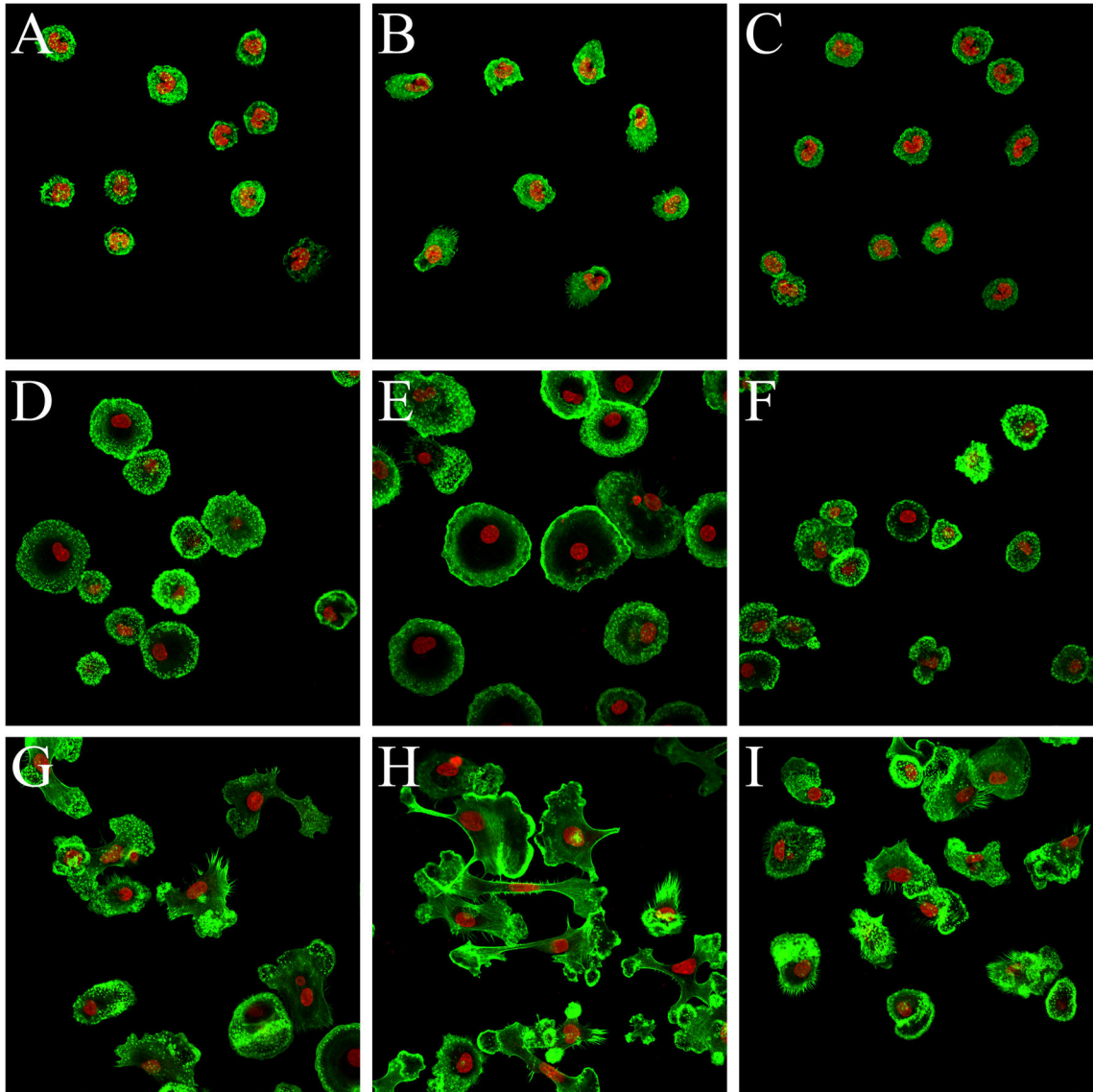


Figure 7. *The contact area of adherent cells after blocking CD11b or CD11c with antibodies. Monocytes (A-C), MDMs (D-F) and MDDCs (G-I) were treated with anti-CD11b (B,E,H), anti-CD11c (C,F,I) or isotype control (A,D,G) antibody, then plated on a fibrinogen coated surface. The actin cytoskeleton was stained with phalloidin-Alexa488 (shown in green), and nuclei were visualized with Draq5 DNA dye (in red). Confocal microscopy images of one representative out of 3 experiment are shown.*

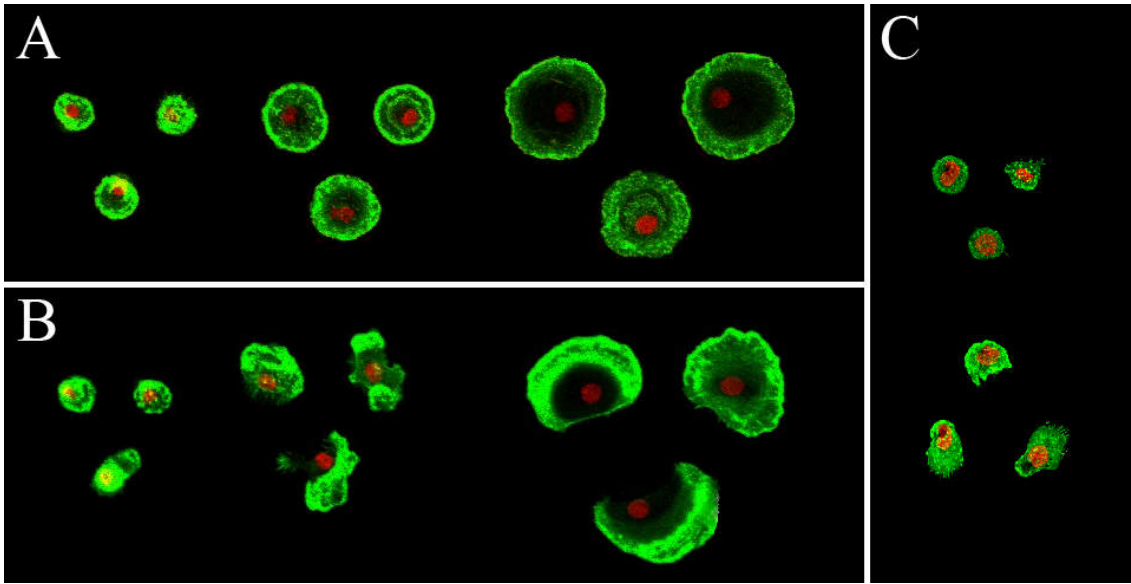


Figure 8. The contact area size categories of adherent cells. Adherent cells were divided into categories based on the size of their contact zones. MDMs (A) and MDDCs (B) were categorised into the following three groups: small (smaller than $800 \mu\text{m}^2$), medium (between $800\text{--}1600 \mu\text{m}^2$), large (bigger than $1600 \mu\text{m}^2$). For monocytes (C) the categories were small (smaller than $400 \mu\text{m}^2$) and large (bigger than $400 \mu\text{m}^2$).

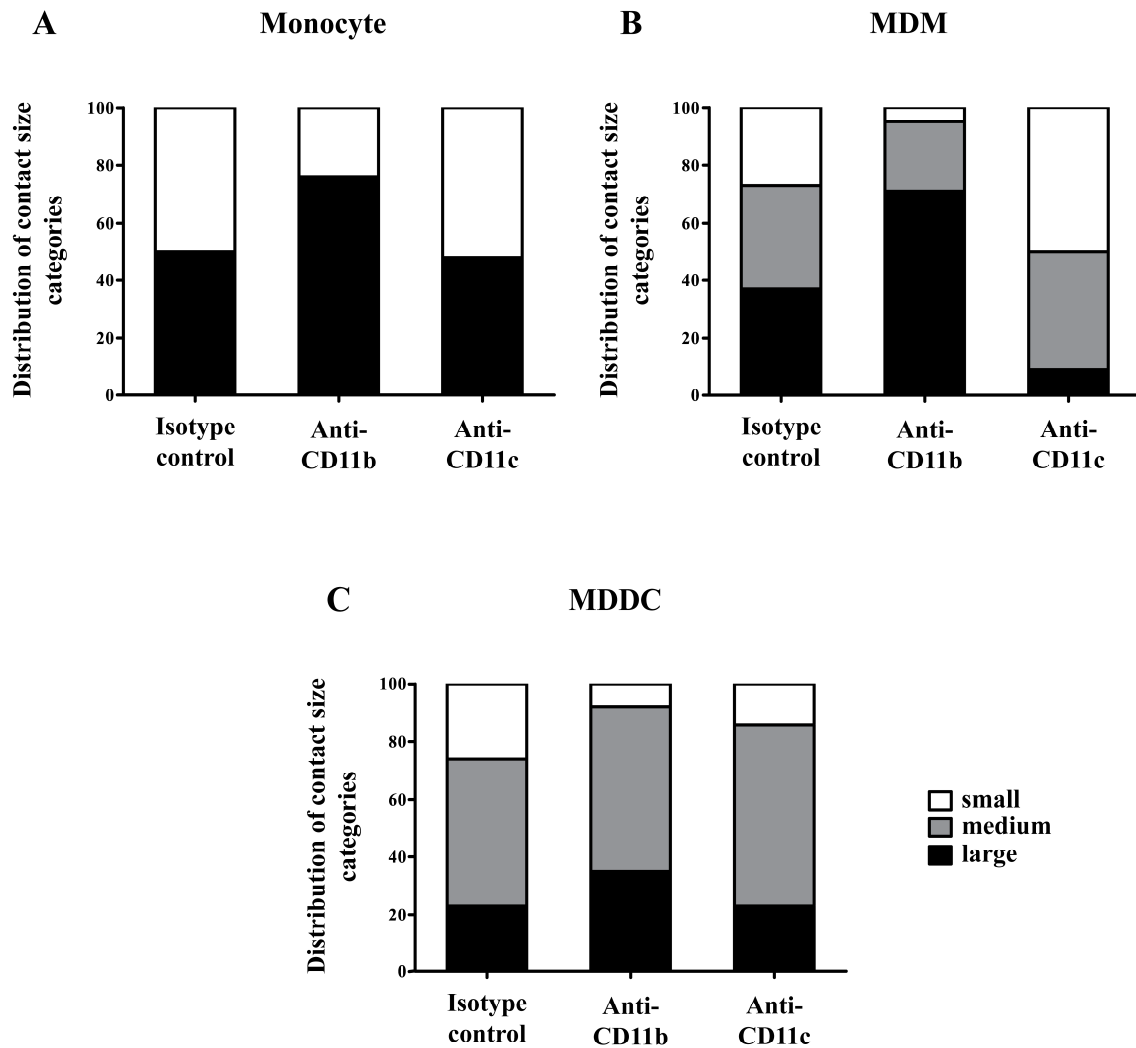


Figure 9. *The distribution of contact zone size categories after blocking CD11b or CD11c with antibodies.* Adherent cells were divided into categories based on the size of their contact zones. MDMs (B) and MDDCs (C) were categorised into the following three groups: small (smaller than $800 \mu\text{m}^2$), medium (between $800\text{--}1600 \mu\text{m}^2$), large (bigger than $1600 \mu\text{m}^2$). For monocytes (A) the categories were small (smaller than $400 \mu\text{m}^2$) and large (bigger than $400 \mu\text{m}^2$). The contact area was measured for 200 cells/sample, one representative is shown out of 3 independent experiments.

4.1.2. The computer controlled micropipette method: CR4 is important for a strong cell attachment

Cell adhesion to fibrinogen was also evaluated using the state-of-the-art biophysical method, namely the force of cell attachment was measured with a computer-controlled micropipette. Cells were let to adhere on a fibrinogen coated surface, and their adhesion force was assessed by trying to pick them up with the micropipette using vacuum induced fluid flow. The pick-up process was repeated several times with increased vacuum, and cells remaining on the surface were counted after each cycle. Applied vacuum was converted to force (μN) based on computer simulations. Cells were treated with ligand binding site specific or an isotype control antibody prior to adhesion, and data are presented as the percent of adhered cells compared to the control samples. In the case of monocytes (Fig. 10A), the force of adhesion decreased with both anti-CD11b and anti-CD11c treatment, that was also observed previously with the classical assay (Fig. 6A). For MDMs and MDDCs the blocking of CD11c decreased the strength of attachment, whereas blocking CD11b increased it (Fig. 10B-C). This opposing effect of the two receptors was also seen in our previous confocal microscopy experiment with the changes of contact area after antibody treatment (Fig 7).

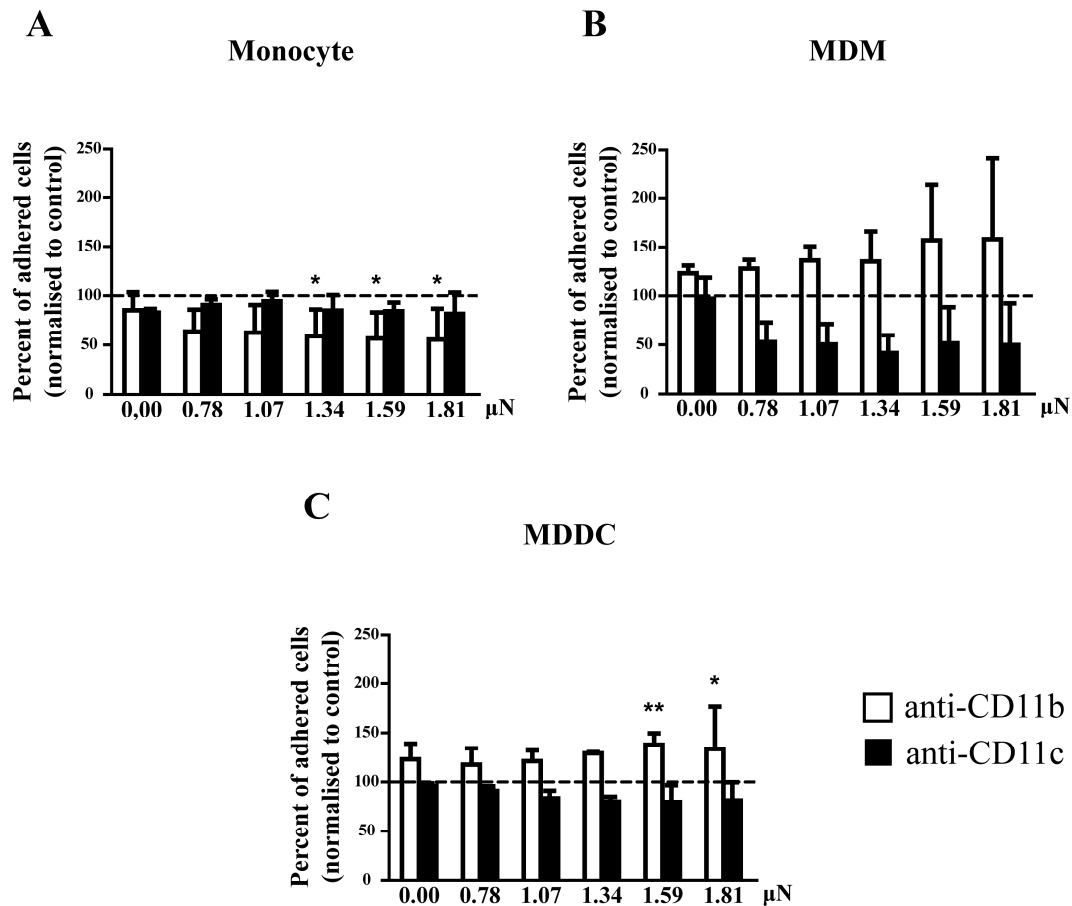


Figure 10. The force of cell adhesion after blocking CD11b or CD11c with antibodies. The force of adhesion was measured using a computer controlled micropipette by trying to pick cells up using vacuum induced fluid flow. This process was repeated several times with increasing amount of vacuum and the number of remaining cells was counted. Applied vacuum was converted to force (μN) based on computer simulations. Monocytes (A), MDMs (B), and MDDCs (C) were treated with monoclonal anti-CD11b or anti-CD11c antibodies prior to adhesion, and data are presented as the percent of adhered cells compared to the isotype control samples. Data presented are mean \pm SD of three independent donors' samples. Two-way ANOVA with Bonferroni post-test was used to determine significant differences compared to control at each force. * = $p < 0.05$; ** = $p < 0.01$.

4.1.3. Analysis of adhesion kinetics using the optical waveguide biosensor: CR4 dominates adhesion over CR3

The second biophysical method we used to study the kinetics of adhesion was the EPIC label free optical waveguide biosensor. This method enables the real-time monitoring of a 100–200 nm width layer over the adhesive surface by analysing the refractive index alterations, detected as the shift of resonant wavelength ($\Delta\lambda$). This volume is only accessible for actively adhering and spread-out cells, thereby non adherent cells are excluded from the measurement. The wavelength shift is proportional with the coverage of the sensor, meaning that we detect a combined signal of the number of the adhered cells and the size and density of their contact area^{213,217}.

Since this is a very sensitive label free method, instead of antibodies we used RNA silencing to study the participation of CR3 and CR4. We used MDMs, where the expression of CD11b or CD11c was downregulated using siRNA. For control, cells were transfected with negative control siRNA. The cell surface expression of CR3 and CR4 was verified using flow cytometry (Fig. 11A-B). To validate our data obtained from siRNA treated cells, we measured the force of adhesion with the micropipette as we have done previously (Fig. 11C). The siRNA silencing resulted in similar changes in the adhesive capacity of MDMs as the receptor blocking with antibodies, confirming the efficiency of this method.

One representative graph of the adhesion kinetics of CD11b or CD11c silenced MDMs is shown on Figure 12A. The downregulation of CD11b resulted in a higher wavelength shift, whereas the silencing of CD11c decreased the detected signal in comparison to the control siRNA treated cells. To compare this with the previous measurements we determined the $\Delta\lambda$ value at the timepoint (30 minutes) we used for the classical and micropipette adhesion assays (Fig. 12B). The adhesive capacity of CD11c siRNA treated MDMs significantly decreased at 30 minutes of adhesion, while it was slightly elevated in the case of CD11b siRNA treatment.

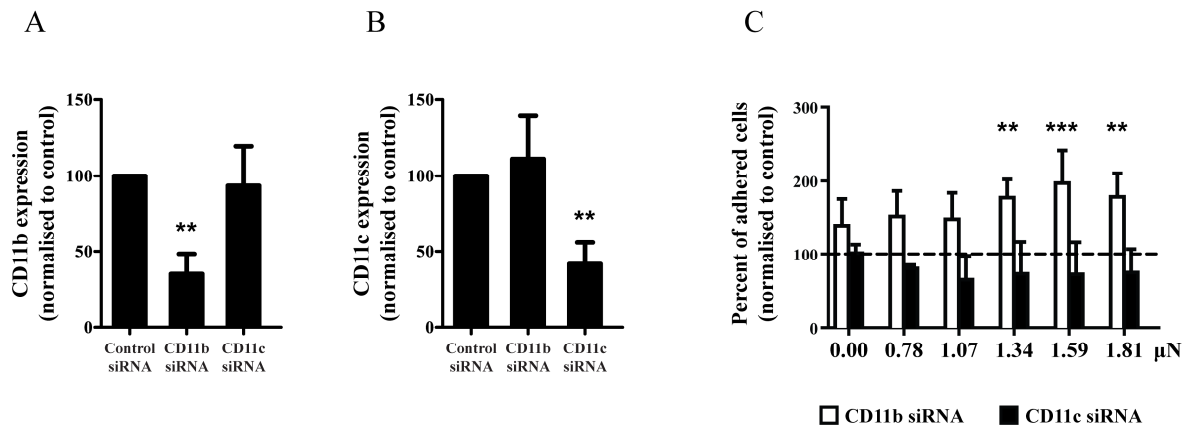


Figure 11. The downregulation of CD11b and CD11c expression with siRNA silencing MDMs were differentiated under conditions where CD11b or CD11c expression was downregulated by receptor specific siRNA. Control cells were treated with negative control siRNA. The expression of CD11b (A) and CD11c (B) was analysed by flow cytometry prior to the functional assays. Data of 4 experiments are presented as the percent of cell surface expression compared to the control siRNA treated samples (mean \pm SD). One-way ANOVA with Tukey's post-test was used to determine significant differences compared to control, **= $p < 0.01$. (C) To validate this method the force of adhesion was measured with the micropipette. Data of 3 experiments are presented as the percent of adhered cells compared to the control siRNA treated samples (mean \pm SD). Two-way ANOVA with Bonferroni post-test was used to determine significant differences compared to control, **= $p < 0.01$; ***= $p < 0.001$.

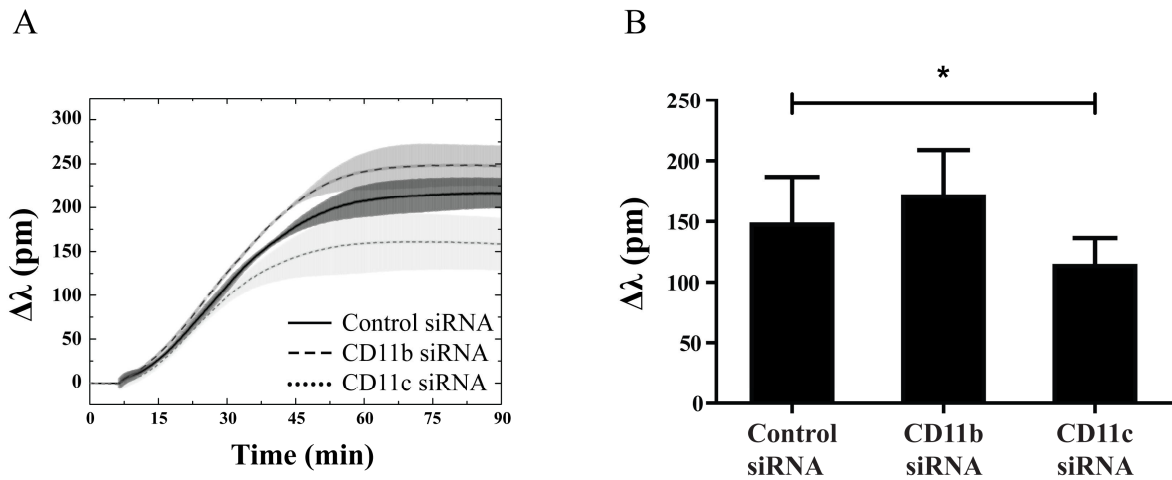


Figure 12. Adhesion of RNA silenced macrophages. (A) Kinetic curves of adhering MDMs was recorded by EPIC optical biosensor. The shift in detected wavelength ($\Delta\lambda$) is plotted against time in the case of CD11b (dashed line), CD11c (dotted line) or negative control (black line) siRNA silenced cells. The shaded area around each line shows the deviation between the parallel samples. One representative measurement out of three is shown. (B) The wavelength shift values ($\Delta\lambda$) were determined at 30 minutes of adhesion, data are shown as mean \pm SD of three independent measurements. Paired t-test was used to determine significant differences compared to control siRNA treated samples, $*=p<0.05$.

4.2. Migration

4.2.1. Both CR3 and CR4 participate in the migration of MDMs and MDDCs

MDMs and immature MDDCs are known to migrate towards N-formylated peptides as they express formyl peptide receptors (FPRs). As a synthetic ligand N-Formylmethionyl-leucyl-phenylalanine (fMLP) was used, which acts similarly on FPRs as the natural ligands. The migration capacity of MDMs and MDDCs was tested using a transwell assay with a 5 μm pore size polycarbonate membrane. To study the involvement of CD11b and CD11c, ligand binding site specific antibodies were employed, and the number of transmigrated cells were counted by flow cytometry. As shown in (Fig. 13) both anti-CD11b and anti-CD11c reduced the number of cells able to migrate through the membrane. For MDMs the blocking of CR3 resulted in a significantly stronger inhibition than the blocking of CR4, while in the case of MDDCs the extent of inhibition was the same for both receptors.

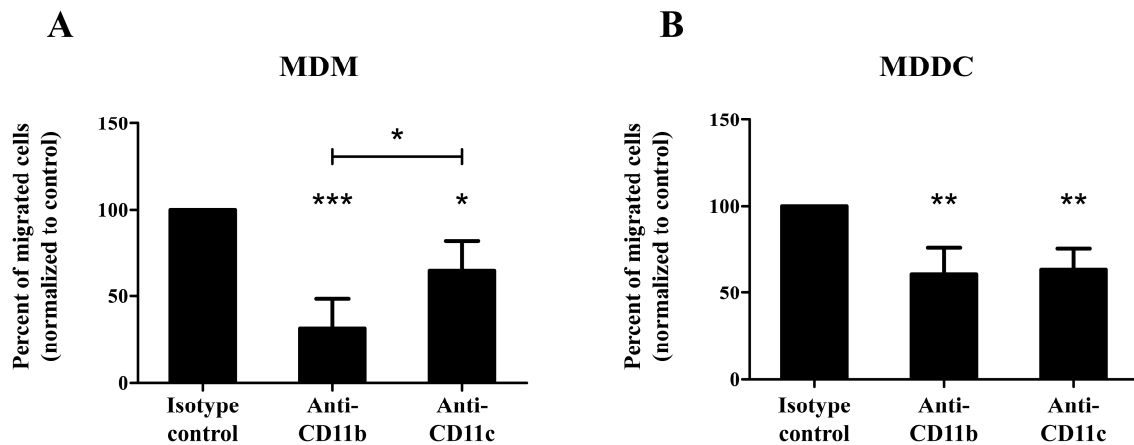


Figure 13. Analysis of migration on MDMs and MDDCs using fMLP as a chemoattractant. MDMs (A) and MDDCs (B) were treated with either anti-CD11b or anti-CD11c ligand binding site specific antibodies before migration, and the number of transmigrated cells were counted by flow cytometry after detachment using EDTA. The number of migrated cells was normalized to the isotype control antibody treated samples, shown as 100%. Results of 4 donors are shown as mean \pm SD. One-way ANOVA with Tukey's post-test was used to determine significant differences compared to control, $*=p < 0.05$; $**=p < 0.01$, $***=p < 0.001$.

4.3. Adhesive structures of human phagocytes – podosomes

Podosomes are adhesive structures known to mediate short-lived adhesion spots that are formed and quickly remodelled during migration. Considering their importance in cell attachment and movement, we set out to study their formation and patterns on various cell types.

4.3.1. Podosome patterns

Podosomes can be examined by confocal microscopy after staining the actin cytoskeleton with phalloidin-Alexa488 (Fig. 14). The actin core of these structures appears as a small, strongly fluorescent dot on the contact surface of cells. We found characteristic podosome patterns in the case of various human phagocytes. Smaller monocytes (Fig. 14A) displayed an even distribution across the substrate contacting surface. The podosomes of MDMs (Fig. 14B) showed either a similar distribution, or a belt like pattern. In MDDCs however (Fig. 14C) podosomes are arranged in clusters or accumulate in the leading edge of polarized cells. Neutrophil granulocytes (Fig. 14D) also have an even distribution of actin cores.

4.3.2. Localization of CD11b and CD11c on the contact surface of adherent cells

The actin core of podosomes is surrounded by cytoskeleton associated proteins and adhesion molecules, such as integrins. The importance of β_2 -integrins in podosome formation and podosome mediated adhesion has been proven, but the individual role of these receptors had not been investigated so far. We studied the localization of CD11b and CD11c in the contact zone of MDMs and MDDCs adhered to a fibrinogen coated surface. The podosome actin cores were visualized using phalloidin-Alexa488 staining (Fig. 15A,D,G,J). Confocal microscopy analysis revealed the presence of both CD11b (Fig. 15C,I) and CD11c (Fig. 15F,L) in the podosome adhesion ring on the contact surface of both cell types. The immunocytochemical staining of CD11b and CD11c showed a wider localization than actin (Fig. 15B,E,H,K), which is in correspondence with data showing an adhesion ring around the core of podosomes^{160,218}.

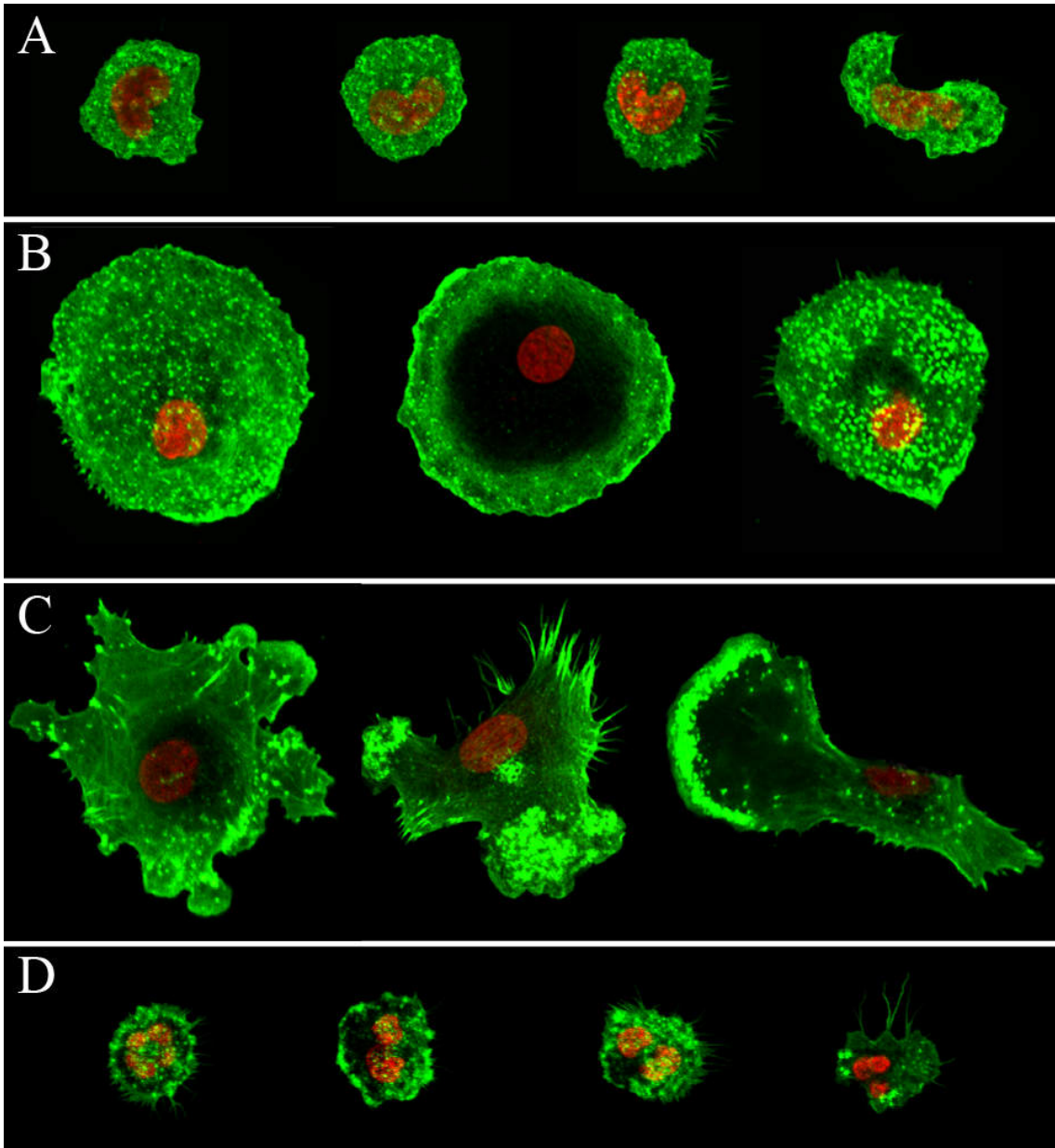


Figure 14. *Podosome patterns of human phagocytes attached to fibrinogen. Different podosome formation can be observed in the case of human monocytes (A), MDMs (B), MDDCs (C) and neutrophil granulocytes (D). Cells were let to adhere for 30 minutes on a fibrinogen coated surface, fixed with paraformaldehyde and unbound cells were washed away. The actin cytoskeleton was stained with phalloidin-Alexa488 (shown in green), nuclei were stained with Draq5 (shown in red). Representative confocal microscopy images were chosen from 3 independent experiments.*

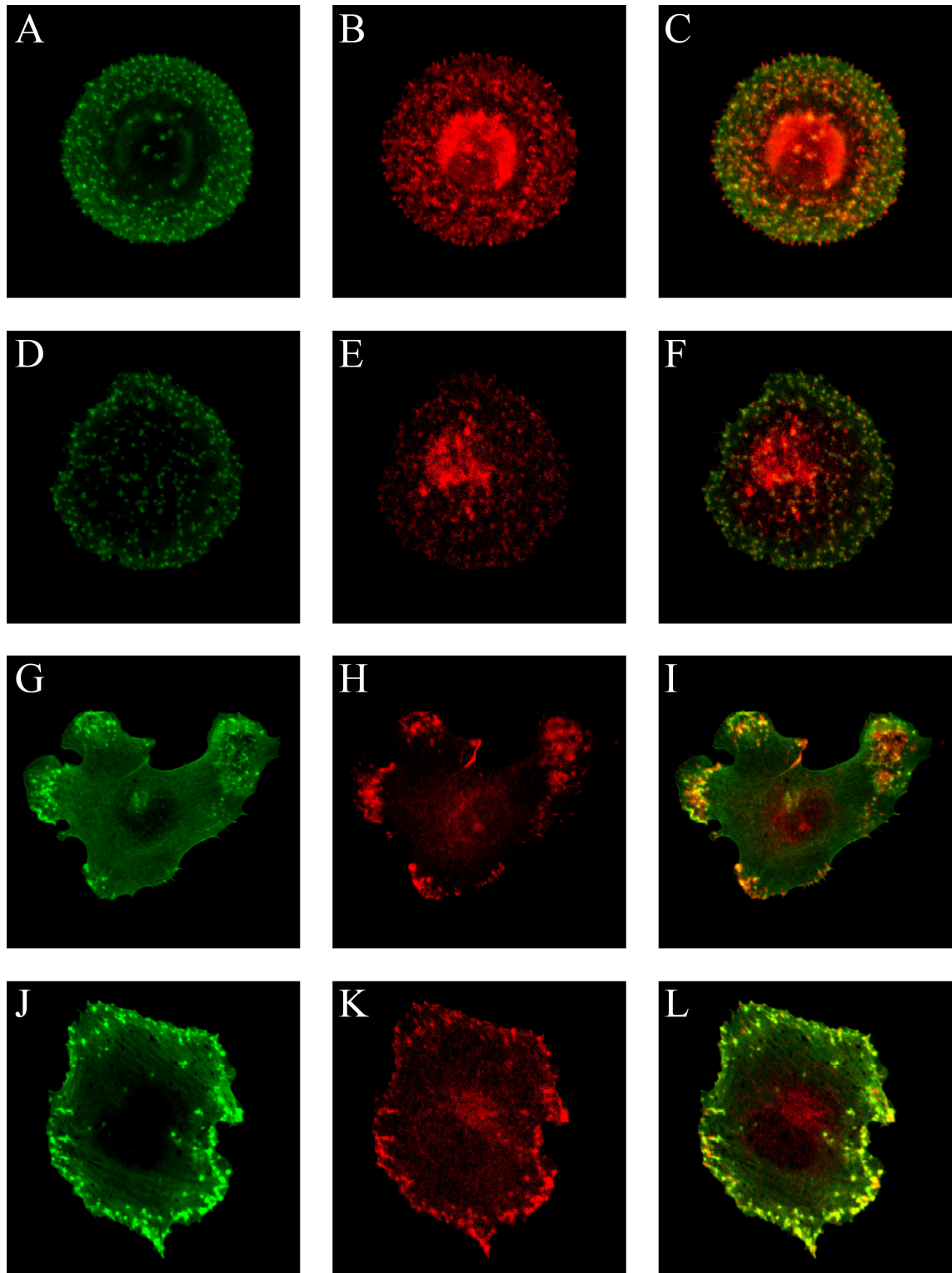


Figure 15. Localization of CD11b and CD11c on the contact surface of human myeloid cells. MDMs (A-F) and MDCCs (G-L) were plated to a fibrinogen coated surface, followed by staining with phalloidin-Alexa488 (A,D,G,J), anti-CD11b (B,H) or anti-CD11c (E,K). Merged images are shown in C,F,I,L. CD11b and CD11c are located around the actin core of podosomes in both cell types. Confocal microscopy images of one representative experiment out of 3 are shown.

4.4. Phagocytosis of iC3b opsonized *Staphylococcus aureus*

One of the most studied functions of CR3 and CR4 are the phagocytosis of complement opsonized microbes. As a model for our experiments we used *Staphylococcus aureus*, an opportunistic pathogen, that is able to inflict skin or respiratory infections²¹⁹. *S. aureus* activates the alternative pathway of the complement system, and iC3b, the main ligand of CR3 and CR4, is deposited on its surface^{215,216}.

4.4.1. Comparing differently labelled S. aureus particles

The phagocytic capacity of monocytes, MDMs, MDDCs and neutrophils was measured using iC3b opsonized *Staphylococcus aureus* conjugated with Alexa488 or pHrodo Green dye. Using bacteria labelled with Alexa488 both surface bound and internalized particles can be detected, while employing the pH sensitive pHrodo Green dye, bacteria are only visible when they reach the acidic milieu of phagolysosomes on the degradative pathway. Representative histograms demonstrating the differences in the detection of bacteria populations are shown in Figure 16 for MDMs (Fig. 16A,B) and MDDCs (Fig. 16C,D). The most prominent difference between the two dyes is revealed when cells are kept on ice (Fig. 16A-D dashed histograms), when the internalization of surface bound particles can not take place. Under these circumstances bacteria labelled with Alexa488 will be detected by flow cytometry although they are only bound on the cell surface. Using this method of labelling the amount of surface bound and internalized bacteria can not be distinguished under physiological conditions, where cells are kept at 37°C in CO₂ incubator during phagocytosis (Fig. 16A,C, solid black histograms). The discrimination of phagocytosed bacteria destined for degradation is only possible with the pH sensitive pHrodo Green dye, where surface bound particles are not detected (Fig. 16B,D). We will refer to these bacteria populations according to the method of their detection: “bound and internalized” for Alexa488 and “digested” for pHrodo Green labelled *S. aureus*.

Comparing the activity of MDMs and MDDCs we found a significant difference in the amount of phagocytosed bacteria measured by Alexa488 (Fig. 16E) and pHrodo Green (Fig. 16F) conjugated *S. aureus*. The lower phagocytic capacity of MDDCs is in agreement with their major role in antigen presentation¹⁵⁰.

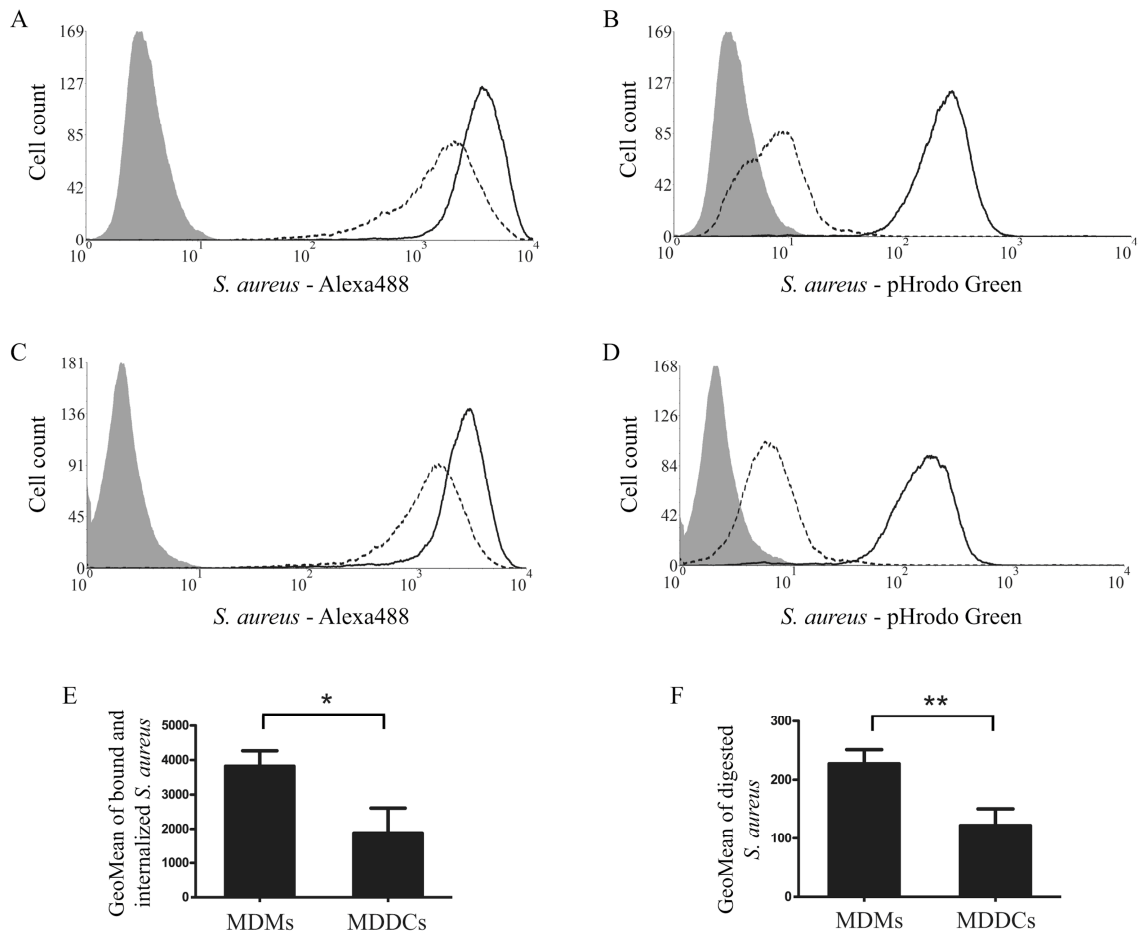


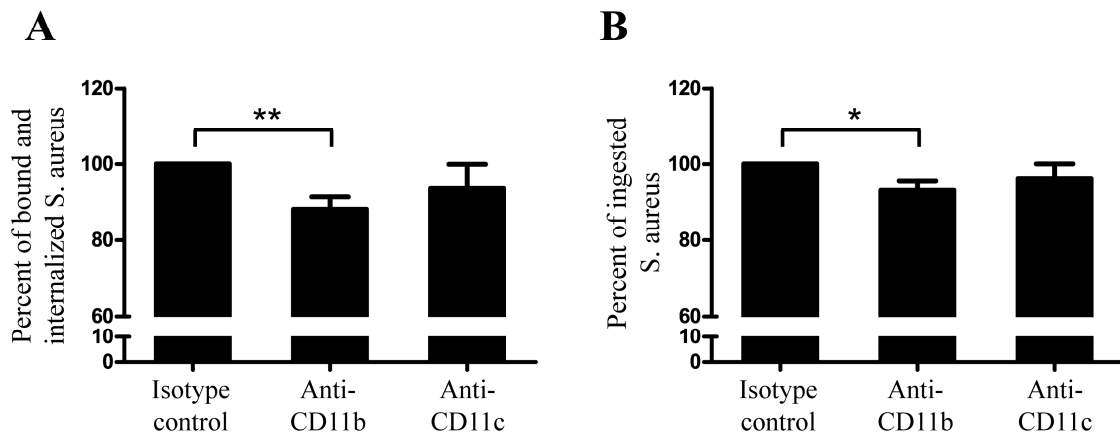
Figure 16. Fluorescence intensity of bound/internalized and digested bacteria by MDMs and MDDCs. Panel A, C and E: results obtained employing *S. aureus* conjugated with Alexa488; panel B, D and F: results obtained with *S. aureus* conjugated with pHrodo Green dye. Representative histograms were chosen of MDMs (6 (A) and 4 (B) independent experiments) and MDDCs (3 (C) and 6 (D) independent experiments). Histograms: grey background: autofluorescence; dashed line: cells were kept on ice; black line: cells were kept at 37°C in CO₂ incubator during phagocytosis. Graphs E and F show the geometric mean fluorescence intensity of bound/internalized and digested *S. aureus* by MDMs and MDDCs, respectively. Mean \pm SD of 3 independent experiments are shown. Unpaired t-test was used to determine significant differences, * = $p < 0.05$; ** = $p < 0.01$.

4.4.2. *The role of CR3 and CR4 in the phagocytosis of iC3b opsonized Staphylococcus aureus*

To determine the participation of CR3 and CR4 in the uptake of opsonized particles, cells were treated with ligand binding site specific blocking antibodies before and during the incubation with the bacteria. The phagocytosis assay was carried out using iC3b opsonized *S. aureus*. In the presence of the CD11b specific antibody monocytes and MDMs showed decreased phagocytosis when employing Alexa488 or PHrodo Green labelled bacteria (Fig. 17). However, when macrophages were treated with the CD11c specific antibody, a significant reduction in the binding of Alexa488 conjugated *S. aureus* (Fig. 17C) could be observed. This blocking effect however was not present when pHrodo Green *S. aureus* was used (Fig. 17D). These findings demonstrate that CD11c participates in the binding of iC3b opsonized *S. aureus*, while further steps leading to the digestion of the coccus are mediated by CD11b in macrophages.

Blocking of CR3 on MDDCs inhibited the phagocytosis of both Alexa488 (Fig. 18A) and pHrodo Green (Fig. 18B) conjugated bacteria, whereas inhibiting CD11c had no effect. Experiments with neutrophil granulocytes (Fig. 18C-D) showed similar results, namely, blocking of CD11b caused a decrease in phagocytosis.

Monocytes



MDMs

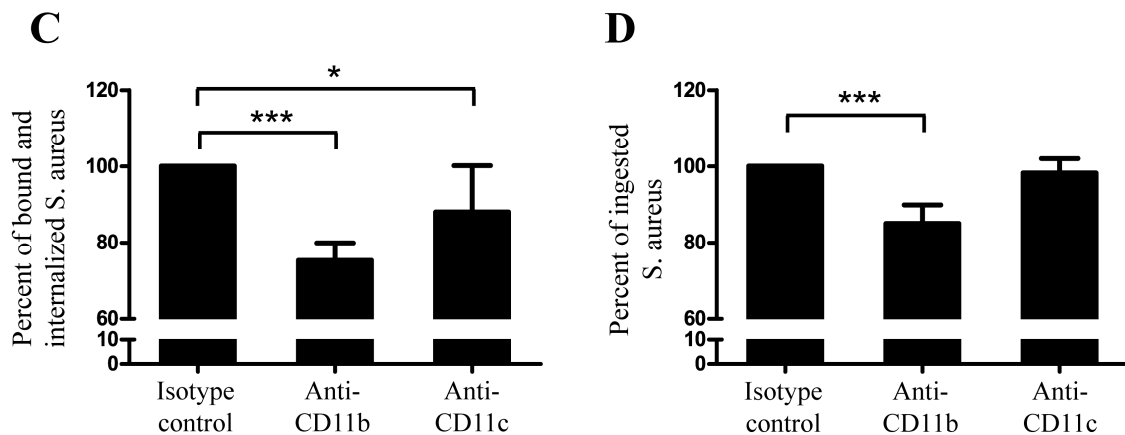
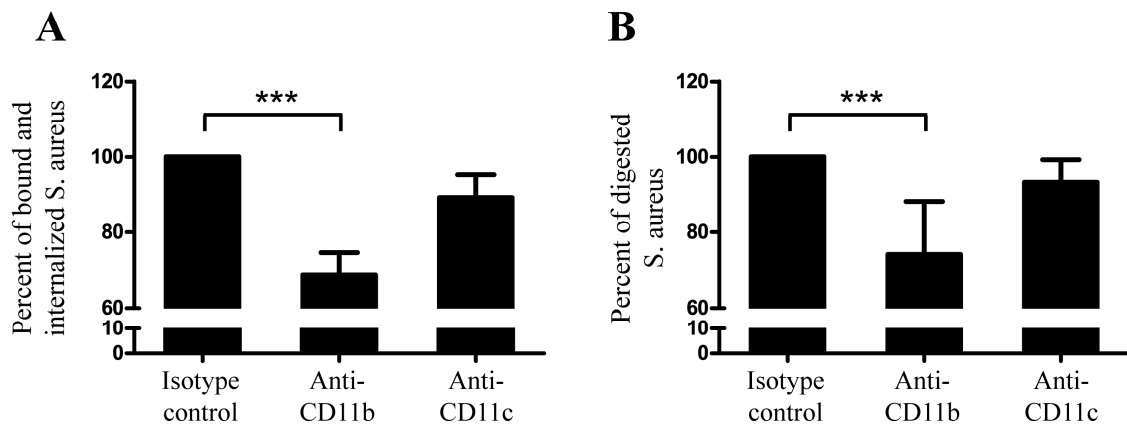


Figure 17. Phagocytic capacity of monocytes and MDMs after blocking CD11b or CD11c with ligand-binding site specific antibodies. Using bacteria labelled with Alexa488 (A and C) both surface bound and internalized particles are detected. With the pH sensitive pHrodo Green dye (B and D) bacteria are only visible when they reach the acidic phagolysosomes. The amount of bound/internalized, vs. digested fluorescently labelled bacteria was measured by flow cytometry. The effect of antibody treatment was compared to isotype control samples, shown as 100%. For monocytes (A and B) results of 4 donors are shown, mean \pm SD, for MDMs (C and D) 6 (C) and 4 (D) donors' results (mean \pm SD) are shown. One way ANOVA with Tukey's post-test was used to determine significant differences compared to control, * = $p < 0.05$; ** = $p < 0.01$; *** = $p < 0.001$.

MDDCs



Neutrophil granulocytes

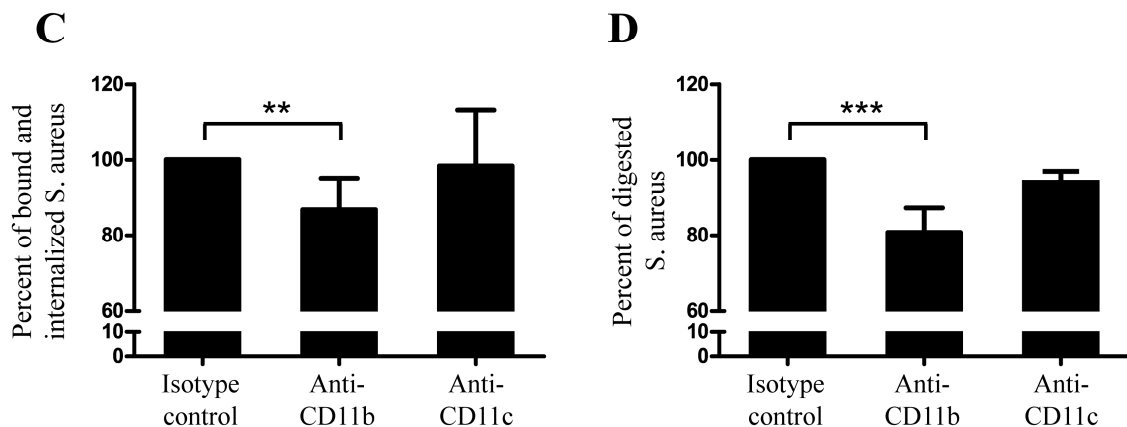


Figure 18. Phagocytic capacity of MDDCs and neutrophil granulocytes after blocking CD11b or CD11c with ligand-binding site specific antibodies. Using bacteria labelled with Alexa488 (A and C) both surface bound and internalized particles are detected. With the pH sensitive pHrodo Green dye (B and D) bacteria are only visible when they reach the acidic phagolysosomes. The amount of bound/internalized vs. digested fluorescently labelled bacteria was measured by flow cytometry. The effect of antibody treatment was compared to isotype control samples, shown as 100%. For MDDCs (A and B) results of 3 (A) and 6 (B) independent donors (mean \pm SD) are shown, for neutrophil granulocytes (C and D) 14 (C) and 4 (D) independent donors' results (mean \pm SD) are shown. One way ANOVA with Tukey's post-test was used to determine significant differences compared to control, **= $p < 0.01$; ***= $p < 0.001$

5. Results II. The function of CR3 and CR4 under inflammatory conditions

The initial phase of an immune response after tissue injury or infection is the recruitment of immune cells and the establishment of an inflammatory environment. The subsequent activation of leukocytes alters their functions and the expression of receptors, costimulatory molecules and cytokines. Additionally, many pathological conditions induce chronic inflammation, where the continuous activation of leukocytes contributes to tissue damage. β_2 -integrins are known to play a critical role in the resolution of infections⁶. An elevated expression of CR3 or CR4 was shown on blood monocytes of rheumatoid arthritis patients²²⁰ and during hypertriglyceridemic conditions²²¹, contributing to enhanced adhesiveness in both cases. Thus we set out to study the function of CR3 and CR4 on macrophages and dendritic cells under inflammatory conditions, where the activating stimulus altering their expression could contribute to changes in their functions.

5.1. Receptor expression, activation status and recycling

5.1.1. Under inflammatory conditions the expression of CR3 and CR4 is regulated differently on MDMs and MDDCs

The expression of CR3 and CR4 was monitored by flow cytometry at different time points during the LPS induced cell activation. Comparing the amount of CR3 and CR4 on the cell surface we found that LPS treatment alters their expression differently on MDMs and MDDCs (Fig. 19). Whereas on MDMs the expression of both CR3 and CR4 decreases, on MDDCs only the expression of CR3 is diminished, CR4 appears at a significantly elevated level.

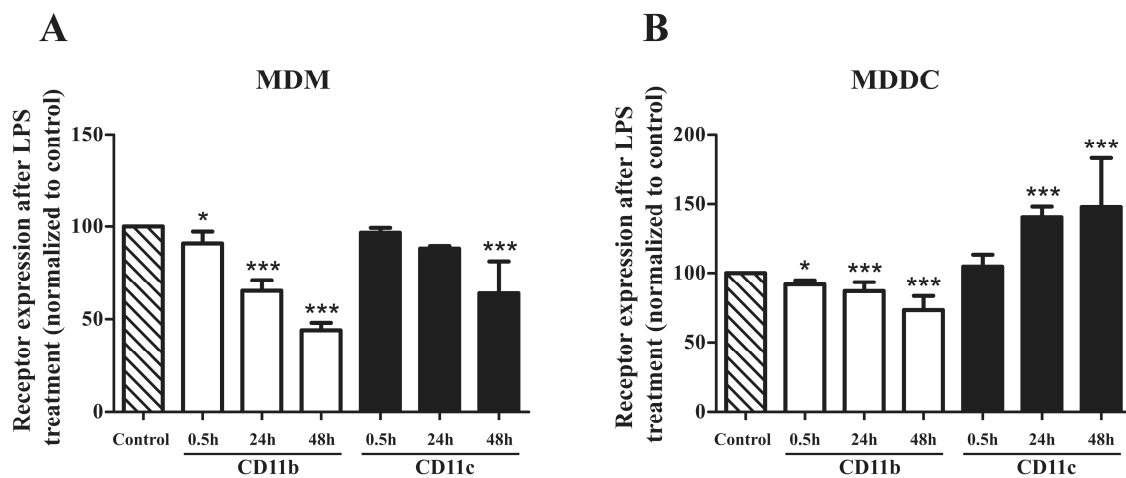


Figure 19. Changes in the expression of CR3 and CR4 after LPS induced activation. The surface expression of CR3 and CR4 was measured at different time points by flow cytometry. The effect of LPS treatment was compared to the appropriate untreated control sample at each time point, shown as 100%. For MDMs (A) results of 3 donors (mean \pm SD), for MDDCs (B) 4 donors' results (mean \pm SD) are shown. Two-way ANOVA with Bonferroni post-test was used to determine significant differences compared to control, $*=p < 0.05$; $**=p < 0.01$; $***=p < 0.001$.

5.1.2. *LPS treatment enhances β_2 -integrin cycling in both MDMs and MDDCs*

The ligand binding affinity of β_2 -integrins is regulated by activation dependent conformational changes, when these receptors switch between an inactive bent and an activated extended structure. The conformational state of the receptors can be checked using the mouse monoclonal mAb24 antibody, which is specific for an activation epitope in the I-like domain of the β_2 chain (CD18). This determinant is revealed only in the high affinity receptor with an open conformation, therefore this antibody does not bind to the receptors of cells kept on ice (Fig. 20 and Fig. 21). Cells were incubated with the Alexa488 labelled mAb24 antibody for 20 minutes on ice, then, without washing, cells were moved to a 37°C incubator. Under the experimental conditions that were used for our functional studies, the receptors were in an active, open conformation, confirmed by the binding of the mAb24 antibody.

Confocal microscopy images showed an even distribution of β_2 -integrins in the cell membrane after 5 minutes of incubation at 37°C, whereas after 30 minutes the labelled receptors accumulated inside the cell (Fig. 20). Integrins are known to have a fast turnover between the cell surface and intracellular pools, leading to the appearance of unlabelled receptors on the cell surface, that bind the mAb24 antibody, increasing the fluorescence intensity with time. When 100 ng/ml LPS was added to the cells during the 37°C incubation time, the mean fluorescence intensity (MFI) was significantly higher, thus LPS enhances the activation and turnover of β_2 -integrins (Fig. 21).

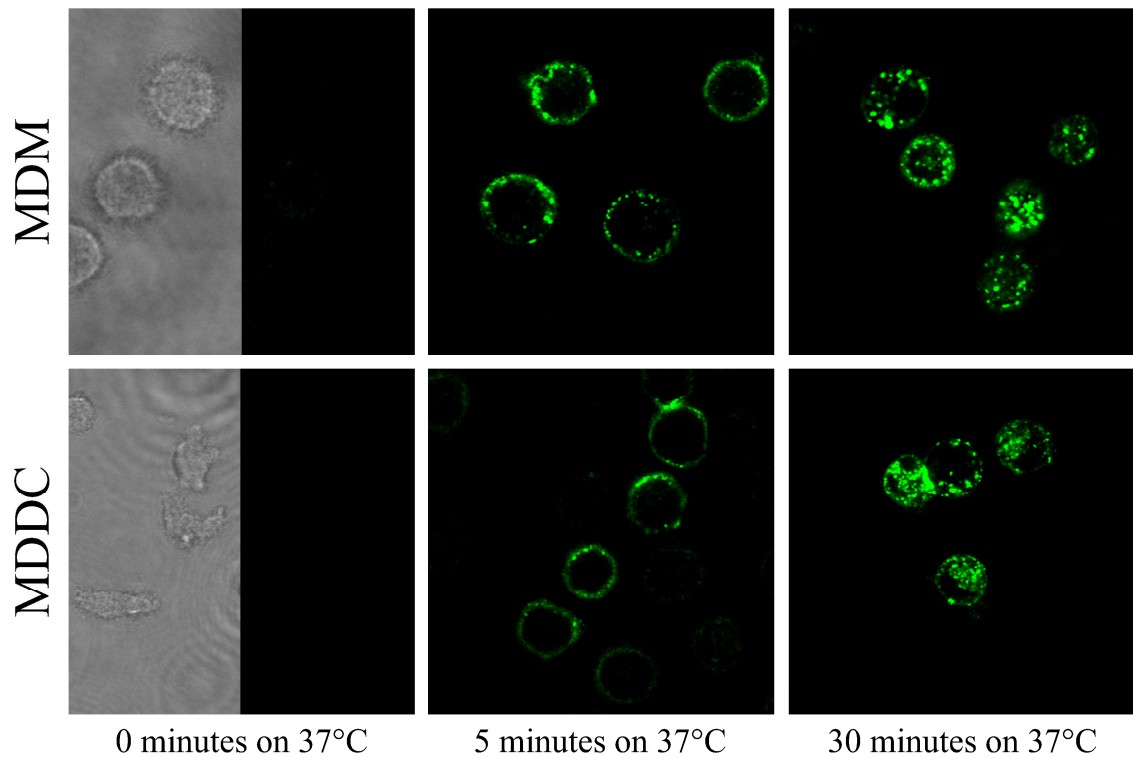


Figure 20. Analysis of β_2 -integrin conformational state by confocal microscopy. Unstimulated cells were incubated with the Alexa488 labelled mAb24 antibody for 20 minutes on ice, then, without washing, cells were moved to 37°C for 5 or 30 minutes or kept on ice (0 minutes). The receptor staining showed an even distribution in the cell membrane after 5 minutes of incubation on 37°C, whereas after 30 minutes the labelled receptors were also accumulating in the cytoplasm of the cell. Representative confocal microscopy images are shown out of 3 donors' results.

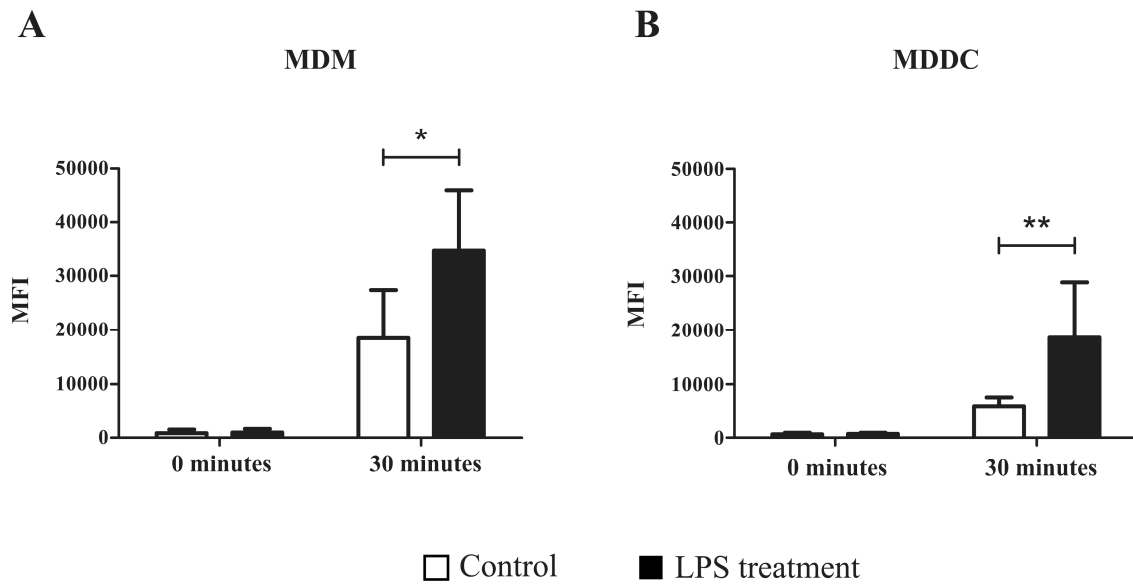


Figure 21. Analysis of β_2 -integrin conformational state by flow cytometry. Cells were incubated with the Alexa488 labelled mAb24 antibody for 20 minutes on ice, then, without washing, cells were moved to a 37°C incubator for 30 minutes or kept on ice, with or without 100 ng/ml LPS. The receptors were in an active, open conformation, confirmed by the binding of the mAb24 antibody, and LPS enhanced the activation and turnover of β_2 -integrins. Mean fluorescence intensity (MFI) data are presented, for MDMs (A) results of 4 donors (mean \pm SD) and for MDDCs (B) 5 donors' results (mean \pm SD) are shown. Two-way ANOVA with Bonferroni post-test was used to determine significant differences, *= $p < 0.05$; **= $p < 0.01$.

5.2. Adhesion to fibrinogen coated surfaces

5.2.1. Under inflammatory conditions both CR3 and CR4 participate in the adhesion to fibrinogen

We set out to study the participation of CR3 and CR4 in the adhesion of MDMs and MDDCs to a fibrinogen coated surface first by a classical method, where the number of adherent cells on a fibrinogen coated surface was counted. To distinguish the function of CR3 and CR4 in adhesion under inflammatory conditions, cells were treated with either anti-CD11b or anti-CD11c antibody prior to the assay. Unbound cells were washed away before counting. We found that in the case of LPS treated MDMs and MDDCs both CR3 and CR4 participated in cell adhesion, as blocking antibodies equally decreased the number of adherent cells compared to the isotype control antibody treated samples (Fig. 22).

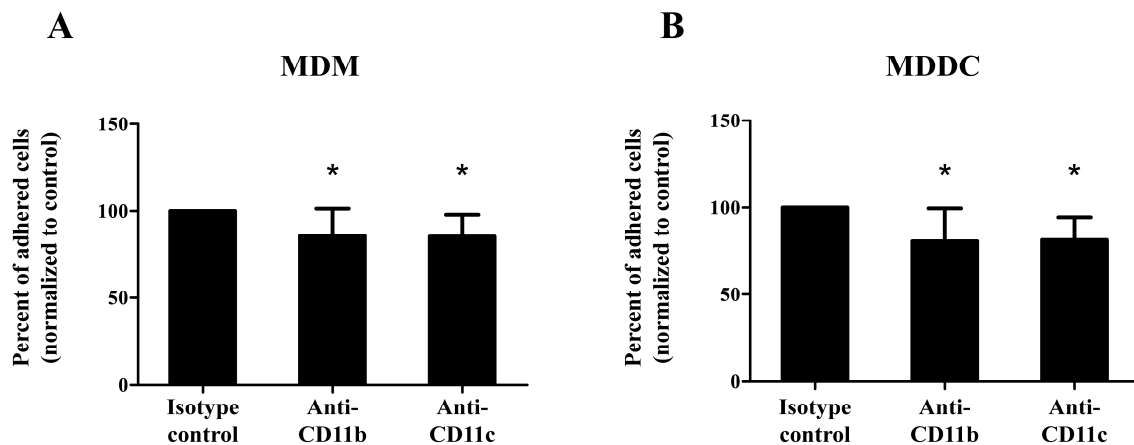


Figure 22. The effect of anti-CD11b and anti-CD11c antibodies on the number of adhered cells. The antibody treated MDMs (A) and MDDCs (B) were let to adhere on a fibrinogen coated surface and after fixation the unbound cells were washed away. Nuclei were stained with Draq5 and the adherent cells were counted. The number of adhered cells was normalized to the isotype control antibody treated samples, shown as 100%. Results of 7 donors are shown as mean \pm SD. One-way ANOVA with Tukey's post-test was used to determine significant differences compared to control, $*=p < 0.05$.

5.2.2. *LPS induced cell maturation decreases the force of adhesion significantly in MDDCs*

In this set of experiments we evaluated cell adhesion to fibrinogen using a state-of-the-art biophysical method, which allows the measurement of the force of cell attachment with a computer-controlled micropipette. Cells were let to adhere on a fibrinogen coated surface, and their adhesion force was assessed by trying to pick them up with the micropipette using vacuum induced fluid flow. The pick-up process was repeated several times with increased vacuum, and cells remaining on the surface were counted after each cycle. Applied vacuum was converted to force (nN) based on computer simulations. Employing the micropipette, we observed a significantly reduced adhesion force for LPS treated MDDCs. In the case of LPS activated MDMs we observed only a slight decrease in the strength of attachment compared to the untreated cells (Fig. 23).

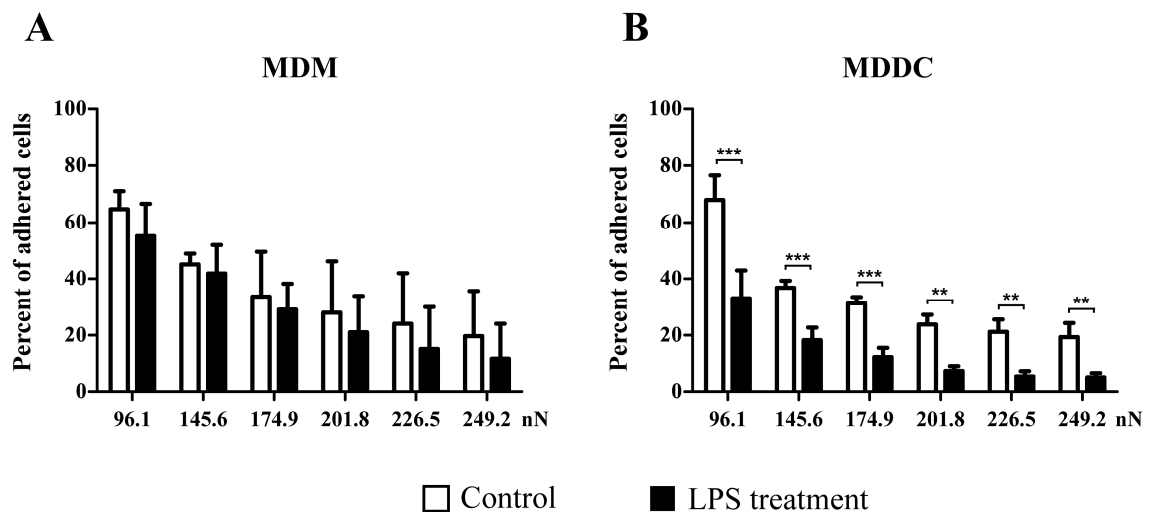


Figure 23. Changes in the force of adhesion during LPS induced maturation. The force of cell attachment was measured with a computer-controlled micropipette using vacuum induced fluid flow. Applied vacuum was converted to force (nN). The percent of adhered cells was calculated by dividing the number of cells remaining on the surface after applying a given vacuum, by the number of cells originally contained in the population. For MDMs (A) and MDDCs (B) results of 3 donors are shown (mean \pm SD). Two-way ANOVA with Bonferroni post-test was used to determine significant differences compared to control, $*=p < 0.05$; $**=p < 0.01$; $***=p < 0.001$.

5.2.3. *CR4 is prominently involved in the strong attachment of MDMs and MDDCs to fibrinogen*

To differentiate the role of CR3 and CR4 in the adhesion to fibrinogen we blocked either CD11b or CD11c by ligand binding site specific monoclonal antibodies. Experimental data are presented as the ratio of blocking antibody treated adherent cells compared to the isotype control treated cells. Previously we proved, that under physiological conditions the blocking of CD11c decreased the adhesion force of MDMs and MDDCs, CD11b did not play a role in cell attachment. Here we demonstrate, that during inflammatory conditions, both receptors become involved in adherence, however the blocking of CD11c resulted in a significantly weaker attachment compared to anti-CD11b treated samples (Fig. 24).

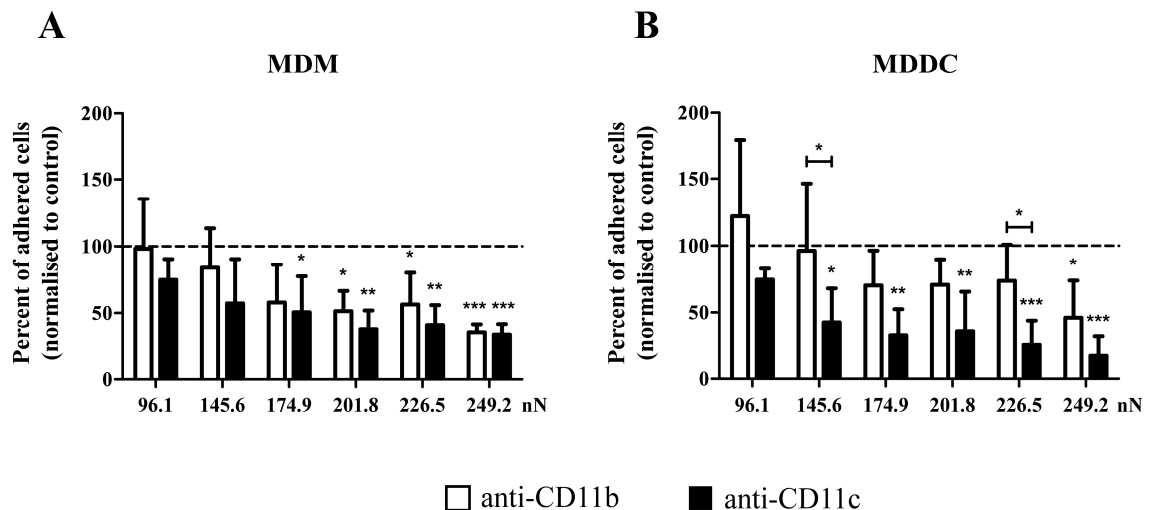


Figure 24. Changes in the force of adhesion after blocking CD11b or CD11c with antibodies. LPS activated cells were treated with anti-CD11b (shown in white) or anti-CD11c (shown in black) blocking antibody before cell adhesion. The force of cell attachment was measured with a computer-controlled micropipette using vacuum induced fluid flow. Applied vacuum was converted to force (nN). Data are presented as the percent of adhered cells staying attached to the fibrinogen coated surface normalized to isotype control antibody treated samples (shown as 100%, represented by the dashed line). For MDMs (A) results of 3 donors (mean \pm SD), for MDDCs (B) 4 donors' results (mean \pm SD) are shown. Two-way ANOVA with Bonferroni post-test was used to determine significant differences compared to control, $*=p < 0.05$; $**=p < 0.01$; $***=p < 0.001$.

5.3. Migration

5.3.1. Under inflammatory conditions both CR3 and CR4 participate in the migration of MDMs and MDDCs

Dendritic cells are known for their capacity to migrate into the lymph nodes for antigen presentation, and during this journey they go through a maturation process¹⁵¹. Maturation induces changes in chemokine receptor expression²²², including CCR7, which is expressed on the cell surface 3 hours after the inflammatory stimuli²²³. Recent studies have shown, that M1 macrophages – i.e. cells activated by LPS and IFN γ – also express CCR7 and migrate in the direction of a CCL19 and CCL21 chemokine gradient²²⁴, which results in their accumulation at inflammatory sites^{225,226}.

The migration capacity of MDMs and MDDCs was studied using a transwell assay and CCL19 as a chemoattractant. Results obtained from these experiments using LPS treated cells shows that both CR3 and CR4 participate in migration (Fig. 25C-D). This figure also shows that blocking with anti-CD11b results in a slightly stronger inhibition, when compared to the effect of anti-CD11c, particularly in the case of unstimulated MDMs.

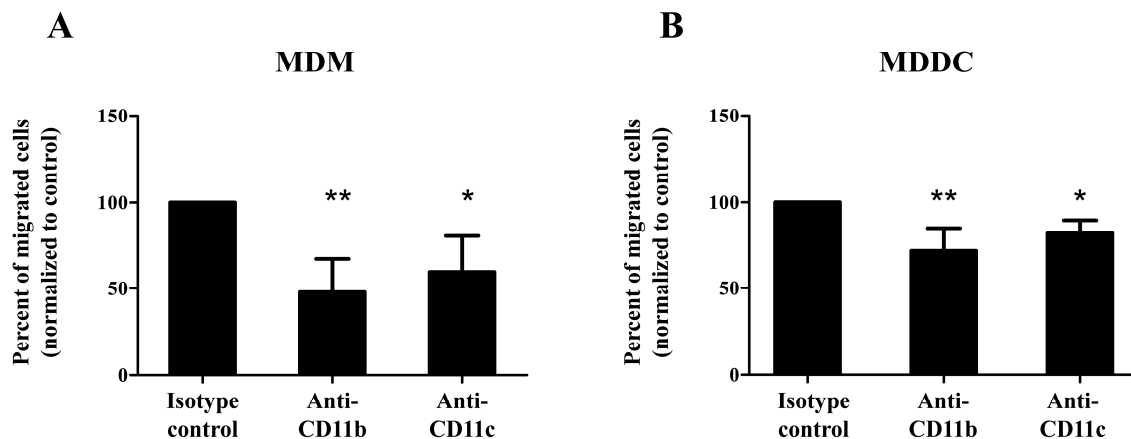


Figure 25. Analysis of migration on MDMs and MDDCs using CCL19 as a chemoattractant. Activated MDMs (A) and mature MDDCs (B) were treated with either anti-CD11b or anti-CD11c ligand binding site specific antibodies before migration, and the number of transmigrated cells were counted by flow cytometry after detachment using EDTA. The number of migrated cells was normalized to the isotype control antibody treated samples, shown as 100%. Results of 4 donors are shown as mean \pm SD. One-way ANOVA with Tukey's post-test was used to determine significant differences compared to control, *= $p < 0.05$; **= $p < 0.01$.

5.4. Adhesive structures of human phagocytes – podosomes

LPS activation induces the maturation of dendritic cells, that involves changes in the expression profile of many proteins and the reorganization of the actin cytoskeleton. These changes can affect their ability for podosome formation and migration. Our aim was to compare the podosome formation and the localization of CD11b and CD11c on the contact surface of MDMs and MDDCs under LPS induced inflammatory conditions.

5.4.1. MDDCs lose their podosomes during LPS induced maturation

Cells were let to adhere on a fibrinogen coated surface, the actin cytoskeleton and nuclei were stained with phalloidin-Alexa488 and Draq5. As it is demonstrated in Figure 26, LPS treatment induced the loss of podosomes in dendritic cells (Fig. 26C-D), whereas activated macrophages preserve these structures (Fig. 26A-B). To quantify these differences, the number of podosomes was counted based on the phalloidin staining of podosome actin cores using ImageJ software (Fig. 26E). These data confirmed, that the number of podosomes is unchanged in MDMs, but drastically decreased in MDDCs after LPS treatment. This remarkable difference in the ability of podosome formation explains the greater reduction in adhesion force of MDDCs compared to MDMs after LPS treatment. Previously we demonstrated that podosomes can be arranged in various patterns in different cell types. In the case of MDMs we observed a belt-like or even distribution, whereas in MDDCs clusters of podosomes appeared. Here we show, that in addition to a difference in podosome arrangement, the number of these structures is significantly lower for MDDCs than MDMs (Fig. 26E).

5.4.2. Localization of CD11b and CD11c on the contact surface of adherent cells under inflammatory conditions

Previously we demonstrated the presence of both CD11b and CD11c in the podosome adhesion ring on the contact surface of MDMs and MDDCs during physiological conditions. Under inflammatory conditions or upon maturation, parallel with the changes in the functions of various cells, podosomes might be lost. In our confocal microscopy study we found that LPS activated MDMs retain their ability to form podosomes with CD11b and CD11c around the actin core (Fig. 27.A-F). In LPS treated mature MDDCs however, with the loss of podosomes, CD11b and CD11c is concentrated in the cell body around the nucleus, and in membrane ruffles on the leading edge (Fig. 27.G-L).

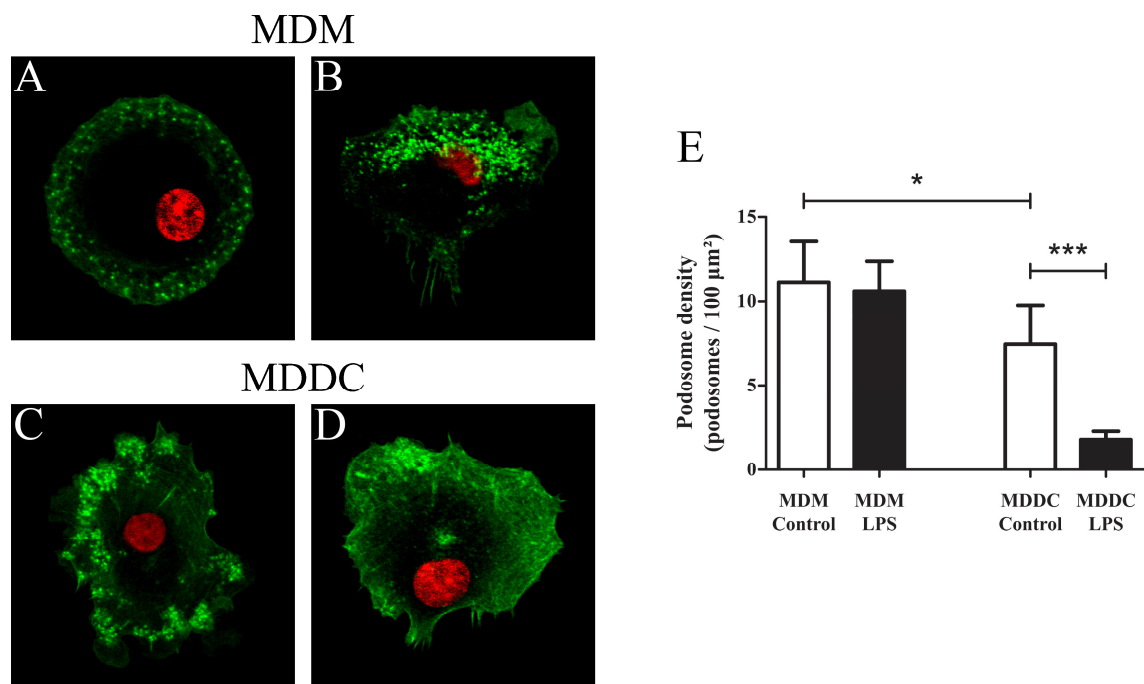


Figure 26. Changes in the arrangement of podosomes in the contact surface of adherent cells upon LPS treatment. The actin cytoskeleton of adherent cells was stained with phalloidin-Alexa488 (shown in green), nuclei were stained with Draq5 DNA dye (shown in red). Both untreated (A) and LPS treated (B) MDMs form podosomes during adhesion, whereas only untreated, immature MDDCs (C) have podosomes, LPS treated mature MDDCs (D) lose their ability for podosome formation. (E) The number of podosomes and cell area were counted with ImageJ software, data are shown as podosome density (number of podosomes per 100μm² of cell covered area). One-way ANOVA with Tukey's post-test was used to determine significant differences compared to control, *=p < 0.05, ***=p < 0.001. Representative confocal microscopy images (A-D) and podosome density data (E) are shown as mean ± SD out of 5 (MDMs) or 7 (MDDCs) donors' results.

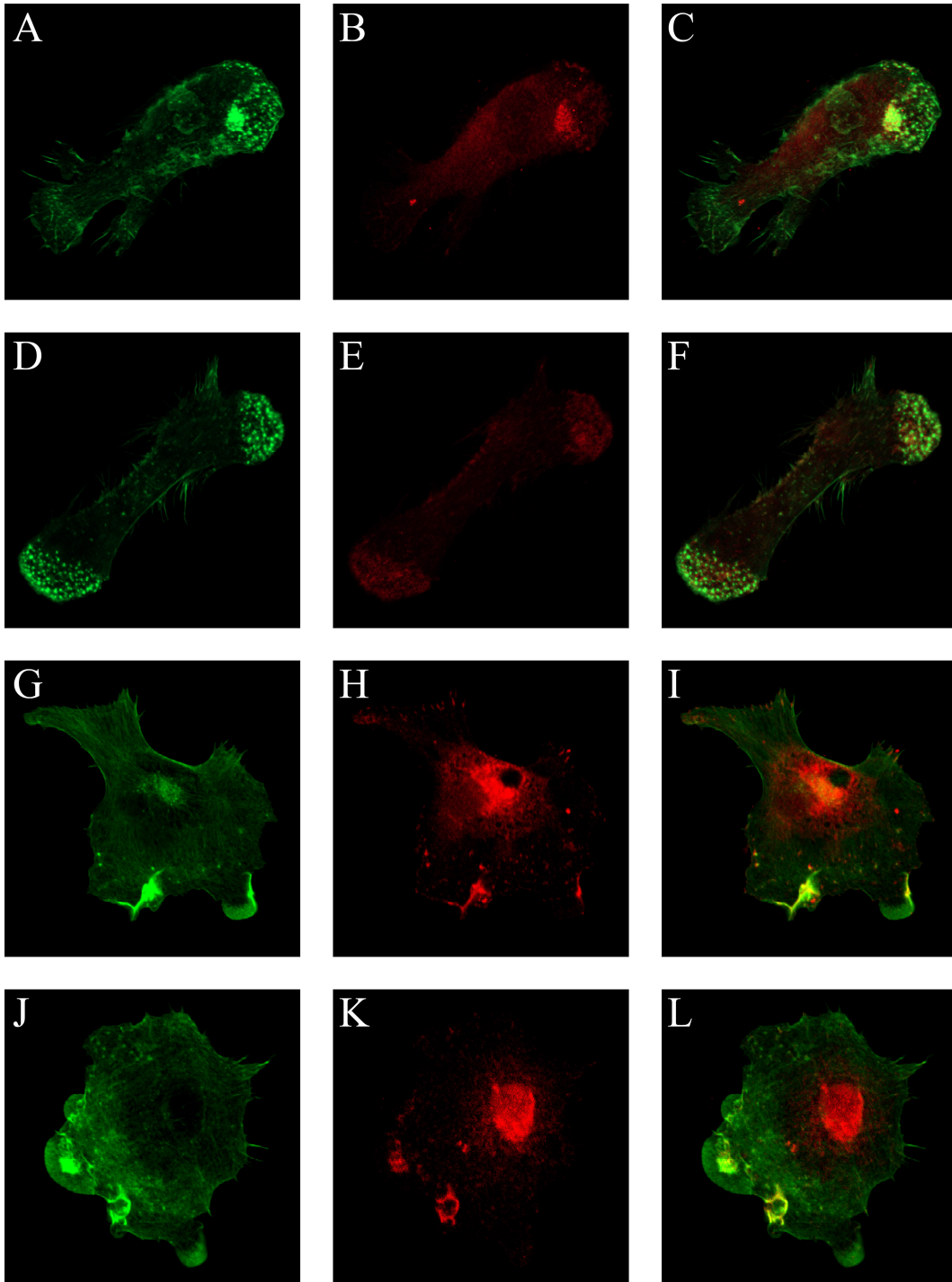


Fig. 27. Localization of CD11b and CD11c on the contact surface changes upon LPS treatment. MDMs (A–F) and MDDCs (G–L) were plated on a fibrinogen coated surface, followed by staining with phalloidin-Alexa488 (A,D,G,J), anti-CD11b (B,H) or anti-CD11c (E,K). Merged images are shown in C,F,I,L. CD11b and CD11c are located around the actin core of podosomes in LPS treated MDMs. In the case of LPS treated mature MDDCs, with the loss of podosomes, CD11b and CD11c is concentrated in the cell body around the nucleus, and in membrane ruffles on the leading edge. Confocal microscopy images of one representative experiment out of 3 are shown.

6. Discussion

The complement receptors CR3 and CR4 belong to the family of β_2 -integrins. These molecules are heterodimeric transmembrane glycoproteins consisting of a non-covalently coupled α and β polypeptide chain, which have a fundamental role in cellular adherence, migration and the clearance of pathogen microbes, tumour- and apoptotic cells by phagocytosis. Their ligands include complement components (iC3b) on the surface of opsonised targets, and adhesion ligands (fibrinogen, ICAM-1)¹⁻³.

The two receptors have a different distribution and expression pattern in mouse and human cells, consequently data obtained in mouse systems can only be applied for human immune cells with great caution⁷. In mice CR4 is expressed on DCs in the highest number, and it is often used as a marker for these cells. Recent data suggests however, that under inflammatory conditions mouse monocytes and macrophages also express CR4, which exerts antimicrobial functions²²⁷. In humans both receptors are constitutively present on monocytes, macrophages, DCs, neutrophils and NK cells²²⁸.

CR3 and CR4 are generally thought to mediate similar functions due to their structural homology and overlapping ligand specificity. The extracellular regions of CD11b and CD11c display 87% similarity, but their intracellular domains, important for signal transduction and connection with the cytoskeleton, differ in length and amino acid sequence displaying only 56% identity^{4,5}. The simultaneous presence of these receptors on leukocytes and their different signalling properties however suggest a separation of functions²²⁹. Our group set out to thoroughly investigate the roles of CR3 and CR4, since studies revealed a pivotal role for of these receptors in leukocyte functions necessary for the resolution of infections⁶.

Firstly, we set out to study the participation of CR3 and CR4 in adhesion, as the importance of this integrin mediated function is clearly evidenced by the serious symptoms of pathological conditions affecting the adhesive capacity of leukocytes, like leukocyte adhesion deficiency (LAD)¹⁸⁰ or Wiskott–Aldrich Syndrome (WAS)¹⁹⁶. We used fibrinogen as an adhesion ligand. It is an acute phase protein that is deposited at the site of injury both intravascularly and in the extracellular matrix, facilitating the adhesion and activation of leukocytes⁹⁹. Both CR3 and CR4 are capable of binding fibrinogen²³⁰, leading to a possible competition between the two receptors for this ligand.

The adhesive capacity of cells was assessed by different approaches: a classical adhesion assay and two state-of-the-art biophysical methods. The classical method consists

of counting the number of cells attached to the fibrinogen coated surface, whereas the biophysical methods allowed us to gain information about the quality of adherence. The computer controlled micropipette is capable of measuring the strength of adhesion while the optical waveguide biosensor records adhesion kinetics. Using these techniques we demonstrated, that under physiological conditions CR4 is the main receptor that mediates strong adhesion of MDMs and MDDCs to fibrinogen. Blocking CD11c with a ligand binding site specific antibody decreased the number of adhered cells and the force of adhesion on MDMs and MDDCs, moreover, it inhibited the spreading of MDMs, resulting in a smaller contact area. Surprisingly, the blocking of CD11b had an opposite effect on these cell types, as we observed no reduction in the number of adhered cell but an enhanced spreading, and this larger contact area provided a stronger attachment for MDMs and MDDCs. These data suggest that although CR3 is able to bind fibrinogen, it can have a negative role in the adhesion of these two cell types. However, in the case of monocytes, both anti-CD11b and anti-CD11c decreased the number of cells adhered to fibrinogen and the force of adhesion.

To resolve this contradiction we propose the following hypothesis: based on the absolute number of cell surface receptors^{6,8}, adhesion to fibrinogen is dependent on the number and ratio of CR3 and CR4 on the cell surface. In a preliminary experiment we found that the number of fibrinogen ligands on the adhesive surface is comparable with the number of receptors found on monocytes. Since there are enough ligands available for both receptors, they take part equally in adhesion without a competition. This idea needs further support by analysing the adhesion of neutrophils, which express the two receptors in similar amounts to monocytes. In previous adhesion studies performed on monocytes and neutrophil granulocytes, both CR3 and CR4 mediated adhesion and spreading, suggesting that the adhesion properties of these cell types are similar^{80,231,232}.

In the case of MDMs and MDDCs however, there is a competition between CR3 and CR4 for accessible fibrinogen ligands, because both receptors are present in high numbers. With the crystal structures available for the ligand binding I-domains of both receptors, Vorup-Jensen et al. showed a ridge of positively charged residues present only in CR4, that results in a differential ligand binding compared to CR3^{233,234}. While CR3 recognizes molecules with a positive charge, CR4 preferentially binds polyanionic species and molecules with a net negative charge, such as fibrinogen. This difference in ligand binding might determine the outcome of cell-ECM interactions when multiple receptors are available.

Circulating leukocytes are guided to the site of injury by chemotactic signals, which initiates adhesion and transmigration through the endothelial cell layer²³⁵. The migratory capacity of MDMs and MDDCs, towards the small chemoattractant peptide fMLP, was assessed by a transwell assay, that simulates the active, integrin-mediated translocation of leukocytes through a barrier. When using ligand binding site specific antibodies, we found that both anti-CD11b and anti-CD11c inhibited the migration of MDMs towards fMLP, but the number of migrated cells was significantly lower when CR3 was blocked. In the case of MDDCs both receptors take part equally. The transwell assay provides a technique to characterize the migration of cells with the participation of all cell surface integrins. To investigate the specific participation of CR3 and CR4 in transmigration, further experiments are required using a fibrinogen coated membrane.

CR3 and CR4 mediate cell adhesion, spreading and migration through the formation of cell-cell and cell-extracellular matrix connections³⁰. To establish these contacts cells use specific structures, called podosomes. They are known to mediate short-lived adhesion spots that are formed and quickly remodelled during migration. These structures have an F-actin core surrounded by adhesion molecules¹⁵⁹ and can be arranged in clusters, rings or belts¹⁶¹. Podosomes are characteristic for monocytic cells, such as monocytes, macrophages, osteoclasts and dendritic cells. Here we studied the podosomes of human phagocytes adhered to a fibrinogen coated surface. Monocytes and MDMs mostly showed an even distribution of podosomes scattered across the contact surface, however a belt like pattern could also be observed for MDMs. The podosomes of dendritic cells were found to be arranged in clusters or condensed in the leading edge of migrating cells. Whether human neutrophils have podosomes is still debated. Neutrophils isolated from mice and pretreated with fMLP formed podosome-like structures, containing an actin core and a vinculin ring, on fibrinogen coated cover slips²³⁶. In this study we detected the formation of actin rich dots evenly spread on the contact surface of human neutrophils adhered to fibrinogen.

The importance of β_2 -integrins in podosome formation and podosome mediated adhesion has been proven, but the individual role of these receptors had not been studied so far. Burns et al. found, that β_2 -integrins are specifically recruited to podosomes in human MDDCs on a fibronectin surface (a ligand for both β_1 - and β_2 -integrins), whereas β_1 -integrins show a disperse distribution¹⁶⁶. In a β_2 -integrin-null mouse model, Gawden-Bone et al. showed that in the absence of β_2 -integrins podosome assembly is disrupted¹⁶⁷.

Here we show that both CR3 and CR4 are located in the adhesion ring of podosomes in human MDMs and MDDCs attached to fibrinogen. Additionally, a strong staining for the

receptors can be observed intracellularly, around the nucleus. Integrins are known to rapidly recycle between the cell membrane and endosomes²⁰, which can occur via distinct routes^{24,25}. In the long loop of recycling integrins go through the perinuclear recycling compartment before returning to the cell surface²⁷. No data is available yet on the exact recycling route used by β_2 -integrins, but the staining pattern we found around the nucleus might implicate a passage through the perinuclear recycling compartment.

The other frequently studied role of CR3 and CR4 is the phagocytosis of complement opsonized microbes. In macrophages the opsonophagocytic function of CR3 has been proven earlier²³⁷, and also a role for CR4 was shown in the uptake of *Mycobacterium tuberculosis* by alveolar macrophages¹⁷³. Though alveolar macrophages differ from monocyte derived macrophages due to their tissue microenvironment and cytokine milieu, several data show that on MDMs both CR3 and CR4 participate in the phagocytosis of opsonized *Cryptococcus neoformans*²³⁸, *Mycobacterium leprae*¹⁷⁹ and *Francisella tularensis*¹⁷⁵. These studies however do not clearly distinguish between the complement receptor mediated binding and digestion of the pathogens. We compared these two different functions using the pH sensitive pHrodo Green labelled *Staphylococcus aureus* and the classical Alexa488 conjugated particles. This approach allowed us to detect bacteria destined for degradation and separate those from the bound and endocytosed ones.

Employing this method, in the case of MDMs we found a collaboration between the two complement receptors. Namely, we observed that blocking CR4 decreased the amount of surface bound particles, while the digestion of iC3b opsonized *S. aureus* was dependent on a functional CR3. However, there are data indicating the existence of two subsets of CR3 and CR4 that can be distinguished based on lateral mobility^{5,239}. Graham et al. showed, that the actin-attached, immobile subset of CR3 was responsible for the phagocytosis of iC3b opsonized particles, despite that the mobile subset could also bind the particles²³⁹. CR3 is also known to associate with other receptors, like Fc γ -receptors, uPAR and CD14²⁴⁰, and the expression and distribution of these interacting receptors can differ between cell types. The different mobility and interacting partners of CR3 and CR4 could influence the outcome of phagocytosis in a cell type specific manner.

Our group demonstrated earlier that blocking of CD11c did not influence the uptake of opsonized yeast or *S. aureus* by MDDCs. We confirmed these results using siRNA; when downregulation of CD11b blocked the phagocytosis of opsonized particles while silencing CD11c had no effect on their uptake²¹⁵. Now we have strengthened these findings by

showing that only CR3 blocking decreases the binding and uptake of *S. aureus*. In contrast to this Ben Nasr et al. demonstrated that blocking both CR3 or CR4 inhibited the phagocytosis of opsonized, live *Francisella tularensis* by human MDDCs²⁴¹. This contradiction might be caused by differences in the pathogens and the capacity of live *Francisella tularensis* to utilize CR4 as well to get into the host cells.

Studies of phagocytosis carried out employing monocytes and neutrophils underline the importance of CR3 expressed by these cells. Monocytes utilize CR3 but not CR4, for the phagocytosis of *Mycobacterium tuberculosis*¹⁷³ and *M. leprae*¹⁷⁰, similarly to neutrophils in the case of *Francisella tularensis*¹⁷⁵. In our present study we show that in the phagocytosis of the extracellular pathogen *S. aureus*, opsonized by iC3b, CR3 plays a dominant role over CR4 by both monocytes and neutrophils.

Taking our results together, we obtained further evidence that under physiological conditions CR3 and CR4 exert distinct functions in human phagocytes. Though both CR3 and CR4 are able to bind fibrinogen and iC3b, we found that either of them dominates the other in various functions, such as antigen uptake and digestion, as well as adhesion and spreading.

Macrophages and dendritic cells are essential in the recognition of invading pathogens and the initiation of immune responses. Both cell types are professional antigen presenting cells, but they have different roles in several aspects. Dendritic cells migrate to lymph nodes after antigen uptake to initiate an adaptive immune response by presenting these antigens to naïve T-cells²⁴². Resident macrophages migrate within the peripheral tissues to the site of infection, where they take part in the elimination of pathogens by phagocytosis, production of reactive intermediates and the establishment of an inflammatory milieu by cytokine secretion²⁴³.

In the initial phase of an immune response after tissue injury or infection immune cells are recruited and an inflammatory environment is established. Additionally, many pathological conditions are known to induce chronic inflammation, where the continuous activation of leukocytes contributes to tissue damage. β_2 -integrins are acknowledged to play a critical role in cell migration and the resolution of infections⁶. An elevated expression of CR3 or CR4 was shown on blood monocytes of rheumatoid arthritis patients²²⁰ and during hypertriglyceridemic conditions²²¹, contributing to enhanced adhesiveness in both cases. These data and our previous results prompted us to investigate in more detail the expression

of CR3 and CR4 on macrophages and dendritic cells and dissect their adhesive and migratory function under inflammatory conditions.

After the lysis of Gram-negative bacteria glycolipids from the outer membrane are released, that serve as potent proinflammatory stimuli for myeloid cells. Bacterial lipopolysaccharides (LPS) are known to bind to Toll-like receptors and β_2 -integrins that promote receptor activation and cell adhesion. Wright et al. identified an LPS binding site in the CR3 α chain that was distinct from the location of iC3b and fibrinogen binding⁷³. Wong et al. showed two putative LPS binding sites in the β_2 I-like domain²⁴⁴ that would explain why LPS binding to either LFA-1, CR3 or CR4 all induce an inflammatory response^{74,245,246}. CR3 was also shown to become associated with CD14 after LPS treatment on neutrophils²⁴⁷, and that it might use the same adaptors for LPS signalling as CD14²⁴⁸.

Antigen uptake and proinflammatory stimuli induce macrophage activation and dendritic cell maturation involving changes in the expression of costimulatory molecules, chemokine and phagocytic receptors²⁴⁹. Upon stimulation by LPS neutrophils quickly, but transiently upregulate the expression of CR3 from intracellular granules, and the receptors on the cell surface switch to high affinity conformation, both events contributing to enhanced adhesiveness^{250,251}.

In the present work we monitored the changes in the expression of CD11b and CD11c upon LPS stimulation. On MDMs and MDDCs treated with LPS for 30 minutes the amount of CD11b slightly decreased, while the amount of CD11c did not change, but after 24 and 48 hours the amount of CD11b decreased on both cell types. At the same time the quantity of CD11c increased in MDDCs but was lower in MDMs, suggesting a cell type specific regulation. In our experiments investigating the conformation of β_2 -integrins, we found a significantly elevated amount of receptors binding mAb24 after 30 minutes of LPS treatment, due to the increased activation and intracellular accumulation of these receptors. Although this antibody is specific for an activation epitope in all β_2 -integrins, LFA-1 was shown to have a very low endocytosis rate compared to CR3, that was not influenced by stimulating agents²⁰. Consequently, the observed increase in internalization and recycling speed can be attributed to CR3 and CR4.

Taking these results together we demonstrated for the first time that the amount of cell surface CR3 and CR4 does not increase immediately after LPS treatment, but their activation status and recycling speed changes. Integrin activation and recycling are most likely linked processes, Arjonen et al. showed that active β_1 -integrins have a higher endocytosis rate, whereas receptors in an inactive state are rapidly recycled to the plasma membrane²⁴. We

propose that at the early stage of LPS stimulation β_2 -integrin activation triggers receptor endocytosis and faster recycling. Thus, a higher endocytosis rate for LPS activated CR3 could explain the decrease in cell surface expression after 30 minutes.

Integrins are known to mediate cell adhesion, spreading and migration through the establishment of cell-cell and cell-extracellular matrix connections³⁰. Our group focuses on clarifying the individual roles of the β_2 -integrins CR3 and CR4, as they are often assumed to have overlapping, or even identical functions. Early studies on human granulocytes and monocytes proved that LFA-1, CR3 and CR4 all contribute to endothelial adhesion^{154,155}, and that the cell type and the stimuli used can influence the participation of these receptors. Georgakopoulos et al. also showed, that the involvement of CR3 and CR4 in adhesion to fibrinogen is dependent on the experimental conditions, namely the type of stimuli and culture conditions of human blood monocytes¹⁵⁷. Earlier we demonstrated that in the lack of inflammatory stimulus CR4 plays a dominant role in the adhesion to fibrinogen⁸.

Here, we studied the adhesive capacity of MDMs and MDDCs after LPS stimulation. We used both the classical, end-point adhesion assay and a computer-controlled micropipette method capable of measuring the force of adhesion. When applying ligand binding site specific antibodies we found that both anti-CD11b and anti-CD11c treatment weakened adhesion to fibrinogen coated surfaces, as verified by the decreased number of adherent cells and force of attachment. Importantly however, while both receptors participated in adhesion, the force of attachment was significantly lower for the anti-CD11c treated cells, proving a dominant role for CR4.

This differential participation of CR3 and CR4 in adhesion confirms our previous hypothesis⁸, namely that ligand availability and the number of cell surface receptors regulates receptor utilization. Based on the absolute number of cell surface receptors^{6,8}, we proved that there is a competition between CR3 and CR4 for accessible fibrinogen ligands on MDMs and MDDCs, where both receptors are present in high amounts. Since LPS treatment altered the cell surface expression of these receptors differently on MDMs and MDDCs, we detected a change in receptor usage. The number of both receptors decreases upon LPS treatment on MDMs, allowing the ligand binding of both CR3 and CR4. In the case of MDDCs the ratio of receptors shifts in favor of CR4, strengthening its dominant role.

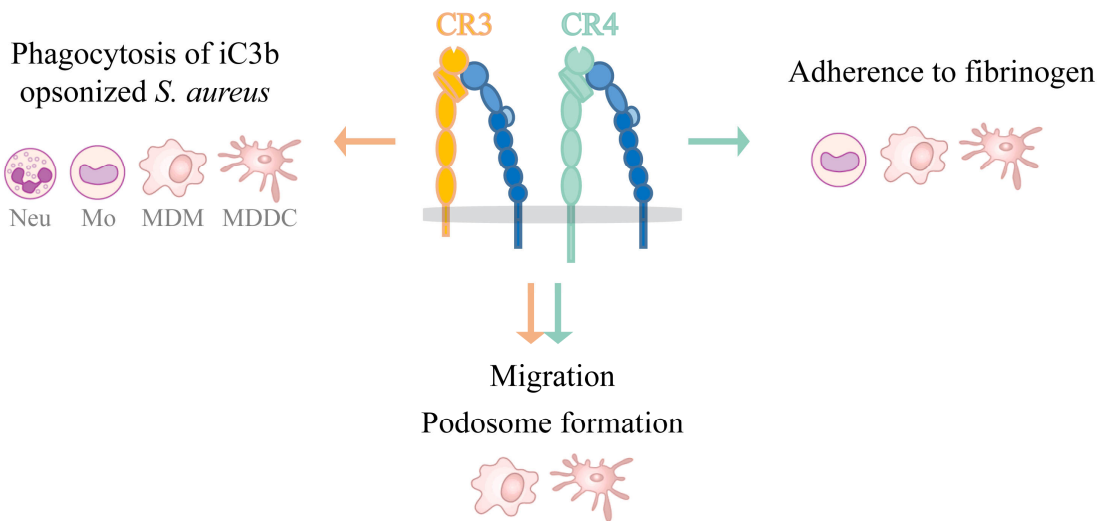
Emerging data on podosomes highlight their importance in myeloid cell adhesion and migration. Considering the differences in immune functions between macrophages and dendritic cells we compared the formation and β_2 -integrin composition of podosomes after inflammatory stimuli on these cell types. During LPS induced maturation dendritic cells go

through cytoskeletal changes, losing their capacity for phagocytosis and podosome formation^{150,166}. In this study we demonstrate, that after 24 hours of LPS treatment MDCCs do not form podosomes on a fibrinogen coated surface, significantly lowering the force of adherence compared to immature cells. In contrast, MDMs preserve these structures after LPS activation and there is only a slight decrease in the adhesion force measured with the computer-controlled micropipette, proving that podosomes ensure a strong attachment.

A crucial and specific role for β_2 -integrins in podosome functions has been demonstrated by others^{166,167}, and we have also proven, that under physiological conditions both CR3 and CR4 are located in the adhesion ring of podosomes in human MDMs and MDCCs attached to fibrinogen¹⁷⁴. Here we show that on LPS matured MDCCs, with the loss of podosomes, CD11b and CD11c are concentrated in the cell body and in membrane protrusions. The strong staining around the nucleus might imply that β_2 -integrins go through the perinuclear recycling compartment in the long loop of integrin cycling before returning to the cell surface²⁵. In the case of LPS activated MDMs, the cells become more elongated, but CD11b and CD11c are localized around the actin core of podosomes, similarly to untreated cells.

Our previous studies proved a “division of labour” between CR3 and CR4 under physiological conditions^{8,174}, with CR3 participating in the phagocytosis of iC3b opsonized *Staphylococcus aureus* and CR4 dominating cell adhesion to fibrinogen. After LPS treatment the expression and role of these receptors changed, proving our hypothesis, that the number and ratio of cell surface receptors influences the outcome of cell-matrix interactions. We also found further evidence underlining the functional differences between macrophages and dendritic cells, and a strong indication that podosomes are essential for firm cell attachment.

Physiological conditions



Inflammatory conditions

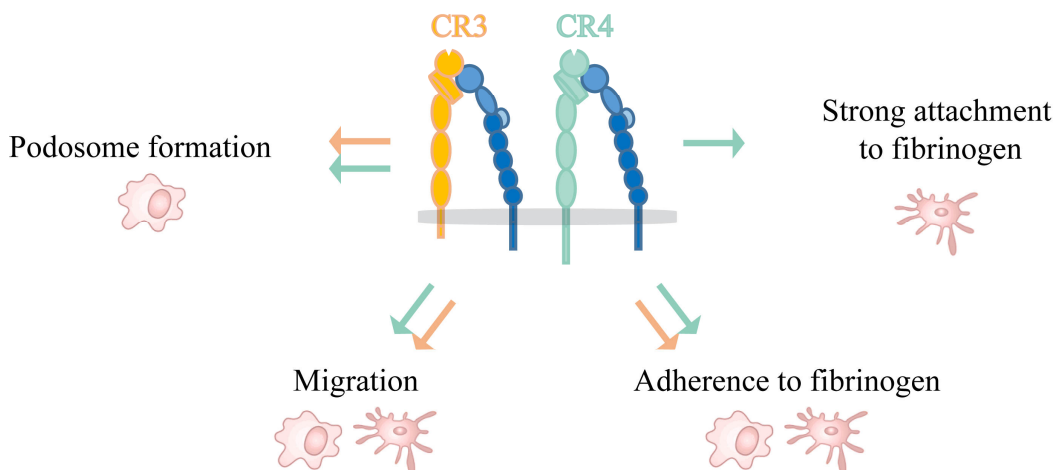


Figure 28. The function of CR3 and CR4 under physiological and inflammatory conditions. Our studies proved a “division of labour” between CR3 and CR4 under physiological conditions, with CR3 participating in the phagocytosis of iC3b opsonized *Staphylococcus aureus* and CR4 dominating cell adhesion to fibrinogen. In the process of migration and podosome formation of MDMs and MDDCs both receptors took part. LPS treatment changed the expression and role of these receptors, both CR3 and CR4 contributed to the adhesion, migration and podosome formation, however in the case of MDDCs CR4 provided a stronger attachment to fibrinogen. Abbreviations: Neu: neutrophil granulocyte; Mo: monocyte; MDM: monocyte derived macrophage; MDDC: monocyte derived dendritic cell.

Summary

CR3 and CR4, the leukocyte specific β_2 -integrins, are involved in cellular adherence, migration and phagocytosis. They are often assumed to mediate similar functions due to their structural homology and overlapping ligand specificity. Our group set out to thoroughly investigate the distinct role of CR3 and CR4 in myeloid cell functions under physiological and inflammatory conditions.

The adhesive capacity of monocytes, monocyte derived macrophages (MDMs) and dendritic cells (MDDCs) was assessed by different approaches: a classical adhesion assay and two biophysical methods. Using these techniques we demonstrated, that under physiological conditions CR4 is the main receptor that mediates strong adhesion of MDMs and MDDCs to fibrinogen. However, in the case of monocytes, both receptors were involved in adhesion, so we proposed the following hypothesis: adhesion to fibrinogen is dependent on the number and ratio of CR3 and CR4 on the cell surface. In the case of monocytes the number of receptors is comparable with the amount of available ligands, but MDMs and MDDCs express these receptors in higher numbers, resulting in a competition for fibrinogen.

We studied the formation and composition of *podosomes*, that are characteristic adhesive structures of myeloid cells. We found different podosome patterns depending on the cell type, namely an even or belt like distribution for monocytes and MDMs, and clusters for MDDCs. Additionally, we showed, that both CR3 and CR4 are located in the adhesion ring of podosomes in the contact zone of MDMs and MDDCs attached to fibrinogen.

The participation of CR3 and CR4 in phagocytosis, with the clear distinction between surface bound and internalized particles, was assessed using iC3b opsonized *Staphylococcus aureus*. Comparing the activity of the two β_2 -integrin type complement receptors we found that CR3 plays a dominant role in the phagocytosis of this pathogen on neutrophil granulocytes, monocytes, MDMs and MDDCs.

To better understand the role of CR3 and CR4 in pathological conditions inducing inflammation, we also studied their functions on LPS activated MDMs and MDDCs. We found that LPS treatment alters the expression of these β_2 -integrins. The amount of CR3 decreases on both cell types, whereas the level of CR4 increases in MDDCs but decreases in MDMs, suggesting a cell type specific regulation. Using mAb24, specific for the high affinity conformation of CD18, we proved that the activation and recycling of β_2 -integrins is significantly enhanced upon LPS treatment.

The adhesion studies on LPS treated cells confirmed our previous hypothesis, with the altered expression of CR3 and CR4 we detected a change in receptor usage. On MDMs the number of both receptors decreases upon LPS treatment, allowing the participation of both CR3 and CR4 in adhesion to fibrinogen. In the case of MDDCs the ratio of receptors shifts in favour of CR4, strengthening its dominant role.

Studying the formation of podosomes under inflammatory conditions, we found major differences between MDMs and MDDCs. While MDMs retain podosome formation after LPS activation, MDDCs lose this ability, which results in a significantly reduced force of adhesion. We show that with the loss of podosomes the distribution of CR3 and CR4 changes, they become concentrated in the cell body and membrane lamellae on the leading edge.

Összefoglalás

A leukocita specifikus β_2 -integrinek családjába tartozó CR3 és CR4 fontos szerepet tölt be az immunsejtek adherenciájában, migrációjában és opsonizált részecskék fagocitózisában. A két receptornak gyakran azonos funkciót tulajdonítanak, hiszen nagyfokú szerkezeti homológiát mutatnak és átfedő a ligandum specificitásuk is. Munkacsoportunk célul tűzte ki e két receptor egyedi funkciójának alapos vizsgálatát a mieloid sejtek funkcióiban, mind fiziológiás, mind gyulladáshoz vezető körülmények között.

A sejtadhézió jellemzésére több különböző módszert használtunk: a klasszikus adhéziónak mellé két biofizikai módszert. Ezen módszerek segítségével kimutattuk, hogy fiziológiás körülmények között a CR4 kulcsszerepet játszik a fibrinogénhez való adherenciában makrofágok és dendritikus sejtek esetén. Mivel monocitákon mindkét receptor blokkolása gátolta az adherenciát, hipotézisünk szerint a fibrinogénhez való adherencia a CR3 és CR4 mennyiségétől és egymáshoz viszonyított arányától függ. Monocitákon a sejt felszíni receptorok mennyisége összemérhető az elérhető fibrinogén ligandumok számával, viszont makrofágok és dendritikus sejtek esetén kompetíció fog kialakulni a két receptor között, mivel ezeken a sejt típusokon egy nagyságrenddel magasabb a receptorszám.

Megvizsgáltuk a mieloid sejtekre jellemző adhéziónak struktúrákat, a *podoszómák* kialakulását és összetételét. Az általunk vizsgált sejt típusok esetében különböző podoszóma mintázatokat találtunk: neutrofilek, monociták és makrofágok felszínén egyenletes vagy övszerű eloszlás volt jellemző, míg dendritikus sejteknél a kisebb csoportokba rendeződés. Továbbá kimutattuk, hogy a fibrinogénnel fedett felszínhez kitapadt makrofágok és dendritikus sejtek kontakt felszínén a CR3 és CR4 megtalálható a podoszómák adhéziónak gyűrűjének területén.

A két receptor részvételét az iC3b-vel opsonizált *Staphylococcus aureus* fagocitózisában neutrofil granulocitákon, monocitákon, makrofágokon és dendritikus sejteken vizsgáltuk, egyértelműen elkülönítve a felszínhez kötődött és internalizált részecskéket. Az összes sejt típus esetén a CR3 domináns szerepét igazoltuk ennek a patogén baktériumnak a fagocitózisában.

A CR3 és CR4 gyulladáshoz vezető patológiás körülmények közötti szerepének feltérképezésére a két receptor szerepét LPS aktivált makrofágokon és dendritikus sejteken is megvizsgáltuk. LPS kezelés hatására a receptorok sejt felszíni expressziója megváltozott.

A CR3 mennyisége mindkét sejtípuson csökkent, míg a CR4 szintje nőtt makrofágokon, de alacsonyabb lett dendritikus sejteken, bizonyítva a két receptor expressziójának sejtspecifikus szabályozását. A CD18 lánc aktív konformációjára specifikus mAb24 ellenanyag használatával kimutattuk, hogy az LPS kezelés fokozza a β_2 -integrinek aktivációját és reciklizációját.

Az LPS aktivált sejteken végzett adhézión kísérletek alátámasztották hipotézisünket, amennyiben a receptorok módosult expressziójával a szerepük is megváltozott. Makrofágokon a CR3 és CR4 mennyisége is csökkent LPS kezelés után, és mindkét receptor részt vett az adherenciában. A receptorok mennyisége dendritikus sejteken ellentétesen változott, eltolva az arányukat a CR4 javára, megerősítve a receptor domináns szerepét az adherenciában.

A podoszómák megjelenésében jelentős különbségeket találtunk makrofágok és dendritikus sejtek esetében gyulladásos körülmények között. Míg makrofágok esetén az LPS kezelés után is megtalálhatók ezek a képletek, a dendritikus sejtek elveszítik a képességüket a podoszómák létrehozására, és ez szignifikánsan lecsökkenti kitapadásuk erejét. Podoszómák hiányában a CR3 és CR4 eloszlása is megváltozik, inkább a sejttest körül és membrán kitüremkedések mentén helyezkednek el.

Acknowledgements

Firstly, I would like to thank my supervisor Prof. Zsuzsa Bajtay for her continuous support during my university and doctoral studies. I am grateful for her ideas and advices she gave me, and the possibility to work in the Complement Research Group.

I wish to thank all members of our research group, for their help and insightful comments during discussions. I am especially grateful to Prof. Anna Erdei and Dr. István Kurucz for their help with the preparation of manuscripts, and Zsuzsa Nagy-Baló, Bernadett Mácsik-Valent, Katinka Nagy and Kliment Kristóf for their practical advices in experiment planning.

I would like to thank Dr. Noémi Sándor for teaching me the experimental methods at the beginning of my studies.

I would like to acknowledge Dr. Bálint Szabó, Rita Ungai-Salánki, Barbara Francz, and Tamás Gerecsei from the Department of Biological Physics and Dr. Róber Horváth, and Norbert Orgován from the Nanobiosensorics “Lendület” Group, Institute of Technical Physics and Material Sciences, for their collaboration during the biophysical adhesion measurements.

I am grateful for my family and friends for their encouragement and support during my studies.

List of publications

Publications connected to the thesis

1. Noémi Sándor*, Szilvia Lukácsi*, Rita Ungai-Salánki, Norbert Orgován, Bálint Szabó, Róbert Horváth, Anna Erdei, Zsuzsa Bajtay

*These authors contributed equally to this work.

CD11c/CD18 Dominates Adhesion of Human Monocytes, Macrophages and Dendritic Cells over CD11b/CD18

PLoS One. 11 (2016) e0163120. doi:10.1371/journal.pone.0163120.

2. Szilvia Lukácsi, Zsuzsa Nagy-Baló, Anna Erdei, Noémi Sándor, Zsuzsa Bajtay

The role of CR3 (CD11b/CD18) and CR4 (CD11c/CD18) in complement-mediated phagocytosis and podosome formation by human phagocytes

Immunology letters, 189 (2017) 64–72. doi:10.1016/j.imlet.2017.05.014.

3. Szilvia Lukácsi, Tamás Gerecsei, Katalin Balázs, Barbara Francz, Bálint Szabó, Anna Erdei, Zsuzsa Bajtay

The differential role of CR3 (CD11b/CD18) and CR4 (CD11c/CD18) in the adherence, migration and podosome formation of human macrophages and dendritic cells under inflammatory conditions

Manuscript under revision

Other publications

1. Anna Erdei, Noémi Sándor, Bernadett Mácsik-Valent, Szilvia Lukácsi, Mariann Kremlitzka, Zsuzsa Bajtay

The versatile functions of complement C3-derived ligands

Immunological reviews, 274 (2016) 127–140. doi:10.1111/imr.12498.

2. Norbert Orgovan, Rita Ungai-Salánki, Szilvia Lukácsi, Noémi Sándor, Zsuzsa Bajtay, Anna Erdei, Bálint Szabó, Róbert Horvath

Adhesion kinetics of human primary monocytes, dendritic cells, and macrophages: Dynamic cell adhesion measurements with a label-free optical biosensor and their comparison with end-point assays

Biointerphases. 11 (2016) 031001. doi:10.1116/1.4954789.

3. Barbara Uzonyi, Bernadett Mácsik-Valent, Szilvia Lukácsi, Richárd Kiss, Katalin Török, Mariann Kremlitzka, Zsuzsa Bajtay, Judit Demeter, Csaba Bödör, Anna Erdei
Functional studies of chronic lymphocytic leukemia B cells expressing β_2 -integrin type complement receptors CR3 and CR4
Immunology letters, 189 (2017) 73–81. doi:10.1016/j.imlet.2017.05.016.

4. Anna Erdei, Szilvia Lukácsi, Bernadett Mácsik-Valent, Zsuzsa Nagy-Baló, István Kurucz, Zsuzsa Bajtay
Non-identical twins: Different faces of CR3 and CR4 in myeloid and lymphoid cells of mice and men
Seminars in cell & developmental biology, 85 (2019) 110–121.
doi:10.1016/j.semcdb.2017.11.025.

References

1. Diamond, M. S., Garcia-Aguilar, J., Bickford, J. K., Corbi, A. L. & Springer, T. A. The I domain is a major recognition site on the leukocyte integrin Mac-1 (CD11b/CD18) for four distinct adhesion ligands. *J. Cell Biol.* **120**, 1031–43 (1993).
2. Rosen, H. & Law, S. K. The leukocyte cell surface receptor(s) for the iC3b product of complement. *Curr. Top. Microbiol. Immunol.* **153**, 99–122 (1990).
3. Lishko, V. K., Yakubenko, V. P., Hertzberg, K. M., Grieninger, G. & Ugarova, T. P. The alternatively spliced alpha(E)C domain of human fibrinogen-420 is a novel ligand for leukocyte integrins alpha(M)beta(2) and alpha(X)beta(2). *Blood* **98**, 2448–55 (2001).
4. Corbi, A. L., Kishimoto, T. K., Miller, L. J. & Springer, T. A. The human leukocyte adhesion glycoprotein Mac-1 (complement receptor type 3, CD11b) alpha subunit. Cloning, primary structure, and relation to the integrins, von Willebrand factor and factor B. *J. Biol. Chem.* **263**, 12403–11 (1988).
5. Ross, G. D., Reed, W., Dalzell, J. G., Becker, S. E. & Hogg, N. Macrophage cytoskeleton association with CR3 and CR4 regulates receptor mobility and phagocytosis of iC3b-opsonized erythrocytes. *J. Leukoc. Biol.* **51**, 109–17 (1992).
6. Erdei, A. *et al.* Non-identical twins: Different faces of CR3 and CR4 in myeloid and lymphoid cells of mice and men. *Semin. Cell Dev. Biol.* **85**, 110–121 (2019).
7. Miller, L. J., Schwarting, R. & Springer, T. A. Regulated expression of the Mac-1, LFA-1, p150,95 glycoprotein family during leukocyte differentiation. *J. Immunol.* **137**, 2891–900 (1986).
8. Sándor, N. *et al.* CD11c/CD18 Dominates Adhesion of Human Monocytes, Macrophages and Dendritic Cells over CD11b/CD18. *PLoS One* **11**, e0163120 (2016).
9. Berger, M. *et al.* Human neutrophils increase expression of C3bi as well as C3b receptors upon activation. *J. Clin. Invest.* **74**, 1566–71 (1984).
10. Sunderkötter, C. *et al.* Subpopulations of mouse blood monocytes differ in maturation stage and inflammatory response. *J. Immunol.* **172**, 4410–7 (2004).
11. Milde, R. *et al.* Multinucleated Giant Cells Are Specialized for Complement-Mediated Phagocytosis and Large Target Destruction. *Cell Rep.* **13**, 1937–48 (2015).
12. Merad, M., Sathe, P., Helft, J., Miller, J. & Mortha, A. The dendritic cell lineage: ontogeny and function of dendritic cells and their subsets in the steady state and the inflamed setting. *Annu. Rev. Immunol.* **31**, 563–604 (2013).
13. Matsushima, H. *et al.* Neutrophil differentiation into a unique hybrid population exhibiting dual phenotype and functionality of neutrophils and dendritic cells. *Blood* **121**, 1677–89 (2013).
14. Ortaldo, J. R., Sharrow, S. O., Timonen, T. & Herberman, R. B. Determination of surface antigens on highly purified human NK cells by flow cytometry with

- monoclonal antibodies. *J. Immunol.* **127**, 2401–9 (1981).
15. Muto, S., Větvička, V. & Ross, G. D. CR3 (CD11b/CD18) expressed by cytotoxic T cells and natural killer cells is upregulated in a manner similar to neutrophil CR3 following stimulation with various activating agents. *J. Clin. Immunol.* **13**, 175–184 (1993).
 16. Postigo, B. A. A., Corbl, A. L., Francisco, S. & Land, M. O. De. Regulated Expression and Function of CD11c/CD18 Integrin on Human B Lymphocytes. Relation between Attachment to Fibrinogen and Triggering of Proliferation through CD11c/CD18. *J. Exp. Med.* **174**, 1313–1322 (1991).
 17. Wagner, C. *et al.* The complement receptor 3, CR3 (CD11b/CD18), on T lymphocytes: Activation-dependent up-regulation and regulatory function. *Eur. J. Immunol.* **31**, 1173–1180 (2001).
 18. Uzonyi, B. *et al.* Functional studies of chronic lymphocytic leukemia B cells expressing β 2-integrin type complement receptors CR3 and CR4. *Immunol. Lett.* **189**, 73–81 (2017).
 19. Wormsley, S. B., Baird, S. M., Gadol, N., Rai, K. R. & Sobol, R. E. Characteristics of CD11c+CD5+ chronic B-cell leukemias and the identification of novel peripheral blood B-cell subsets with chronic lymphoid leukemia immunophenotypes. *Blood* **76**, 123–30 (1990).
 20. Bretscher, M. S. Circulating integrins: alpha 5 beta 1, alpha 6 beta 4 and Mac-1, but not alpha 3 beta 1, alpha 4 beta 1 or LFA-1. *EMBO J.* **11**, 405–10 (1992).
 21. Lobert, V. H. *et al.* Ubiquitination of alpha 5 beta 1 integrin controls fibroblast migration through lysosomal degradation of fibronectin-integrin complexes. *Dev. Cell* **19**, 148–59 (2010).
 22. Moreno-Layseca, P., Icha, J., Hamidi, H. & Ivaska, J. Integrin trafficking in cells and tissues. *Nat. Cell Biol.* **21**, 122–132 (2019).
 23. Zhen, Y. & Stenmark, H. Cellular functions of Rab GTPases at a glance. *J. Cell Sci.* **128**, 3171–6 (2015).
 24. Arjonen, A., Alanko, J., Veltel, S. & Ivaska, J. Distinct recycling of active and inactive β 1 integrins. *Traffic* **13**, 610–25 (2012).
 25. Jones, M. C., Caswell, P. T. & Norman, J. C. Endocytic recycling pathways: emerging regulators of cell migration. *Curr. Opin. Cell Biol.* **18**, 549–57 (2006).
 26. Roberts, M., Barry, S., Woods, A., van der Sluijs, P. & Norman, J. PDGF-regulated rab4-dependent recycling of alphavbeta3 integrin from early endosomes is necessary for cell adhesion and spreading. *Curr. Biol.* **11**, 1392–402 (2001).
 27. Caswell, P. T., Vadrevu, S. & Norman, J. C. Integrins: masters and slaves of endocytic transport. *Nat. Rev. Mol. Cell Biol.* **10**, 843–853 (2009).
 28. Fabbri, M. *et al.* A tyrosine-based sorting signal in the beta2 integrin cytoplasmic domain mediates its recycling to the plasma membrane and is required for ligand-supported migration. *EMBO J.* **18**, 4915–25 (1999).

29. Monica Fabbri,*† Silvia Di Meglio, †, Gagliani, M. C., Elisa Consonni,* Raffaella Molteni, J. R. B., Tacchetti, C. & Pardi*, and R. Dynamic Partitioning into Lipid Rafts Controls the Endo- Exocytic Cycle of the α L/ β 2 Integrin, LFA-1, during Leukocyte Chemotaxis. *Mol. Biol. Cell* **17**, 1018–1032 (2006).
30. Hynes, R. O. Integrins: bidirectional, allosteric signaling machines. *Cell* **110**, 673–87 (2002).
31. Tan, S. The leucocyte β 2 (CD18) integrins: the structure, functional regulation and signalling properties. *Biosci. Rep.* **32**, 241–269 (2012).
32. Xie, C. *et al.* Structure of an integrin with an alphaI domain, complement receptor type 4. *EMBO J.* **29**, 666–79 (2010).
33. Tan, S. M. *et al.* The N-terminal region and the mid-region complex of the integrin beta 2 subunit. *J. Biol. Chem.* **276**, 36370–6 (2001).
34. Shi, M. *et al.* The crystal structure of the plexin-semaphorin-integrin domain/hybrid domain/I-EGF1 segment from the human integrin beta2 subunit at 1.8-Å resolution. *J. Biol. Chem.* **280**, 30586–93 (2005).
35. Sen, M. & Springer, T. A. Leukocyte integrin α L β 2 headpiece structures: The α I domain, the pocket for the internal ligand, and concerted movements of its loops. *Proc. Natl. Acad. Sci. U. S. A.* **113**, 2940–5 (2016).
36. Xiong, J.-P. *et al.* Crystal structure of the extracellular segment of integrin alpha Vbeta3 in complex with an Arg-Gly-Asp ligand. *Science* **296**, 151–5 (2002).
37. Lee, J. H., Choi, J. & Nham, S.-U. Critical residues of alphaX I-domain recognizing fibrinogen central domain. *Biochem. Biophys. Res. Commun.* **355**, 1058–63 (2007).
38. Bajic, G., Yatime, L., Sim, R. B., Vorup-Jensen, T. & Andersen, G. R. Structural insight on the recognition of surface-bound opsonins by the integrin I domain of complement receptor 3. *Proc. Natl. Acad. Sci. U. S. A.* **110**, 16426–31 (2013).
39. Michishita, M., Videm, V. & Arnaout, M. A. A novel divalent cation-binding site in the A domain of the beta 2 integrin CR3 (CD11b/CD18) is essential for ligand binding. *Cell* **72**, 857–67 (1993).
40. Lee, J. O., Rieu, P., Arnaout, M. a & Liddington, R. Crystal structure of the A domain from the alpha subunit of integrin CR3 (CD11b/CD18). *Cell* **80**, 631–8 (1995).
41. Luo, B.-H., Carman, C. V & Springer, T. a. Structural basis of integrin regulation and signaling. *Annu. Rev. Immunol.* **25**, 619–47 (2007).
42. Nishida, N. *et al.* Activation of leukocyte beta2 integrins by conversion from bent to extended conformations. *Immunity* **25**, 583–94 (2006).
43. Xie, C. *et al.* The integrin alpha-subunit leg extends at a Ca²⁺-dependent epitope in the thigh/genu interface upon activation. *Proc. Natl. Acad. Sci. U. S. A.* **101**, 15422–7 (2004).
44. Shi, M. *et al.* A structural hypothesis for the transition between bent and extended

- conformations of the leukocyte beta2 integrins. *J. Biol. Chem.* **282**, 30198–206 (2007).
45. Bhunia, A., Tang, X.-Y., Mohanram, H., Tan, S.-M. & Bhattacharjya, S. NMR solution conformations and interactions of integrin alphaLbeta2 cytoplasmic tails. *J. Biol. Chem.* **284**, 3873–84 (2009).
 46. García-Alvarez, B. *et al.* Structural determinants of integrin recognition by talin. *Mol. Cell* **11**, 49–58 (2003).
 47. Sampath, R., Gallagher, P. J. & Pavalko, F. M. Cytoskeletal interactions with the leukocyte integrin beta2 cytoplasmic tail. Activation-dependent regulation of associations with talin and alpha-actinin. *J. Biol. Chem.* **273**, 33588–94 (1998).
 48. Das, M., Subbayya Ithychanda, S., Qin, J. & Plow, E. F. Mechanisms of talin-dependent integrin signaling and crosstalk. *Biochim. Biophys. Acta - Biomembr.* **1838**, 579–588 (2014).
 49. Thome, S., Begandt, D., Pick, R., Salvermoser, M. & Walzog, B. Intracellular β 2 integrin (CD11/CD18) interacting partners in neutrophil trafficking. *Eur. J. Clin. Invest.* **48 Suppl 2**, e12966 (2018).
 50. Anthis, N. J. *et al.* The structure of an integrin/talin complex reveals the basis of inside-out signal transduction. *EMBO J.* **28**, 3623–32 (2009).
 51. Kim, M., Carman, C. V & Springer, T. A. Bidirectional transmembrane signaling by cytoplasmic domain separation in integrins. *Science* **301**, 1720–5 (2003).
 52. Lee, J. O., Bankston, L. A. & Robert C Liddington, M. A. A. and. Two conformations of the integrin A-domain (I-domain): a pathway for activation? *Structure* **3**, 1333–1340 (1995).
 53. Chen, X. *et al.* Requirement of open headpiece conformation for activation of leukocyte integrin alphaXbeta2. *Proc. Natl. Acad. Sci. U. S. A.* **107**, 14727–32 (2010).
 54. Shimaoka, M. *et al.* Stabilizing the integrin alpha M inserted domain in alternative conformations with a range of engineered disulfide bonds. *Proc. Natl. Acad. Sci. U. S. A.* **99**, 16737–41 (2002).
 55. Jin, M., Andricioaei, I. & Springer, T. A. Conversion between three conformational states of integrin I domains with a C-terminal pull spring studied with molecular dynamics. *Structure* **12**, 2137–2147 (2004).
 56. Takagi, J., Petre, B. M., Walz, T. & Springer, T. A. Global conformational rearrangements in integrin extracellular domains in outside-in and inside-out signaling. *Cell* **110**, 599–11 (2002).
 57. Tng, E., Tan, S.-M., Ranganathan, S., Cheng, M. & Law, S. K. A. The integrin alpha L beta 2 hybrid domain serves as a link for the propagation of activation signal from its stalk regions to the I-like domain. *J. Biol. Chem.* **279**, 54334–9 (2004).
 58. Mould, A. P. *et al.* Conformational changes in the integrin beta A domain provide a

- mechanism for signal transduction via hybrid domain movement. *J. Biol. Chem.* **278**, 17028–35 (2003).
59. Astrof, N. S., Salas, A., Shimaoka, M., Chen, J. & Springer, T. A. Importance of force linkage in mechanochemistry of adhesion receptors. *Biochemistry* **45**, 15020–8 (2006).
 60. Li, J. & Springer, T. A. Integrin extension enables ultrasensitive regulation by cytoskeletal force. *Proc. Natl. Acad. Sci. U. S. A.* **114**, 4685–4690 (2017).
 61. Zhu, J. *et al.* Structure of a complete integrin ectodomain in a physiologic resting state and activation and deactivation by applied forces. *Mol. Cell* **32**, 849–61 (2008).
 62. Puklin-Faucher, E. & Sheetz, M. P. The mechanical integrin cycle. *J. Cell Sci.* **122**, 179–86 (2009).
 63. Ghandour, H., Cullere, X., Alvarez, A., Lusinskas, F. W. & Mayadas, T. N. Essential role for Rap1 GTPase and its guanine exchange factor CalDAG-GEFI in LFA-1 but not VLA-4 integrin mediated human T-cell adhesion. *Blood* **110**, 3682–90 (2007).
 64. Caron, E., Self, A. J. & Hall, A. The GTPase Rap1 controls functional activation of macrophage integrin α M β 2 by LPS and other inflammatory mediators. *Curr. Biol.* **10**, 974–8 (2000).
 65. Lim, J., Dupuy, A. G., Critchley, D. R. & Caron, E. Rap1 controls activation of the α (M) β (2) integrin in a talin-dependent manner. *J. Cell. Biochem.* **111**, 999–1009 (2010).
 66. Lee, H.-S., Lim, C. J., Puzon-McLaughlin, W., Shattil, S. J. & Ginsberg, M. H. RIAM activates integrins by linking talin to ras GTPase membrane-targeting sequences. *J. Biol. Chem.* **284**, 5119–27 (2009).
 67. Lagarrigue, F., Kim, C. & Ginsberg, M. H. The Rap1-RIAM-talin axis of integrin activation and blood cell function. *Blood* **128**, 479–87 (2016).
 68. Klapproth, S. *et al.* Loss of the Rap1 effector RIAM results in leukocyte adhesion deficiency due to impaired β 2 integrin function in mice. *Blood* **126**, 2704–12 (2015).
 69. Lim, J., Thompson, J., May, R. C., Hotchin, N. A. & Caron, E. Regulator of G-Protein Signalling-14 (RGS14) Regulates the Activation of α M β 2 Integrin during Phagocytosis. *PLoS One* **8**, e69163 (2013).
 70. Medraño-Fernandez, I. *et al.* RIAM (Rap1-interacting adaptor molecule) regulates complement-dependent phagocytosis. *Cell. Mol. Life Sci.* **70**, 2395–410 (2013).
 71. Stritt, S. *et al.* Rap1-GTP-interacting adaptor molecule (RIAM) is dispensable for platelet integrin activation and function in mice. *Blood* **125**, 219–22 (2015).
 72. O’Brien, X. M. *et al.* Lectin site ligation of CR3 induces conformational changes and signaling. *J. Biol. Chem.* **287**, 3337–48 (2012).
 73. Wright, S. D., Levin, S. M., Jong, M. T., Chad, Z. & Kabbash, L. G. CR3 (CD11b/CD18) expresses one binding site for Arg-Gly-Asp-containing peptides and

- a second site for bacterial lipopolysaccharide. *J. Exp. Med.* **169**, 175–83 (1989).
74. Ingalls, R. R. & Golenbock, D. T. CD11c/CD18, a transmembrane signaling receptor for lipopolysaccharide. *J. Exp. Med.* **181**, 1473–9 (1995).
 75. Losse, J., Zipfel, P. F. & Józsi, M. Factor H and factor H-related protein 1 bind to human neutrophils via complement receptor 3, mediate attachment to *Candida albicans*, and enhance neutrophil antimicrobial activity. *J. Immunol.* **184**, 912–21 (2010).
 76. Malhotra, V., Hogg, N. & Sim, R. B. Ligand binding by the p150,95 antigen of U937 monocytic cells: properties in common with complement receptor type 3 (CR3). *Eur. J. Immunol.* **16**, 1117–23 (1986).
 77. Józsi, M., Schneider, A. E., Kárpáti, É. & Sándor, N. Complement factor H family proteins in their non-canonical role as modulators of cellular functions. *Semin. Cell Dev. Biol.* 1–10 (2018). doi:10.1016/j.semcdb.2017.12.018
 78. Wright, S. D. *et al.* Complement receptor type three (CD11b/CD18) of human polymorphonuclear leukocytes recognizes fibrinogen. *Proc. Natl. Acad. Sci. U. S. A.* **85**, 7734–8 (1988).
 79. Altieri, D. C. & Edgington, T. S. The saturable high affinity association of factor X to ADP-stimulated monocytes defines a novel function of the Mac-1 receptor. *J. Biol. Chem.* **263**, 7007–15 (1988).
 80. Loike, J. D. *et al.* CD11c/CD18 on neutrophils recognizes a domain at the N terminus of the A alpha chain of fibrinogen. *Proc. Natl. Acad. Sci. U. S. A.* **88**, 1044–8 (1991).
 81. Thompson, H. L. & Matsushima, K. Human polymorphonuclear leucocytes stimulated by tumour necrosis factor-alpha show increased adherence to extracellular matrix proteins which is mediated via the CD11b/18 complex. *Clin. Exp. Immunol.* **90**, 280–5 (1992).
 82. Monboisse, J. C., Garnotel, R., Randoux, A., Dufer, J. & Borel, J. P. Adhesion of human neutrophils to and activation by type-I collagen involving a beta 2 integrin. *J. Leukoc. Biol.* **50**, 373–80 (1991).
 83. Nathan, C. *et al.* Cytokine-induced respiratory burst of human neutrophils: Dependence on extracellular matrix proteins and CD11/CD18 integrins. *J. Cell Biol.* **109**, 1341–1349 (1989).
 84. Garnotel, R. *et al.* Human blood monocytes interact with type I collagen through alpha x beta 2 integrin (CD11c-CD18, gp150-95). *J. Immunol.* **164**, 5928–34 (2000).
 85. Gahmberg, C. G. Leukocyte adhesion: CD11/CD18 integrins and intercellular adhesion molecules. *Curr. Opin. Cell Biol.* **9**, 643–50 (1997).
 86. Santoso, S. *et al.* The junctional adhesion molecule 3 (JAM-3) on human platelets is a counterreceptor for the leukocyte integrin Mac-1. *J. Exp. Med.* **196**, 679–91 (2002).
 87. Blackford, J., Reid, H. W., Pappin, D. J., Bowers, F. S. & Wilkinson, J. M. A

- monoclonal antibody, 3/22, to rabbit CD11c which induces homotypic T cell aggregation: evidence that ICAM-1 is a ligand for CD11c/CD18. *Eur. J. Immunol.* **26**, 525–31 (1996).
88. Sadhu, C. *et al.* CD11c/CD18: novel ligands and a role in delayed-type hypersensitivity. *J. Leukoc. Biol.* **81**, 1395–1403 (2007).
 89. Ihanus, E., Uotila, L. M., Toivanen, A., Varis, M. & Gahmberg, C. G. Red-cell ICAM-4 is a ligand for the monocyte/macrophage integrin CD11c/CD18: characterization of the binding sites on ICAM-4. *Blood* **109**, 802–10 (2007).
 90. O'Brien, X. M. & Reichner, J. S. Neutrophil Integrins and Matrix Ligands and NET Release. *Front. Immunol.* **7**, 363 (2016).
 91. Muchowski, P. J. *et al.* Functional interaction between the integrin antagonist neutrophil inhibitory factor and the I domain of CD11b/CD18. *J. Biol. Chem.* **269**, 26419–23 (1994).
 92. Ishibashi, Y., Claus, S. & Relman, D. A. Bordetella pertussis filamentous hemagglutinin interacts with a leukocyte signal transduction complex and stimulates bacterial adherence to monocyte CR3 (CD11b/CD18). *J. Exp. Med.* **180**, 1225–33 (1994).
 93. Coulson, B. S., Londrigan, S. L. & Lee, D. J. Rotavirus contains integrin ligand sequences and a disintegrin-like domain that are implicated in virus entry into cells. *Proc. Natl. Acad. Sci. U. S. A.* **94**, 5389–94 (1997).
 94. Janssen, B. J. C. *et al.* Structures of complement component C3 provide insights into the function and evolution of immunity. *Nature* **437**, 505–11 (2005).
 95. Xu, S., Wang, J., Wang, J.-H. & Springer, T. A. Distinct recognition of complement iC3b by integrins $\alpha X\beta 2$ and $\alpha M\beta 2$. *Proc. Natl. Acad. Sci. U. S. A.* **114**, 3403–3408 (2017).
 96. Chen, X., Yu, Y., Mi, L.-Z., Walz, T. & Springer, T. a. Molecular basis for complement recognition by integrin $\alpha X\beta 2$. *Proc. Natl. Acad. Sci. U. S. A.* **109**, 4586–91 (2012).
 97. Forneris, F. *et al.* Regulators of complement activity mediate inhibitory mechanisms through a common C3b-binding mode. *EMBO J.* **35**, 1133–49 (2016).
 98. Molmenti, E. P., Ziambaras, T. & Perlmutter, D. H. Evidence for an acute phase response in human intestinal epithelial cells. *J. Biol. Chem.* **268**, 14116–24 (1993).
 99. Guadiz, G., Sporn, L. a & Simpson-Haidaris, P. J. Thrombin cleavage-independent deposition of fibrinogen in extracellular matrices. *Blood* **90**, 2644–53 (1997).
 100. Flick, M. J., Du, X. & Degen, J. L. Fibrin(ogen)-alpha M beta 2 interactions regulate leukocyte function and innate immunity in vivo. *Exp. Biol. Med. (Maywood)*. **229**, 1105–10 (2004).
 101. Luyendyk, J. P., Schoenecker, J. G. & Flick, M. J. The multifaceted role of fibrinogen in tissue injury and inflammation. *Blood* **133**, 511–520 (2019).

102. Mosesson, M. W. Fibrinogen and fibrin structure and functions. *J. Thromb. Haemost.* **3**, 1894–904 (2005).
103. Altieri, D. C., Bader, R., Mannucci, P. M. & Edgington, T. S. Oligospecificity of the cellular adhesion receptor Mac-1 encompasses an inducible recognition specificity for fibrinogen. *J. Cell Biol.* **107**, 1893–900 (1988).
104. Altieri, D. C., Plescia, J. & Plow, E. F. The structural motif glycine 190-valine 202 of the fibrinogen gamma chain interacts with CD11b/CD18 integrin (alpha M beta 2, Mac-1) and promotes leukocyte adhesion. *J. Biol. Chem.* **268**, 1847–53 (1993).
105. Ugarova, T. P. *et al.* Identification of a novel recognition sequence for integrin alphaM beta2 within the gamma-chain of fibrinogen. *J. Biol. Chem.* **273**, 22519–27 (1998).
106. Podolnikova, N. P. *et al.* Sequence γ 377–395(P2), but Not γ 190–202(P1), Is the Binding Site for the α M I-Domain of Integrin α M β 2 in the γ C-Domain of Fibrinogen †. *Biochemistry* **42**, 9365–9373 (2003).
107. Flick, M. J. *et al.* Leukocyte engagement of fibrin(ogen) via the integrin receptor alphaMbeta2/Mac-1 is critical for host inflammatory response in vivo. *J. Clin. Invest.* **113**, 1596–606 (2004).
108. Ugarova, T. P. & Yakubenko, V. P. Recognition of fibrinogen by leukocyte integrins. *Ann. N. Y. Acad. Sci.* **936**, 368–85 (2001).
109. Nham, S. U. Characteristics of fibrinogen binding to the domain of CD11c, an alpha subunit of p150,95. *Biochem. Biophys. Res. Commun.* **264**, 630–4 (1999).
110. Lishko, V. K., Kudryk, B., Yakubenko, V. P., Yee, V. C. & Ugarova, T. P. Regulated unmasking of the cryptic binding site for integrin alpha M beta 2 in the gamma C-domain of fibrinogen. *Biochemistry* **41**, 12942–51 (2002).
111. Kollman, J. M., Pandi, L., Sawaya, M. R., Riley, M. & Doolittle, R. F. Crystal structure of human fibrinogen. *Biochemistry* **48**, 3877–86 (2009).
112. Dupuy, A. G. & Caron, E. Integrin-dependent phagocytosis: spreading from microadhesion to new concepts. *J. Cell Sci.* **121**, 1773–83 (2008).
113. Stuart, L. M. & Ezekowitz, R. A. B. Phagocytosis: elegant complexity. *Immunity* **22**, 539–50 (2005).
114. Jin, T., Xu, X. & Hereld, D. Chemotaxis, chemokine receptors and human disease. *Cytokine* **44**, 1–8 (2008).
115. Sozzani, S. *et al.* Migration of dendritic cells in response to formyl peptides, C5a, and a distinct set of chemokines. *J. Immunol.* **155**, 3292–5 (1995).
116. Lee, H. Y., Lee, M. & Bae, Y.-S. Formyl Peptide Receptors in Cellular Differentiation and Inflammatory Diseases. *J. Cell. Biochem.* **118**, 1300–1307 (2017).
117. Le, Y., Oppenheim, J. J. & Wang, J. M. Pleiotropic roles of formyl peptide receptors. *Cytokine Growth Factor Rev.* **12**, 91–105 (2001).

118. Yang, D. *et al.* Differential regulation of responsiveness to fMLP and C5a upon dendritic cell maturation: correlation with receptor expression. *J. Immunol.* **165**, 2694–702 (2000).
119. Weiß, E. & Kretschmer, D. Formyl-Peptide Receptors in Infection, Inflammation, and Cancer. *Trends Immunol.* **39**, 815–829 (2018).
120. Liu, M. *et al.* Formylpeptide receptors are critical for rapid neutrophil mobilization in host defense against *Listeria monocytogenes*. *Sci. Rep.* **2**, 786 (2012).
121. Anna, E., Gabriella, S. & József, P. *Immunológia. Med. Könyvkiadó Zrt.* (2012).
122. Varricchi, G., Raap, U., Rivellese, F., Marone, G. & Gibbs, B. F. Human mast cells and basophils-How are they similar how are they different? *Immunol. Rev.* **282**, 8–34 (2018).
123. Ravin, K. A. & Loy, M. The Eosinophil in Infection. *Clin. Rev. Allergy Immunol.* **50**, 214–27 (2016).
124. Mayadas, T. N., Cullere, X. & Lowell, C. A. The multifaceted functions of neutrophils. *Annu. Rev. Pathol.* **9**, 181–218 (2014).
125. Kolaczkowska, E. & Kubes, P. Neutrophil recruitment and function in health and inflammation. *Nat. Rev. Immunol.* **13**, 159–75 (2013).
126. Ziegler-Heitbrock, L. Blood monocytes and their subsets: Established features and open questions. *Front. Immunol.* **6**, 1–5 (2015).
127. Guilliams, M., Mildner, A. & Yona, S. Developmental and Functional Heterogeneity of Monocytes. *Immunity* **49**, 595–613 (2018).
128. Ginhoux, F. & Guilliams, M. Tissue-Resident Macrophage Ontogeny and Homeostasis. *Immunity* **44**, 439–449 (2016).
129. Samstein, M. *et al.* Essential yet limited role for CCR2⁺ inflammatory monocytes during *Mycobacterium tuberculosis*-specific T cell priming. *Elife* **2**, e01086 (2013).
130. Rivollier, A., He, J., Kole, A., Valatas, V. & Kelsall, B. L. Inflammation switches the differentiation program of Ly6Chi monocytes from antiinflammatory macrophages to inflammatory dendritic cells in the colon. *J. Exp. Med.* **209**, 139–55 (2012).
131. Jakubzick, C. V., Randolph, G. J. & Henson, P. M. Monocyte differentiation and antigen-presenting functions. *Nat. Rev. Immunol.* **17**, 349–362 (2017).
132. Serbina, N. V., Salazar-Mather, T. P., Biron, C. a, Kuziel, W. a & Pamer, E. G. TNF/iNOS-producing dendritic cells mediate innate immune defense against bacterial infection. *Immunity* **19**, 59–70 (2003).
133. Kratofil, R. M., Kubes, P. & Deniset, J. F. Monocyte Conversion During Inflammation and Injury. *Arterioscler. Thromb. Vasc. Biol.* **37**, 35–42 (2017).
134. Auffray, C. *et al.* Monitoring of blood vessels and tissues by a population of monocytes with patrolling behavior. *Science* **317**, 666–70 (2007).

135. Patel, A. A. *et al.* The fate and lifespan of human monocyte subsets in steady state and systemic inflammation. *J. Exp. Med.* **214**, 1913–1923 (2017).
136. Mukherjee, R. *et al.* Non-Classical monocytes display inflammatory features: Validation in Sepsis and Systemic Lupus Erythematosus. *Sci. Rep.* **5**, 13886 (2015).
137. Belge, K.-U. *et al.* The proinflammatory CD14+CD16+DR++ monocytes are a major source of TNF. *J. Immunol.* **168**, 3536–42 (2002).
138. Davies, L. C., Jenkins, S. J., Allen, J. E. & Taylor, P. R. Tissue-resident macrophages. *Nat. Immunol.* **14**, 986–95 (2013).
139. Gautier, E. L. *et al.* Gene-expression profiles and transcriptional regulatory pathways that underlie the identity and diversity of mouse tissue macrophages. *Nat. Immunol.* **13**, 1118–28 (2012).
140. Varol, C., Mildner, A. & Jung, S. Macrophages: development and tissue specialization. *Annu. Rev. Immunol.* **33**, 643–75 (2015).
141. Mills, C. D., Kincaid, K., Alt, J. M., Heilman, M. J. & Hill, A. M. M-1/M-2 macrophages and the Th1/Th2 paradigm. *J. Immunol.* **164**, 6166–73 (2000).
142. Martinez, F. O., Sica, A., Mantovani, A. & Locati, M. Macrophage activation and polarization. *Front. Biosci.* **13**, 453–61 (2008).
143. Gordon, S. & Martinez, F. O. Alternative activation of macrophages: mechanism and functions. *Immunity* **32**, 593–604 (2010).
144. Jetten, N. *et al.* Anti-inflammatory M2, but not pro-inflammatory M1 macrophages promote angiogenesis in vivo. *Angiogenesis* **17**, 109–18 (2014).
145. Mosser, D. M. & Edwards, J. P. Exploring the full spectrum of macrophage activation. *Nat. Rev. Immunol.* **8**, 958–69 (2008).
146. Murray, P. J. *et al.* Macrophage activation and polarization: nomenclature and experimental guidelines. *Immunity* **41**, 14–20 (2014).
147. Sapozhnikov, A. *et al.* Organ-dependent in vivo priming of naive CD4+, but not CD8+, T cells by plasmacytoid dendritic cells. *J. Exp. Med.* **204**, 1923–33 (2007).
148. Reizis, B., Bunin, A., Ghosh, H. S., Lewis, K. L. & Sisirak, V. Plasmacytoid dendritic cells: recent progress and open questions. *Annu. Rev. Immunol.* **29**, 163–83 (2011).
149. Gilliet, M., Cao, W. & Liu, Y.-J. Plasmacytoid dendritic cells: sensing nucleic acids in viral infection and autoimmune diseases. *Nat. Rev. Immunol.* **8**, 594–606 (2008).
150. Savina, A. & Amigorena, S. Phagocytosis and antigen presentation in dendritic cells. *Immunol. Rev.* **219**, 143–56 (2007).
151. Steinman, R. M. The dendritic cell system and its role in immunogenicity. *Annu. Rev. Immunol.* **9**, 271–96 (1991).
152. Ding, Z. M. *et al.* Relative contribution of LFA-1 and Mac-1 to neutrophil adhesion and migration. *J. Immunol.* **163**, 5029–38 (1999).

153. Lu, H. *et al.* LFA-1 is sufficient in mediating neutrophil emigration in Mac-1-deficient mice. *J. Clin. Invest.* **99**, 1340–50 (1997).
154. Arnaout, M. A., Lanier, L. L. & Faller, D. V. Relative contribution of the leukocyte molecules Mo1, LFA-1, and p150,95 (LeuM5) in adhesion of granulocytes and monocytes to vascular endothelium is tissue- and stimulus-specific. *J. Cell. Physiol.* **137**, 305–9 (1988).
155. Anderson, D. C., Miller, L. J., Schmalstieg, F. C., Rothlein, R. & Springer, T. a. Contributions of the Mac-1 glycoprotein family to adherence-dependent granulocyte functions: structure-function assessments employing subunit-specific monoclonal antibodies. *J. Immunol.* **137**, 15–27 (1986).
156. Thacker, R. I. & Retzinger, G. S. Adsorbed fibrinogen regulates the behavior of human dendritic cells in a CD18-dependent manner. *Exp. Mol. Pathol.* **84**, 122–30 (2008).
157. Georgakopoulos, T., Moss, S. T. & Kanagasundaram, V. Integrin CD11c contributes to monocyte adhesion with CD11b in a differential manner and requires Src family kinase activity. *Mol. Immunol.* **45**, 3671–81 (2008).
158. Destaing, O., Saltel, F., Géminard, J.-C., Jurdic, P. & Bard, F. Podosomes display actin turnover and dynamic self-organization in osteoclasts expressing actin-green fluorescent protein. *Mol. Biol. Cell* **14**, 407–16 (2003).
159. Linder, S. & Aepfelbacher, M. Podosomes: adhesion hot-spots of invasive cells. *Trends Cell Biol.* **13**, 376–385 (2003).
160. Calle, Y., Burns, S., Thrasher, A. J. & Jones, G. E. The leukocyte podosome. *Eur. J. Cell Biol.* **85**, 151–7 (2006).
161. Linder, S. & Wiesner, C. Tools of the trade: podosomes as multipurpose organelles of monocytic cells. *Cell. Mol. Life Sci.* **72**, 121–35 (2015).
162. Meddens, M. B. M., van den Dries, K. & Cambi, A. Podosomes revealed by advanced bioimaging: what did we learn? *Eur. J. Cell Biol.* **93**, 380–7 (2014).
163. Alonso, F., Spuul, P., Daubon, T., Kramer, Ij. & Génot, E. Variations on the theme of podosomes: A matter of context. *Biochim. Biophys. acta. Mol. cell Res.* **1866**, 545–553 (2019).
164. Veillat, V. *et al.* Podosomes: Multipurpose organelles? *Int. J. Biochem. Cell Biol.* **65**, 52–60 (2015).
165. Proag, A. *et al.* Working together: spatial synchrony in the force and actin dynamics of podosome first neighbors. *ACS Nano* **9**, 3800–13 (2015).
166. Burns, S. *et al.* Maturation of DC is associated with changes in motile characteristics and adherence. *Cell Motil. Cytoskeleton* **57**, 118–32 (2004).
167. Gawden-Bone, C. *et al.* A crucial role for β 2 integrins in podosome formation, dynamics and Toll-like-receptor-signaled disassembly in dendritic cells. *J. Cell Sci.* **127**, 4213–24 (2014).

168. Bajtay, Z., Speth, C., Erdei, A. & Dierich, M. P. Cutting edge: productive HIV-1 infection of dendritic cells via complement receptor type 3 (CR3, CD11b/CD18). *J. Immunol.* **173**, 4775–8 (2004).
169. Hajishengallis, G. *et al.* Subversion of innate immunity by periodontopathic bacteria via exploitation of complement receptor-3. *Adv. Exp. Med. Biol.* **632**, 203–19 (2008).
170. Schlesinger, L. S. & Horwitz, M. A. Phagocytosis of leprosy bacilli is mediated by complement receptors CR1 and CR3 on human monocytes and complement component C3 in serum. *J. Clin. Invest.* **85**, 1304–14 (1990).
171. Hawley, K. L. *et al.* CD14 cooperates with complement receptor 3 to mediate MyD88-independent phagocytosis of *Borrelia burgdorferi*. *Proc. Natl. Acad. Sci. U. S. A.* **109**, 1228–32 (2012).
172. Zhou, J. *et al.* CD14(hi)CD16⁺ monocytes phagocytose antibody-opsonised *Plasmodium falciparum* infected erythrocytes more efficiently than other monocyte subsets, and require CD16 and complement to do so. *BMC Med.* **13**, 154 (2015).
173. Hirsch, C. S., Ellner, J. J., Russell, D. G. & Rich, E. A. Complement receptor-mediated uptake and tumor necrosis factor- α -mediated growth inhibition of *Mycobacterium tuberculosis* by human alveolar macrophages. *J. Immunol.* **152**, 743–53 (1994).
174. Lukácsi, S., Nagy-Baló, Z., Erdei, A., Sándor, N. & Bajtay, Z. The role of CR3 (CD11b/CD18) and CR4 (CD11c/CD18) in complement-mediated phagocytosis and podosome formation by human phagocytes. *Immunol. Lett.* **189**, 64–72 (2017).
175. Schwartz, J. T. *et al.* Natural IgM mediates complement-dependent uptake of *Francisella tularensis* by human neutrophils via complement receptors 1 and 3 in nonimmune serum. *J. Immunol.* **189**, 3064–77 (2012).
176. van Bruggen, R. *et al.* Complement receptor 3 and Toll-like receptor 4 act sequentially in uptake and intracellular killing of unopsonized *Salmonella enterica* serovar Typhimurium by human neutrophils. *Infect. Immun.* **75**, 2655–60 (2007).
177. Peyron, P., Bordier, C., N'Diaye, E. N. & Maridonneau-Parini, I. Nonopsonic phagocytosis of *Mycobacterium kansasii* by human neutrophils depends on cholesterol and is mediated by CR3 associated with glycosylphosphatidylinositol-anchored proteins. *J. Immunol.* **165**, 5186–91 (2000).
178. Levitz, S. M. & Tabuni, A. Binding of *Cryptococcus neoformans* by human cultured macrophages. Requirements for multiple complement receptors and actin. *J. Clin. Invest.* **87**, 528–35 (1991).
179. Schlesinger, L. S. & Horwitz, M. a. Phagocytosis of *Mycobacterium leprae* by human monocyte-derived macrophages is mediated by complement receptors CR1 (CD35), CR3 (CD11b/CD18), and CR4 (CD11c/CD18) and IFN- γ activation inhibits complement receptor function and phagocytosis of this bacte. *J. Immunol.* **147**, 1983–94 (1991).
180. Anderson, D. C. & Springer, T. A. Leukocyte adhesion deficiency: an inherited defect in the Mac-1, LFA-1, and p150,95 glycoproteins. *Annu. Rev. Med.* **38**, 175–

- 94 (1987).
181. Schmidt, S., Moser, M. & Sperandio, M. The molecular basis of leukocyte recruitment and its deficiencies. *Mol. Immunol.* **55**, 49–58 (2013).
 182. Etzioni, A. Genetic etiologies of leukocyte adhesion defects. *Curr. Opin. Immunol.* **21**, 481–486 (2009).
 183. Kishimoto, T. K., Hollander, N., Roberts, T. M., Anderson, D. C. & Springer, T. A. Heterogeneous mutations in the beta subunit common to the LFA-1, Mac-1, and p150,95 glycoproteins cause leukocyte adhesion deficiency. *Cell* **50**, 193–202 (1987).
 184. Anderson, D. C. *et al.* The severe and moderate phenotypes of heritable Mac-1, LFA-1 deficiency: their quantitative definition and relation to leukocyte dysfunction and clinical features. *J. Infect. Dis.* **152**, 668–89 (1985).
 185. von Andrian, U. H. *et al.* In vivo behavior of neutrophils from two patients with distinct inherited leukocyte adhesion deficiency syndromes. *J. Clin. Invest.* **91**, 2893–7 (1993).
 186. Gresham, H. D., Graham, I. L., Anderson, D. C. & Brown, E. J. Leukocyte adhesion-deficient neutrophils fail to amplify phagocytic function in response to stimulation. Evidence for CD11b/CD18-dependent and -independent mechanisms of phagocytosis. *J. Clin. Invest.* **88**, 588–97 (1991).
 187. Yong, K., Addison, I. E., Johnson, B., Webster, A. D. B. & Linch, D. C. Role of leukocyte integrins in phagocyte responses to granulocyte-macrophage colony stimulating factor (GM-CSF): In vitro and in vivo studies on leukocyte adhesion deficiency neutrophils. *Br. J. Haematol* **77**, 150–157 (1991).
 188. van de Vijver, E. *et al.* Hematologically important mutations: leukocyte adhesion deficiency (first update). *Blood Cells. Mol. Dis.* **48**, 53–61 (2012).
 189. Svensson, L. *et al.* Leukocyte adhesion deficiency-III is caused by mutations in KINDLIN3 affecting integrin activation. *Nat. Med.* **15**, 306–12 (2009).
 190. Malinin, N. L. *et al.* A point mutation in KINDLIN3 ablates activation of three integrin subfamilies in humans. *Nat. Med.* **15**, 313–8 (2009).
 191. Sorio, C. *et al.* Mutations of Cystic Fibrosis Transmembrane Conductance Regulator Gene Cause a Monocyte-Selective Adhesion Deficiency. *Am. J. Respir. Crit. Care Med.* **193**, 1123–33 (2016).
 192. Fan, Z. & Ley, K. Leukocyte Adhesion Deficiency IV. Monocyte Integrin Activation Deficiency in Cystic Fibrosis. *Am. J. Respir. Crit. Care Med.* **193**, 1075–7 (2016).
 193. Bosticardo, M. *et al.* Recent advances in understanding the pathophysiology of Wiskott-Aldrich syndrome. *Blood* **113**, 6288–6295 (2009).
 194. Bouma, G., Burns, S. O. & Thrasher, A. J. Wiskott-Aldrich Syndrome: Immunodeficiency resulting from defective cell migration and impaired immunostimulatory activation. *Immunobiology* **214**, 778–90 (2009).

195. Badolato, R. *et al.* Monocytes from Wiskott-Aldrich patients display reduced chemotaxis and lack of cell polarization in response to monocyte chemoattractant protein-1 and formyl-methionyl-leucyl-phenylalanine. *J. Immunol.* **161**, 1026–33 (1998).
196. Zhang, H. *et al.* Impaired Integrin-Dependent Function in Wiskott-Aldrich Syndrome Protein-Deficient Murine and Human Neutrophils. *Immunity* **25**, 285–295 (2006).
197. Zicha, D. *et al.* Chemotaxis of macrophages is abolished in the Wiskott-Aldrich syndrome. *Br. J. Haematol.* **101**, 659–665 (1998).
198. de Noronha, S. *et al.* Impaired dendritic-cell homing in vivo in the absence of Wiskott-Aldrich syndrome protein. *Blood* **105**, 1590–7 (2005).
199. Linder, S., Nelson, D., Weiss, M. & Aepfelbacher, M. Wiskott-Aldrich syndrome protein regulates podosomes in primary human macrophages. *Proc. Natl. Acad. Sci. U. S. A.* **96**, 9648–9653 (1999).
200. Burns, S., Thrasher, A. J., Blundell, M. P., Machesky, L. & Jones, G. E. Configuration of human dendritic cell cytoskeleton by Rho GTPases, the WAS protein, and differentiation. *Blood* **98**, 1142–9 (2001).
201. Gahmberg, C. G. *et al.* Regulation of integrin activity and signalling. *Biochim. Biophys. Acta* **1790**, 431–44 (2009).
202. Bouma, G. *et al.* Cytoskeletal remodeling mediated by WASp in dendritic cells is necessary for normal immune synapse formation and T-cell priming. *Blood* **118**, 2492–2501 (2011).
203. Han, S. *et al.* Evaluation of imputation-based association in and around the integrin-alpha-M (ITGAM) gene and replication of robust association between a non-synonymous functional variant within ITGAM and systemic lupus erythematosus (SLE). *Hum. Mol. Genet.* **18**, 1171–80 (2009).
204. MacPherson, M., Lek, H. S., Prescott, A. & Fagerholm, S. C. A systemic lupus erythematosus-associated R77H substitution in the CD11b chain of the Mac-1 integrin compromises leukocyte adhesion and phagocytosis. *J. Biol. Chem.* **286**, 17303–17310 (2011).
205. Rhodes, B. *et al.* The rs1143679 (R77H) lupus associated variant of ITGAM (CD11b) impairs complement receptor 3 mediated functions in human monocytes. *Ann. Rheum. Dis.* **71**, 2028–34 (2012).
206. Fossati-Jimack, L. *et al.* Phagocytosis Is the Main CR3-Mediated Function Affected by the Lupus-Associated Variant of CD11b in Human Myeloid Cells. *PLoS One* **8**, (2013).
207. Rosetti, F. *et al.* A Lupus-Associated Mac-1 Variant Has Defects in Integrin Allosteric and Interaction with Ligands under Force. *Cell Rep.* **10**, 1655–1664 (2015).
208. Etzioni, A., Doerschuk, C. M. & Harlan, J. M. Of man and mouse: leukocyte and endothelial adhesion molecule deficiencies. *Blood* **94**, 3281–8 (1999).

209. Prechtel, A. T., Turza, N. M., Theodoridis, A. a. & Steinkasserer, A. CD83 knockdown in monocyte-derived dendritic cells by small interfering RNA leads to a diminished T cell stimulation. *J. Immunol.* **178**, 5454–64 (2007).
210. Ungai-Salánki, R. *et al.* Automated single cell isolation from suspension with computer vision. *Sci. Rep.* **6**, 20375 (2016).
211. Salánki, R. *et al.* Single cell adhesion assay using computer controlled micropipette. *PLoS One* **9**, e111450 (2014).
212. Környei, Z. *et al.* Cell sorting in a Petri dish controlled by computer vision. *Sci. Rep.* **3**, 1088 (2013).
213. Orgovan, N. *et al.* In-situ and label-free optical monitoring of the adhesion and spreading of primary monocytes isolated from human blood: Dependence on serum concentration levels. *Biosens. Bioelectron.* **54**, 339–344 (2014).
214. Cervero, P., Panzer, L. & Linder, S. Podosome reformation in macrophages: assays and analysis. *Methods Mol. Biol.* **1046**, 97–121 (2013).
215. Sándor, N. *et al.* CR3 is the dominant phagocytotic complement receptor on human dendritic cells. *Immunobiology* **218**, 652–63 (2013).
216. Turner, M. W., Grant, C., Seymour, N. D., Harvey, B. & Levinsky, R. J. Evaluation of C3b/C3bi opsonization and chemiluminescence with selected yeasts and bacteria using sera of different opsonic potential. *Immunology* **58**, 111–5 (1986).
217. Orgovan, N. *et al.* Dependence of cancer cell adhesion kinetics on integrin ligand surface density measured by a high-throughput label-free resonant waveguide grating biosensor. *Sci. Rep.* **4**, 4034 (2015).
218. Schachtner, H., Calaminus, S. D. J., Thomas, S. G. & Machesky, L. M. Podosomes in adhesion, migration, mechanosensing and matrix remodeling. *Cytoskeleton* **70**, 572–589 (2013).
219. Mehraj, J. *et al.* Epidemiology of Staphylococcus aureus Nasal Carriage Patterns in the Community. *Curr. Top. Microbiol. Immunol.* **398**, 55–87 (2016).
220. Lioté, F., Boval-Boizard, B., Weill, D., Kuntz, D. & Wautier, J. L. Blood monocyte activation in rheumatoid arthritis: increased monocyte adhesiveness, integrin expression, and cytokine release. *Clin. Exp. Immunol.* **106**, 13–9 (1996).
221. Gower, R. M. *et al.* CD11c/CD18 expression is upregulated on blood monocytes during hypertriglyceridemia and enhances adhesion to vascular cell adhesion molecule-1. *Arterioscler. Thromb. Vasc. Biol.* **31**, 160–6 (2011).
222. Sallusto, F. *et al.* Rapid and coordinated switch in chemokine receptor expression during dendritic cell maturation. *Eur. J. Immunol.* **28**, 2760–9 (1998).
223. Dieu, M. C. *et al.* Selective recruitment of immature and mature dendritic cells by distinct chemokines expressed in different anatomic sites. *J. Exp. Med.* **188**, 373–86 (1998).
224. Xuan, W., Qu, Q., Zheng, B., Xiong, S. & Fan, G.-H. The chemotaxis of M1 and

- M2 macrophages is regulated by different chemokines. *J. Leukoc. Biol.* **97**, 61–9 (2015).
225. Halvorsen, B. *et al.* Increased levels of CCR7 ligands in carotid atherosclerosis: different effects in macrophages and smooth muscle cells. *Cardiovasc. Res.* **102**, 148–56 (2014).
 226. Damås, J. K. *et al.* Enhanced expression of the homeostatic chemokines CCL19 and CCL21 in clinical and experimental atherosclerosis: possible pathogenic role in plaque destabilization. *Arterioscler. Thromb. Vasc. Biol.* **27**, 614–20 (2007).
 227. Jawhara, S., Pluskota, E., Cao, W., Plow, E. F. & Soloviev, D. A. Distinct Effects of Integrins $\alpha X\beta 2$ and $\alpha M\beta 2$ on Leukocyte Subpopulations during Inflammation and Antimicrobial Responses. *Infect. Immun.* **85**, 1–17 (2017).
 228. Mazzone, A. & Ricevuti, G. Leukocyte CD11/CD18 integrins: Biological and clinical relevance. *Haematologica* **80**, 161–175 (1995).
 229. Thinn, A. M. M., Wang, Z. & Zhu, J. The membrane-distal regions of integrin α cytoplasmic domains contribute differently to integrin inside-out activation. *Sci. Rep.* **8**, 5067 (2018).
 230. Vorup-Jensen, T. *et al.* Exposure of acidic residues as a danger signal for recognition of fibrinogen and other macromolecules by integrin $\alpha X\beta 2$. *Proc. Natl. Acad. Sci. U. S. A.* **102**, 1614–9 (2005).
 231. Berton, G., Laudanna, C., Sorio, C. & Rossi, F. Generation of signals activating neutrophil functions by leukocyte integrins: LFA-1 and gp150/95, but not CR3, are able to stimulate the respiratory burst of human neutrophils. *J. Cell Biol.* **116**, 1007–17 (1992).
 232. Keizer, G. D., Te Velde, a a, Schwarting, R., Figdor, C. G. & De Vries, J. E. Role of p150,95 in adhesion, migration, chemotaxis and phagocytosis of human monocytes. *Eur. J. Immunol.* **17**, 1317–1322 (1987).
 233. Vorup-Jensen, T., Ostermeier, C., Shimaoka, M., Hommel, U. & Springer, T. A. Structure and allosteric regulation of the alpha X beta 2 integrin I domain. *Proc. Natl. Acad. Sci. U. S. A.* **100**, 1873–8 (2003).
 234. Vorup-Jensen, T. & Jensen, R. K. Structural Immunology of Complement Receptors 3 and 4. *Front. Immunol.* **9**, 1–20 (2018).
 235. Nourshargh, S. & Alon, R. Leukocyte migration into inflamed tissues. *Immunity* **41**, 694–707 (2014).
 236. Szczur, K., Xu, H., Atkinson, S., Zheng, Y. & Filippi, M. D. Rho GTPase CDC42 regulates directionality and random movement via distinct MAPK pathways in neutrophils. *Blood* **108**, 4205–4213 (2006).
 237. Aderem, A. & Underhill, D. M. Mechanisms of phagocytosis in macrophages. *Annu. Rev. Immunol.* **17**, 593–623 (1999).
 238. Levitz, S. M. Receptor-mediated recognition of *Cryptococcus neoformans*. *Nihon Ishinkin Gakkai Zasshi* **43**, 133–6 (2002).

239. Graham, I. L., Gresham, H. D. & Brown, E. J. An immobile subset of plasma membrane CD11b/CD18 (Mac-1) is involved in phagocytosis of targets recognized by multiple receptors. *J. Immunol.* **142**, 2352–8 (1989).
240. Ross, G. D. Role of the lectin domain of Mac-1/CR3 (CD11b/CD18) in regulating intercellular adhesion. *Immunol. Res.* **25**, 219–227 (2002).
241. Ben Nasr, A. *et al.* Critical role for serum opsonins and complement receptors CR3 (CD11b/CD18) and CR4 (CD11c/CD18) in phagocytosis of *Francisella tularensis* by human dendritic cells (DC): uptake of *Francisella* leads to activation of immature DC and intracellular survival of. *J. Leukoc. Biol.* **80**, 774–786 (2006).
242. Banchereau, J. *et al.* Immunobiology of dendritic cells. *Annu. Rev. Immunol.* **18**, 767–811 (2000).
243. Murray, P. J. & Wynn, T. A. Protective and pathogenic functions of macrophage subsets. *Nat. Rev. Immunol.* **11**, 723–37 (2011).
244. Wong, K.-F., Luk, J. M., Cheng, R. H., Klickstein, L. B. & Fan, S.-T. Characterization of two novel LPS-binding sites in leukocyte integrin betaA domain. *FASEB J.* **21**, 3231–9 (2007).
245. Flaherty, S. F., Golenbock, D. T., Milham, F. H. & Ingalls, R. R. CD11/CD18 leukocyte integrins: new signaling receptors for bacterial endotoxin. *J. Surg. Res.* **73**, 85–9 (1997).
246. Wright, S. D. & Jong, M. T. Adhesion-promoting receptors on human macrophages recognize *Escherichia coli* by binding to lipopolysaccharide. *J. Exp. Med.* **164**, 1876–88 (1986).
247. Zarewych, D. M., Kindzelskii, A. L., Todd, R. F. & Petty, H. R. LPS induces CD14 association with complement receptor type 3, which is reversed by neutrophil adhesion. *J. Immunol.* **156**, 430–3 (1996).
248. Ingalls, R. R., Arnaout, M. a & Golenbock, D. T. Outside-in signaling by lipopolysaccharide through a tailless integrin. *J. Immunol.* **159**, 433–8 (1997).
249. Rescigno, M., Granucci, F., Citterio, S., Foti, M. & Ricciardi-Castagnoli, P. Coordinated events during bacteria-induced DC maturation. *Immunol. Today* **20**, 200–3 (1999).
250. Wright, S. D., Ramos, R. A., Hermanowski-Vosatka, A., Rockwell, P. & Detmers, P. A. Activation of the adhesive capacity of CR3 on neutrophils by endotoxin: dependence on lipopolysaccharide binding protein and CD14. *J. Exp. Med.* **173**, 1281–6 (1991).
251. Lo, S. K., Detmers, P. A., Levin, S. M. & Wright, S. D. Transient adhesion of neutrophils to endothelium. *J. Exp. Med.* **169**, 1779–93 (1989).

ADATLAP

a doktori értekezés nyilvánosságra hozatalához*

I. A doktori értekezés adatai

A szerző neve: **Lukácsi Szilvia Zsófia**

MTMT-azonosító: **10055879**

A doktori értekezés címe és alcíme: **The differential role of CR3 (CD11b/CD18) and CR4 (CD11c/CD18) complement receptors in human phagocytes (A CR3 és CR4 komplementreceptorok eltérő szerepe humán fagociták funkcióiban)**

DOI-azonosító⁴⁶: **10.15476/ELTE.2019.154**

A doktori iskola neve: **Biológia Doktori Iskola**

A doktori iskolán belüli doktori program neve: **Immunológia**

A témavezető neve és tudományos fokozata: **Bajtay Zsuzsa, Ph.D., D.Sc.**

A témavezető munkahelye: **ELTE TTK Immunológiai Tanszék**

II. Nyilatkozatok

1. A doktori értekezés szerzőjeként

a) hozzájárulok, hogy a doktori fokozat megszerzését követően a doktori értekezésem és a tézisek nyilvánosságra kerüljenek az ELTE Digitális Intézményi Tudástárban. Felhatalmazom a Természettudományi kar Dékáni Hivatal Doktori, Habilitációs és Nemzetközi Ügyek Csoportjának ügyintézőjét, hogy az értekezést és a téziseket feltöltse az ELTE Digitális Intézményi Tudástárba, és ennek során kitöltse a feltöltéshez szükséges nyilatkozatokat.

b) kérem, hogy a mellékelt kérelemben részletezett szabadalmi, illetőleg oltalmi bejelentés közzétételéig a doktori értekezést ne bocsássák nyilvánosságra az Egyetemi Könyvtárban és az ELTE Digitális Intézményi Tudástárban;

c) kérem, hogy a nemzetbiztonsági okból minősített adatot tartalmazó doktori értekezést a minősítés (*dátum*)-ig tartó időtartama alatt ne bocsássák nyilvánosságra az Egyetemi Könyvtárban és az ELTE Digitális Intézményi Tudástárban;

d) kérem, hogy a mű kiadására vonatkozó mellékelt kiadó szerződésre tekintettel a doktori értekezést a könyv megjelenéséig ne bocsássák nyilvánosságra az Egyetemi Könyvtárban, és az ELTE Digitális Intézményi Tudástárban csak a könyv bibliográfiai adatait tegyék közzé. Ha a könyv a fokozatszerzést követően egy évig nem jelenik meg, hozzájárulok, hogy a doktori értekezésem és a tézisek nyilvánosságra kerüljenek az Egyetemi Könyvtárban és az ELTE Digitális Intézményi Tudástárban.

2. A doktori értekezés szerzőjeként kijelentem, hogy

a) az ELTE Digitális Intézményi Tudástárba feltöltendő doktori értekezés és a tézisek saját eredeti, önálló szellemi munkám és legjobb tudomásom szerint nem sértem vele senki szerzői jogait;

b) a doktori értekezés és a tézisek nyomtatott változatai és az elektronikus adathordozón benyújtott tartalmak (szöveg és ábrák) mindenben megegyeznek.

3. A doktori értekezés szerzőjeként hozzájárulok a doktori értekezés és a tézisek szövegének plágiumkereső adatbázisba helyezéséhez és plágiumellenőrző vizsgálatok lefuttatásához.

Kelt: *Bp. 2019. 07. 11.*

Lukácsi Szilvia

a doktori értekezés szerzőjének aláírása